Magnetic Fields and Magnetic Diagnostics

for

Tokamak Plasmas

Alan Wootton

INTRODUCTION

This series of notes tries to lay the foundations for the interpretation of magnetic fields and fluxes, often in terms of equilibrium plasma parameters. The title, 'magnetic diagnostics', is taken to mean those diagnostics which are used to measure magnetic fields and fluxes using induction, or pick-up, coils. More specifically, what is often inferred is a question: "How much can we tell about a plasma given certain measurements of magnetic fields, and fluxes, outside that plasma?" I don't consider here diagnostics which measure the plasma current density distribution utilizing phenomena such as the motional Stark effect, or Faraday rotation; these are found in a series of notes on Plasma Diagnostics..

The measurements themselves are in principle simple, although in practice they are always complicated by unwanted field components, for example from misaligned pick-up coils. There is also the problem of allowing for image currents flowing in nearby conductors; dealing with these image currents becomes a large part of the problem. Including the effects of an iron core also leads to complications.

Many people think the topic under consideration is boring, in that there is nothing new to do. You have only to read current issues of plasma physics journals to recognize that there is still much interest in the topic. For example, equilibrium and its determination, axisymmetric stability and disruptions are all of current interest, and all involve 'magnetic diagnostics'. The subject does appear to be difficult (students starting in the topic have a hard time).

The layout of the notes is as given in the list of contents. Generally I have included topics which I have found useful in trying to understand tokamaks. Some basic concepts (inductances, fluxes, etc.) are included, because they are made use of throughout the notes. There is also a section on plasma equilibrium, in which the large aspect ratio, circular tokamak is described. The fluxes and fields from this model are used as examples for application of certain ideas in the remainder of the text.

References I find useful include:
- B. J. Braams, The interpretation of tokamak diagnostics: status and prospects, IPP Garching report IPP 5/2, 1985.
- L. E. Zakharov and V. D. Shafranov, Equilibrium of current carrying plasmas in toroidal configurations, in Reviews of Plasma Physics volume 11, edited by M. A. Leontovich, Consultants Bureau, New York (1986).
- V. S. Mukhovatov and V. D. Shafranov, Nucl. Fusion 11 (1971) 605.
- V. D. Shafranov, Plasma Physics 13 (1971) 757.
- L. E. Zakharov and V. D. Shafranov, Sov. Phys. Tech. Phys. 18 (1973) 151

o J. A. Wesson, in Tokamaks, Oxford Science Publications, Clarendon press, Oxford, 1987.
o P. Shkarofsky, Evaluation of multipole moments over the current density in a tokamak
    with magnetic probes, Phys. Fluids <u>25</u> (1982) 89.

1. SOME CONCEPTS AND DEFINITIONS

Maxwell's equations

We are going to make extensive use of Maxwell's equations. In vector form, these are

$$\nabla \times \mathbf{B} = \mu \left(\mathbf{j} + \frac{\partial \mathbf{D}}{\partial t} \right) \qquad\qquad 1.1$$

$$\nabla \cdot \mathbf{B} = 0 \qquad\qquad 1.2$$

$$\nabla \times \mathbf{E} = -\frac{\partial \mathbf{B}}{\partial t} \qquad\qquad 1.3$$

$$\nabla \cdot \mathbf{D} = \rho \qquad\qquad 1.4$$

If charge is conserved we can add to these the continuity equation. We shall ignore the displacement current $\partial D/\partial t$, and take $\mu = \mu_o$, the free space value, inside a plasma. Without the last term Equation 1.1 is Amperes law. We have effectively restricted ourselves to assuming $n_i = n_e = n$, the charge neutral assumption, and that any waves have frequencies much less than the electron plasma frequency, with characteristic lengths much greater than the Debye length . We have <u>not</u> said E or $\nabla \cdot \mathbf{E} = 0$. When considering plasma equilibrium we shall also assume the electron mass m_e approaches 0. This allows electrons to have an infinitely fast response time.

Pick-up or Induction Coils

This is the heart of the matter. Magnetic fields are usually measured with pick-up or induction coil circuits. Changing the magnetic flux in a circuit generates a current; the direction of this current is in a direction such as to set up a magnetic flux opposing the change. The electromotence or voltage ε ($\nabla\, \varepsilon$ = -**E**, the electric field intensity) in Volts induced in a circuit equals the rate of change of flux N = $\oint_S \mathbf{B} \cdot \mathbf{n} dS$ in Webers per second, i.e.

$$\varepsilon = \frac{dN}{dt} \qquad\qquad 1.5$$

The flux can be changed either by changing its strength, changing the shape of the circuit, or moving the circuit. Then

$$\oint_l \mathbf{E} \cdot \mathbf{dl} = -\frac{d}{dt} \oint_S \mathbf{B} \cdot \mathbf{n} dS \qquad\qquad 1.6$$

for any path l, with n the normal to a two sided surface S. Applying Stokes theorem ($\oint_l \mathbf{A} \bullet \mathbf{dl} = \int_S \mathbf{n} \bullet \nabla \times \mathbf{A} dS$ for any vector **A**) to the left hand side of Equation 1.6 gives Equation 1.3. *Figure 1.1* shows the geometry of a coil used in applying Equation 1.6, Faraday's Law. The output signal must be time integrated to obtain the required flux. By taking a small enough coil the local field B can then be determined. This becomes difficult if very small scale variations in field exist, because the pick-up coils must then be very small themselves. The surface S includes any area between the leads; this is minimized by twisting them together. A hand drill is particularly useful for this.
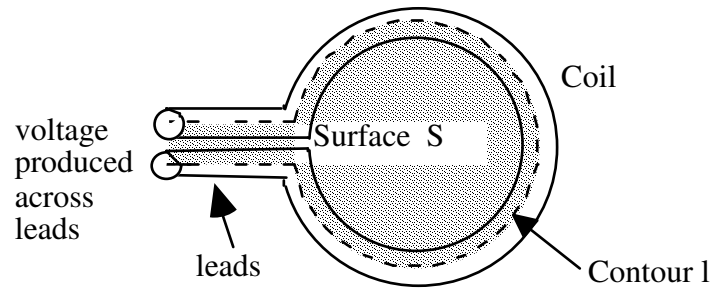
Figure 1.1. The contour l and surface S of a pick-up coil.

Integration

The time integration required to obtain the magnetic field B from the pick-up coil output ε can be performed either digitally or by an analog circuit.
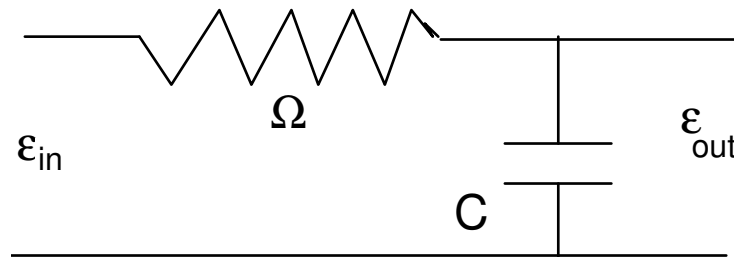
Figure 1.2. A passive "ΩC" integration circuit.

The simplest thing to do is to use a capacitor (C) and resistor (Ω) network, as shown in *Figure 1.2*. The output voltage is given by

$$\frac{d\varepsilon_{out}}{dt} + \frac{\varepsilon_{out}}{\tau} = \frac{\varepsilon_{in}}{\tau} \qquad\qquad 1.7$$

with $\tau = \Omega C$ called the integrator time constant. The solution to this equation is

$$\varepsilon_{out} = e^{-t/\tau} \int_0^t \left(e^{-t'/\tau} \right) \varepsilon_{in}(t') \frac{dt'}{\tau}$$
1.8

For example, suppose at t = 0 we start an input voltage $\varepsilon_{in} = \varepsilon_{in0} \sin(\omega t)$, so that the required integral is $\varepsilon_{int} = \varepsilon_{in0} (1-\cos(\omega t))/\omega$. The output from the passive circuit is (obtained using Laplace transforms)

$$\varepsilon_{out} = \varepsilon_{in0} \left(\frac{\omega\tau}{e^{t/\tau}\left(1+(\omega\tau)^2\right)} + \frac{\sin(\omega t) - \omega\tau\cos(\omega t)}{\left(1+(\omega\tau)^2\right)} \right)$$
1.9

Now consider two extremes. First, if $\omega\tau \gg 1$ and $t \ll \tau$ we have

$$\varepsilon_{out} = \frac{\varepsilon_{in0}}{\omega\tau}(1-\cos(\omega t))$$
1.10

That is, $\varepsilon_{out} = 1/\tau$ times the required integral. In this limit we have integrated the input signal. If $\omega\tau \ll 1$ and $t \gg \tau$, then $\varepsilon_{out} = \varepsilon_{in}$.

As an example, we show in *Figure 1.3* the output from the passive integrator ("integrator output", dotted line) for a sinusoidal voltage input of 1V at a frequency of 100 Hz ("coil input", solid line), with an integrator time $\tau = 0.1$s. The exact integral ("field") divided by τ is shown as the broken line. The integral is only performed accurately for times $t \ll \tau$; as the pulse proceeds there is a "droop", and significant errors result. We can imagine the curve "field" represents a specified magnetic field time history $B = B_0(1-\cos(\omega t))/(\omega\tau)$, with $B_0 = \tau/(nA)$ T, and B/τ is plotted. The curve "coil output" represents the unintegrated output from a magnetic pick-up coil with area nA m^2, (n turns each of area A), which becomes the input voltage to a passive integrator $\varepsilon_{in} = \sin(\omega t)$. Finally the curve "integrator output" represents the output from the passive integrator, which we would interpret as the original magnetic field.

A common situation is that the required signal from the pick-up coil has a low frequency component of angular frequency ω_0, and superimposed upon this is a higher frequency unwanted "noise" signal of angular frequency ω_1. By carefully choosing the time constant τ of our passive integrator so that $\omega_0\tau \ll 1$ ($\varepsilon_{out} = \varepsilon_{in}$) but $\omega_1\tau \gg 1$ (integration) we filter the noise, leaving the required slowly time varying voltage. As an example, *Figure 1.4* shows the passive integrator output ε_{out} (dashed line) for an input voltage ε_{in} (solid line) comprising a slow ($\omega_0 = 10$ rs^{-1}, $\varepsilon_{in0} = 1$ V) and fast ($\omega_1 = 2 \times 10^3$ rs^{-1}, $\varepsilon_{in1} = 0.2$ V) component. The time constant $\tau = 0.01$ s, so that

$\omega_0\tau = 0.1$ (<< 1) and $\omega_1\tau = 100$ (>> 1). The output voltage is filtered, as required. The dashed line shows the exact integral divided by τ, for comparison.
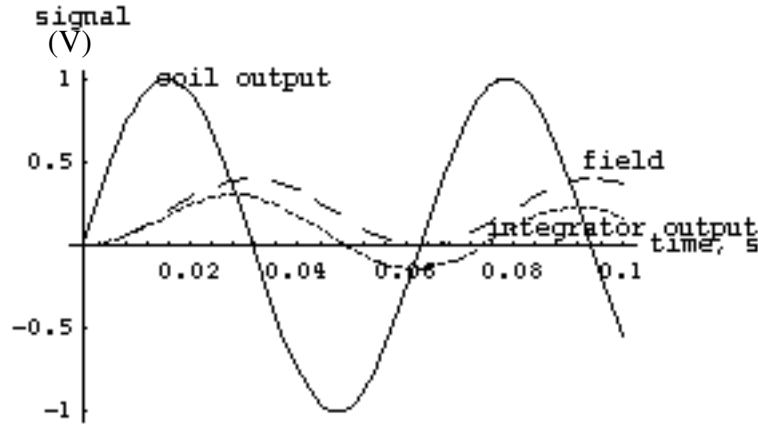
Figure 1.3. The input ("coil input", solid line) sinusoidal voltage with f = 100 Hz and output ("integrator output", dotted line) of a passive integrator circuit with $\tau = \Omega C = 0.1$ s. The (exact integral)/τ is denoted by "field", the broken line.
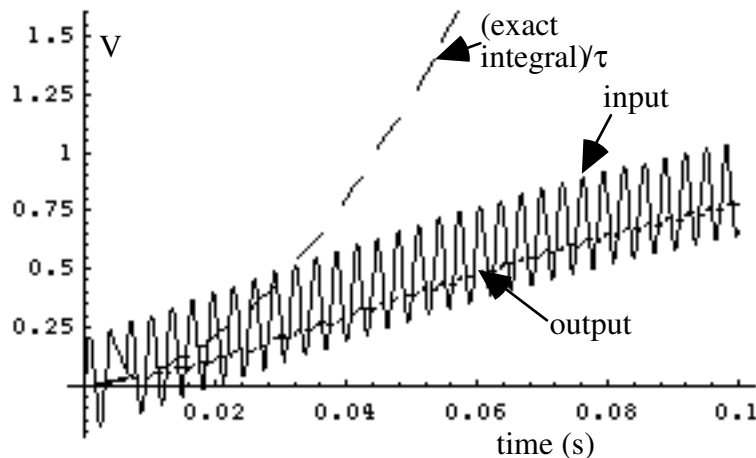
Figure 1.4. The output of a passive integrator circuit used as a filter. An input voltage (solid line) with summed sinusoidal voltages is smoothed to give the dash-dot line. The exact integral divided by $\tau = \Omega C$ is shown as the dashed line.

A more common system to perform the time integration is an active integrator, but in many cases an input filter consisting of a passive integrator is still used. Active integration is performed using a circuit such as shown in *Figure 1.5*; the output voltage $\varepsilon_{out} = \dfrac{1}{\Omega C}\int\limits_{t_1}^{t}\varepsilon_{in}dt$. The example shown grounds one side of the coil. A useful feature shown is the integrator gate, which defines

10

the time t_1 the integration starts. On tokamaks this gate is often used to help reduce errors from misaligned pick-up coils. For example, tokamaks have a large toroidal field and a much smaller poloidal field. Therefore if the pick-up coil used to measure the poloidal field is misaligned even by a small amount, the resulting component of the toroidal field which is picked up (as dB/dt) can be significant. However the toroidal field usually evolves on a much slower time scale than the poloidal field, and in fact it is usually time independent at the time the poloidal field is initiated. Therefore the integrator gate can be opened when the toroidal field is time independent, and therefore the induced voltage in the misaligned pick-up coil is independent of the toroidal field.
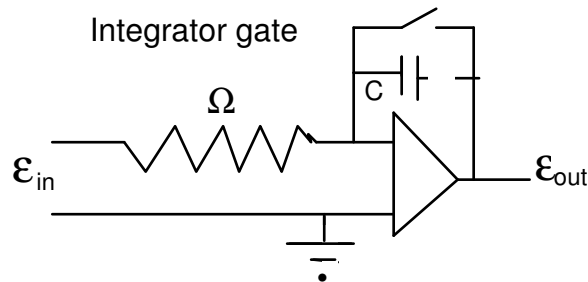
Figure 1.5. An active integrator circuit.

If the data is digitized, integration can be performed numerically. Sufficiently fast systems now exist for "real time" integration; the integration can be performed in μs so that integrated signals suitable for real time feedback control can be obtained. A p bit digitizer has a resolution of 1 part in 10^p, e.g. an 8 bit system has a resolution of 1 in 256, while a 10 bit system has a resolution of 1 part in 1024. This can be a limitation if we intend to investigate large but low frequency magnetic fields in the presence of small, high frequency fields. An example is that of trying to measure the equilibrium poloidal field in the presence of Mirnov oscillations. The pick-up coil output is dominated by the voltage produced by the time derivative of the small but high frequency component. Avoiding saturating the input by the higher voltage, high frequency component means that the resolution of the low frequency fields is now restricted. If we want to use the full capability of the digitizer in recording the lower frequency fields, then the solution is to filter the signal and only allow frequencies below a certain value to be recorded, i.e. use the filter described above with reference to *Figures 1.2* and *1.4*.

Intuition suggests that if a time varying wave form is sampled sufficiently fast then the original wave form can be recovered. However, we must determine how close the samples must be, and how to interpolate between adjacent points. The sampling theorem provides answers to these questions. An original signal x(t) can be recovered from sample values $x(nt_s)$, with t_s the sample time, by locating sinc functions at nt_s with amplitudes $x(nt_s)$. The signal x(t) can only be

recovered if the signal bandwidth $b \leq f_s/2$, with f_s the sampling frequency $= 1/t_s$. If this is not done, aliasing occurs.

If $b > f_s/2$ then the high frequency signal can appear as a low frequency signal. The fact that spoked wheels in films sometimes appear to rotate backwards is a manifestation of aliasing. Aliasing can be avoided using a passive filter to remove the high frequencies $f > f_s/2$. For example, sampling at 5 kHz (i.e. a sample every 0.2 ms) then an "anti aliasing" filter with $\tau = 0.5$ ms can be used.

Vector potential

In describing plasma equilibria we shall make use of the vector potential **A**. It is related to the poloidal flux, and used to determine self and mutual inductances. It is defined through the equation

$$\nabla \times \mathbf{A} = \mathbf{B} \qquad\qquad 1.11$$

In cylindrical geometry (R,ϕ,z), which we shall use a lot, this is

$$B_R = \frac{1}{R}\frac{\partial A_z}{\partial \phi} - \frac{\partial A_\phi}{\partial z}$$

$$B_\phi = \frac{\partial A_R}{\partial z} - \frac{\partial A_z}{\partial R} \qquad\qquad 1.12$$

$$B_z = \frac{1}{R}\frac{\partial (RA_\phi)}{\partial R} - \frac{1}{R}\frac{\partial A_R}{\partial \phi}$$

Then the electric intensity **E** is proportional to the vector potential **A** whose change produces it:

$$\mathbf{E} = -\frac{d\mathbf{A}}{dt} \qquad\qquad 1.13$$

From Equation 1.1 (ignoring D and ρ) we then have that **A** is given in terms of the current density **j** (the current per unit area) by Poisson's equation:

$$\nabla^2 \mathbf{A} = -\mu\mathbf{j} \qquad\qquad 1.14$$

which has a solution

$$A = \frac{\mu}{4\pi}\int_V \frac{jdV}{r} = \frac{\mu}{4\pi}\oint \frac{Idl}{r} \qquad\qquad 1.15$$

where the total current I flows inside the volume V, the line element dl is along the direction of the total current I, and r is the distance from the line element to the point of interest. A useful example for us is the vector potential of a circular filament. This is used to represent windings (vertical field, shaping, ohmic heating) on the tokamak, and elements of the plasma current itself.
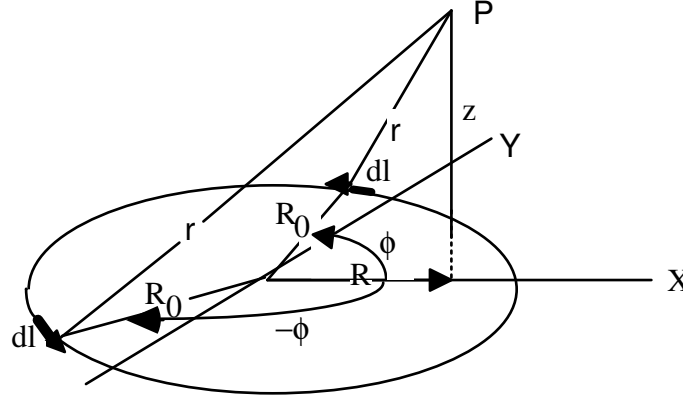
Figure 1.6. The geometry used to evaluate the vector potential of a circular filament.

Consider a circular filament of radius R_0, with current I in the ϕ direction. A_ϕ must be independent of ϕ, so choose the point of interest P in the (X,z) plane of *Figure 1.6*, where $\phi = 0$. Pairing equidistant elements dl shown in thickened lines at $\pm\phi$ we see the resultant is normal to (R,z). Therefore only consider the component dl_ϕ of dl in the direction normal to the plane (R,z); $dl_\phi = R_0\cos(\phi)d\phi$. The radial distance r from the point P to the element is given by $r^2 = z^2 + R_0^2 + R^2 - 2R_0 R\cos(\phi)$. Then

$$A_\phi = \frac{\mu}{4\pi}\oint\frac{Idl_\phi}{r} = \frac{\mu I}{2\pi}\int_0^\pi\frac{R_0\cos(\phi)d\phi}{\left(R_0^2 + R^2 + z^2 - 2R_0 R\cos(\phi)\right)^{1/2}} \qquad 1.16$$

Far from the loop (i.e. a small loop) we have $r_0 = (R^2+z^2)^{1/2} \gg R_0$, and the integral becomes

$$A_\phi = \frac{\mu I}{2\pi}\int_0^\pi\frac{R_0\cos(\phi)}{r_0}\left(1 + \frac{RR_0\cos(\phi)}{r_0^2}\right)d\phi$$

$$\approx \frac{RR_0^2\mu I}{4r^3} = \mu\frac{(\mathbf{M}\times\mathbf{r})}{4\pi r^3} \qquad\qquad 1.17$$

Here we have written the magnetic moment of the loop $M = \pi R_0^2 I$, directed upwards.

If the loop is not small, then let $\phi = \pi + 2\theta$, so $d\phi = 2\ d\theta$ and $\cos(\phi) = 2\sin^2(\theta) - 1$, and we obtain

$$A_\phi = \frac{\mu R_0 I}{\pi} \int_0^{\pi/2} \frac{\left(2\sin^2(\theta) - 1\right)d\theta}{\left(\left(R_0 + R\right)^2 + z^2 - 4R_0 R \sin^2(\theta)\right)^{1/2}}$$

1.18

This can be re-written in terms of $K(k^2)$ and $E(k^2)$, the complete elliptic integrals of the first and second kind, $\left(E(m) = \int_0^{\frac{\pi}{2}} \sqrt{\left(1 - m\sin^2(\theta)\right)}d\theta,\ K(m) = \int_0^{\frac{\pi}{2}} \frac{d\theta}{\sqrt{\left(1 - m\sin^2(\theta)\right)}} \right.$ as

$$A_\Phi = \frac{\mu I}{\pi k}\left(\frac{R_0}{R}\right)^{1/2}\left[\left(1 - \frac{k^2}{2}\right)K - E\right]$$

$$k^2 = 4R_0 R\left[\left(R_0 + R\right)^2 + z^2\right]^{-1}$$

1.19
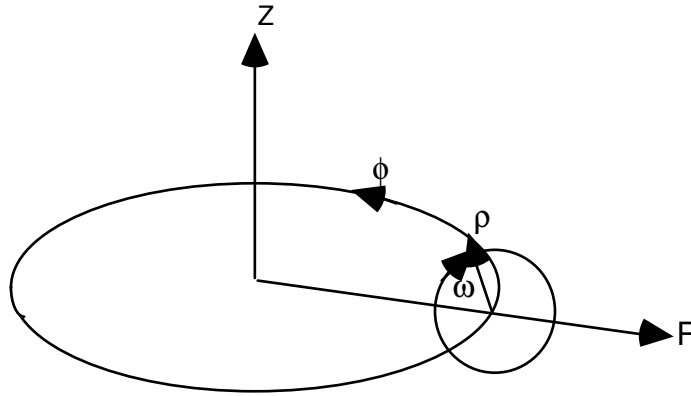
Figure 1.7. Cylindrical (R,ϕ,z) and quasi cylindrical (ρ,ω,ϕ) coordinate systems. Both are right handed

Going into a quasi-cylindrical coordinate system (ρ,ω,ϕ) shown in *Figure 1.7*, based on the current path, then

$$R = R_0 - \rho\cos(\omega)$$

$$z = \rho\sin(\omega)$$

1.20

Expanding k we find that keeping terms of order ρ/R_0 then $k^2 \approx 1$. We must go to higher order (to find $k < 1$) because $K(1) = \infty$. Keeping terms of order $(\rho/R_0)^4$ we find $k^2 \approx 1 - \frac{1}{4}\frac{\rho^2}{R_0^2} - \frac{\rho^3}{R_0^3}\frac{\cos(\omega)}{4}) - \frac{\rho^4}{R_0^4}\frac{\left(1 + 2\cos(2\omega)\right)}{16}$. Using the expansions for E and K found in the Handbook of Mathematical Tables, Abramowitz, Dover Publications, and after some rearranging, we obtain up to order $(\rho/R_0)^2$ $E \approx 1 + \frac{\rho^2}{8R_0^2}\left(1 + \ln\left(\frac{2R_0}{\rho}\right)\right)$ and

$$K \approx \ln\left(\frac{8R_0}{\rho}\right) - \frac{\rho}{2R_0}\cos(\omega) + \frac{\rho^2}{16R_0^2}\left(\ln\left(\frac{2R_0}{\rho}\right) + \frac{1}{2}(1 + 4\cos(2\omega))\right).$$ Finally we can write an

expression for the vector potential near the loop keeping terms of order (ρ/R_0):

$$A_\phi \approx \frac{\mu_0 I}{2\pi}\left[\left(\ln\left(\frac{8R_0}{\rho}\right) - 2\right) + \frac{\rho}{R_0}\frac{\cos(\omega)}{2}\left(\ln\left(\frac{8R_0}{\rho}\right) - 3\right)\right] \qquad 1.21$$

Figures 1.8 and *1.9* show a comparison between the approximate (Equation 1.21) and exact (Equation 1.19) solutions for a case with current I = 1/μ, and a major radius R_0 = 1.0 m. For the approximate solutions we show results both for zero order (i.e. neglecting terms proportional to ρ/R_0) and including first order corrections (i.e. including terms proportional to ρ/R_0). *Figure 1.8* shows a cut in the plane of the coil (z = 0), while *Figure 1.9* shows contours for A_ϕ = 0.15, 0.2, 0.3 and 0.4. We see that it is sufficient to consider only the zero order terms, that is the terms proportional to ρ/R_0 can be neglected. In fact in *Figure 1.8* the effects of including the first order terms cannot be detected. The simple approximation $A_\phi \approx \frac{\mu_0 I}{2\pi}\left(\ln\left(\frac{8R_0}{\rho}\right) - 2\right)$ is excellent.

The field components are given, in the original circular coordinate system (R,ϕ,z), as

$$B_R = -\frac{\partial A_\phi}{\partial z} = \frac{\mu_0 I}{2\pi}\frac{z}{R\left[(R+R_0)^2 + z^2\right]^{1/2}}\left[-K + \frac{R_0^2 + R^2 + z^2}{(R_0 - R)^2 + z^2}E\right]$$

$$B_z = \frac{1}{R}\frac{\partial(RA_\phi)}{\partial R} = \frac{\mu_0 I}{2\pi}\frac{1}{\left[(R+R_0)^2 + z^2\right]^{1/2}}\left[K + \frac{R_0^2 - R^2 - z^2}{(R_0 - R)^2 + z^2}E\right] \qquad 1.22$$

where we have made use of

$$\frac{\partial K}{\partial k} = \frac{E}{k(1-k^2)} - \frac{K}{k}; \frac{\partial E}{\partial k} = \frac{E}{k} - \frac{K}{k};$$

$$\frac{\partial k}{\partial z} = -\frac{zk^3}{4R_0 R}; \frac{\partial k}{\partial R} = \frac{k}{2R} - \frac{k^3}{4R} - \frac{k^3}{4R_0} \qquad 1.23$$

On the axis R = 0 we have B_R = 0 and $B_z = \frac{\mu_0 I R_0^2}{2(R_0^2 + z^2)^{3/2}}$.
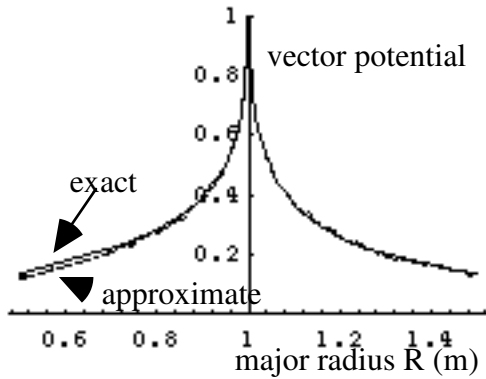
Figure 1.8. The exact (solid line), the approximate zero order (dashed line) and the approximate first order (dotted line) solutions in the z = 0 plane for the vector potential from a circular current filament with current I = 1/μ.
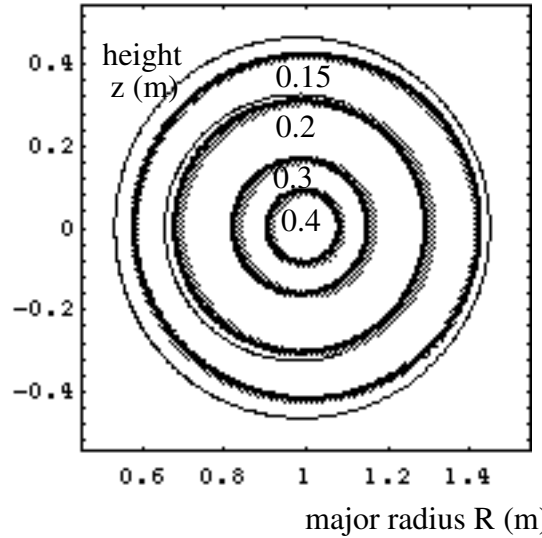
Figure 1.9. Contours of vector potential from the exact solution (thin dark line), the zero order approximation (thick gray line) and including first order corrections (intermediate thickness dark line) for a circular current filament with current I = 1/μ. Contours of potential equal to 0.15, 0.2, 0.3 and 0.4 are shown.

Mutual inductance

We shall use mutual and self inductances, often between circular filaments. They can be used to derive the vertical field necessary to maintain a plasma equilibrium, and to analyze axisymmetric instabilities. We are interested in the relationships between mutual and self inductances and fluxes, and how to write energy in terms of mutual and self inductances.

The mutual inductance M_{12} between two circuits is defined as the flux N_{12} through circuit 1 produced by unit current in circuit 2. Then

$$M_{12} = \oint_{l_1} \frac{A_2}{I_2} dl_1$$

1.24

with A_2 the total vector potential due to current 2 in circuit 2. That is,

$$M_{12} = \frac{\mu}{4\pi} \oint_{l_1} \oint_{l_2} \frac{dl_1 dl_2}{r} = M_{21}$$

1.25

The electromotance through circuit 1 due to a current I_2 in circuit 2 is

16

$$\varepsilon_1 = M_{12}\frac{dI_2}{dt} \qquad\qquad 1.26$$

The total energy (in a volume V) associated with two circuits is

$$W_t = \frac{1}{2\mu}\int_V (\mathbf{B}_1 + \mathbf{B}_2) \bullet (\mathbf{B}_1 + \mathbf{B}_2)dV$$

$$= \frac{1}{2\mu}\int_V B_1^2 dV + \frac{1}{2\mu}\int_V B_2^2 dV + \frac{1}{\mu}\int_V \mathbf{B}_1 \bullet \mathbf{B}_2 dV \qquad 1.27$$

The first two terms represent the energy required to establish the currents I_1 and I_2 producing the fields B_1 and B_2 in circuits 1 and 2. The third term is the energy used in bringing the two circuits together. This mutual energy between the two circuits W_{12} is

$$W_{12} = M_{12}I_1 I_2 = \frac{1}{\mu}\int_V B_1 B_2 dV \qquad\qquad 1.28$$

Self inductance

The magnetic energy density W of a single circuit carrying current I_1 is used to define the self inductance L_{11} of the circuit:

$$W = \frac{1}{2\mu}\int_V B^2 dV = \frac{1}{2}L_{11}I_1^2 \qquad\qquad 1.29$$

To maintain the current I_1 a power source must, in each second, do an amount of work

$$\varepsilon_1 I_1 = I_1\frac{dN_1}{dt} \qquad\qquad 1.30$$

(because $\varepsilon = dN/dt$) in addition to working against resistance Ω. The stored energy per second in the magnetic field equals dW/dt, so that

$$I_1\frac{dN_1}{dt} = L_{11}I_1\frac{dI_1}{dt} \qquad\qquad 1.31$$

i.e.

$$N_{11} = L_{11}I_1 \qquad\qquad 1.32$$

Therefore we can also define the self inductance of a circuit through the change in flux linking that circuit when the current changes by one unit:

$$\varepsilon_1 = \frac{dN_{11}}{dt} = L_{11}\frac{dI_1}{dt} \qquad\qquad 1.33$$

Poloidal flux

Suppose that a system consists only of toroidally wound loops producing only poloidal fields. In a cylindrical coordinate system R,φ,z shown in *Figure 1.7* (φ is also the 'toroidal' angle in a quasi cylindrical coordinate system) nothing depends on the angle φ. Then

$$M_{12} = 2\pi R_1 \frac{A_2}{I_2} \qquad\qquad 1.34$$

and A has only a toroidal component A_ϕ. In this case the fields are given by (**B** $=\nabla\times$**A**):

$$B_R = -\frac{\partial A_\phi}{\partial z}$$
$$B_\phi = 0 \qquad\qquad 1.35$$
$$B_z = \frac{1}{R}\frac{\partial(RA_\phi)}{\partial R}$$

These poloidal fields are also expressed in terms of the transverse (poloidal) flux function Ψ: Ψ(R,z) = constant defines the form of the equilibrium magnetic surfaces, proved later:

$$\mathbf{B} = \frac{1}{2\pi R}\left(\nabla\Psi\times\mathbf{e}_\phi\right) \qquad\qquad 1.36$$

with $\mathbf{e}_\phi$ a unit vector in the toroidal (φ) direction, so that

$$B_z = \frac{1}{2\pi R}\frac{\partial\Psi}{\partial R}$$
$$B_R = -\frac{1}{2\pi R}\frac{\partial\Psi}{\partial z} \qquad\qquad 1.37$$

But we know that we can write, in terms of the vector potential for our toroidally symmetric system ($\partial/\partial\phi = 0$),

$$B_R = -\frac{\partial A_\phi}{\partial z}$$
$$B_z = \frac{1}{R}\frac{\partial(RA_\phi)}{\partial R} \qquad\qquad 1.38$$

That is, the poloidal flux can be written as (with subscripts implied but not given):

$$\Psi = 2\pi R A_\phi = MI = 2\pi \int_0^R B_z R dR \qquad\qquad 1.39$$

That is, for the system we are considering, the poloidal flux at a position R is simply the vertical field B_z integrated across a circle of radius R. Note that sometimes in the literature the flux function $\psi = \Psi/(2\pi)$ is used.

As an example we show in *Figure 1.10* the poloidal flux ψ produced by a single circular filament (see the section on vector potentials for the derivation of A_ϕ) of radius $R_0 = 1$ m, current $I = 1/\mu_0$. Results are shown in the plane of the coil (z = 0). The exact results are shown as the solid line. Also shown are two approximate solutions; the very near field solution and the far field solution. Near the current ("near field") we can write

$$\psi = R A_\phi \approx \frac{\mu_0 I R_0}{2\pi}\left[\left(\ln\left(\frac{8R_0}{\rho}\right) - 2\right) - \left(\frac{\rho}{R_0}\right)\frac{\cos(\omega)}{2}\left(\ln\left(\frac{8R_0}{\rho}\right) - 1\right)\right] \qquad 1.40$$

The very near field solution is the zero order in ρ/R_0 term, i.e. $\psi_0 = \frac{\mu_0 I R_0}{2\pi}\left(\ln\left(\frac{8R_0}{\rho}\right) - 2\right)$. Far from the loop ("far field") we can write

$$\psi = \frac{MR^2}{\left(R^2 + z^2\right)^{3/2}} \qquad\qquad 1.41$$

We see that neither the very near or far field solutions are good for distances of about half a coil radius from the coil itself. However, if we use the full expansion expression including terms of order ρ/R_0 (Equation 1.40) then the results are very near to the exact solution. This is shown in *Figure 1.11*.
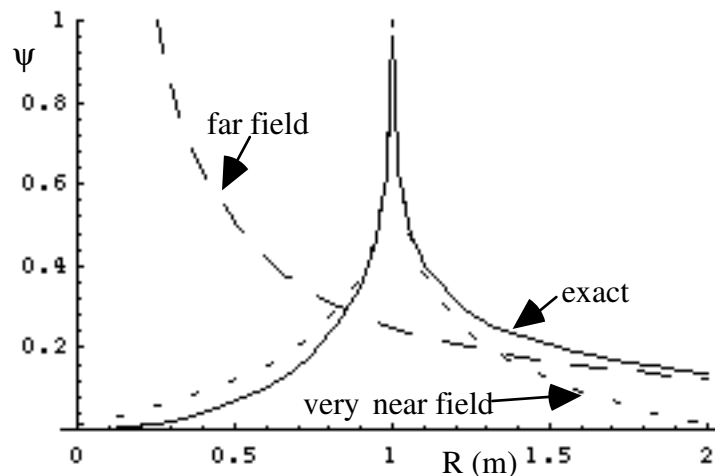
Figure 1.10. The poloidal flux ψ in the plane z = 0 for a circular current loop, radius 1 m, current I = 1/μ_0. The solid line is the exact solution, the long dash line is the far field solution, and the short dash line is the very near field solution (zero order in ρ/R terms only).
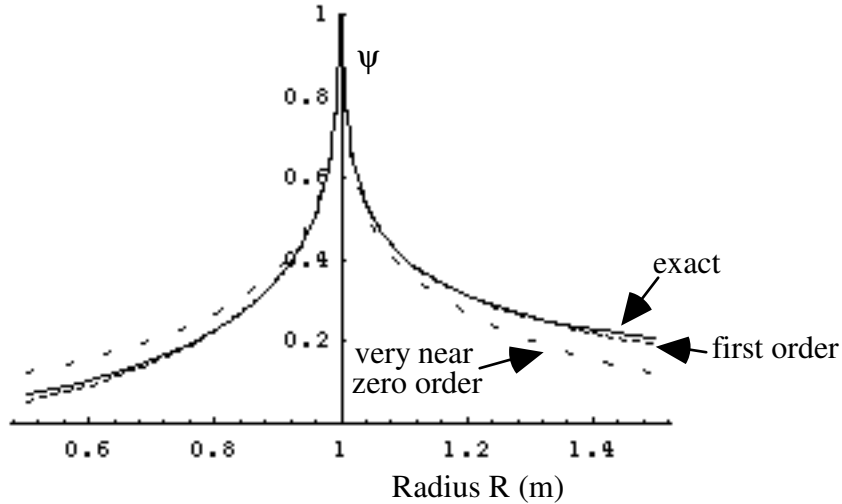
Figure 1.11 The poloidal flux ψ in the plane z = 0 for a circular current loop, radius 1 m, current I = 1/μ_0. The solid line is the exact solution, the short dash line is the first order expansion in ρ/R_0 solution keeping terms of order ρ/R_0, and the long dash line is the very near field solution (zero order in ρ/R terms only).

We can also compare the zero order, first order and exact solutions by plotting contours of ψ in (R,z) space. This is done in *Figure 1.12*, for the conditions described in the caption of *Figure 1.11*. We see that it is very important to include the first order in ρ/R_0 terms; even then the solution contours are significantly different from the exact solution contours. This is very different from the case of the vector potential, where the zero order solution was accurate.
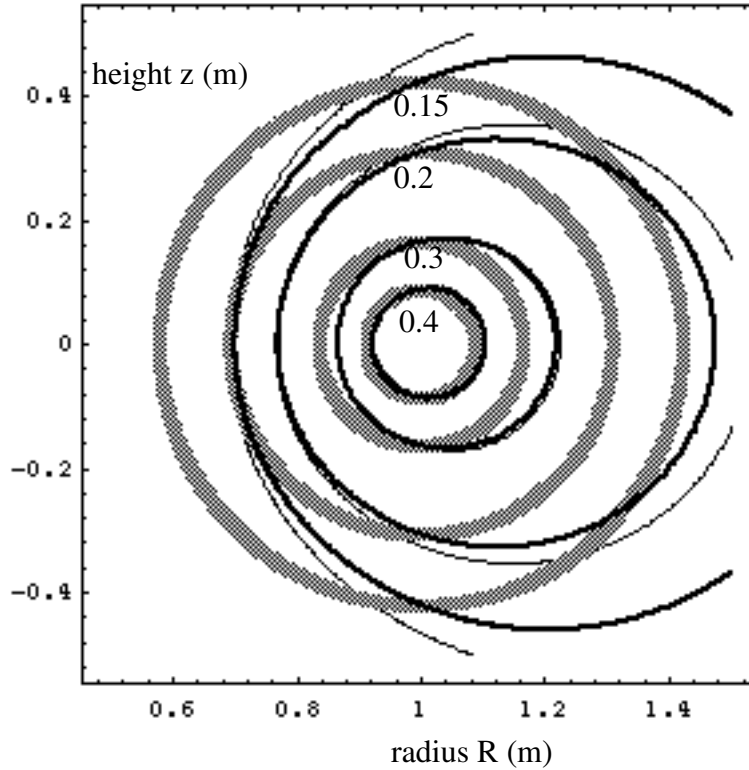
Figure 1.12 Contours of flux ψ from the exact solution (thin dark line), the zero order approximation (thick gray line) and including first order corrections (intermediate thickness dark line) for a circular current filament with current I = 1/μ. Contours of flux equal to 0.15, 0.2, 0.3 and 0.4 are shown.

Field lines and flux surfaces

Before starting on TOKAMAK EQUILIBRIUM, I want to discuss the field line equation, and apply it to a case very similar to a tokamak. The field line equation is

$$\frac{dx}{B_x} = \frac{dy}{B_y} = \frac{dz}{B_z}$$
1.42

or, in cylindrical geometry (the system (R,ϕ,z) of *Figure 1.7*)

$$\frac{dR}{B_R} = \frac{dz}{B_z} = \frac{R B_\phi}{B_\phi}$$
1.43

This is easy to see in two dimensions, as illustrated in *Figure 1.13*.

21

$$\alpha = \ dz/dx = B_z/B_x$$
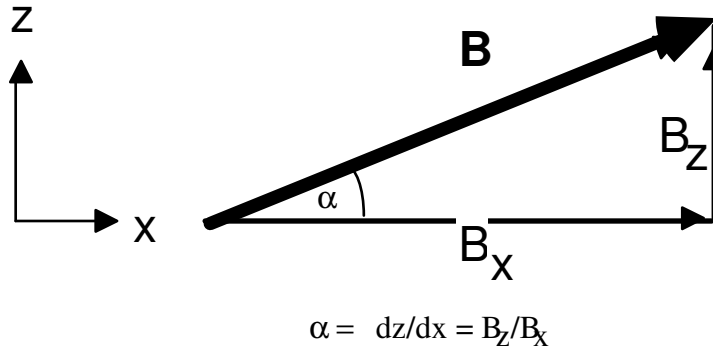
Figure 1.13. A field line made up from two components B_x and B_z.

If the length along a field line is l, then these equations are equivalent to dl/B = constant (B is the magnitude of **B**). Now a magnetic surface is defined by an equation $\psi(R)$ = constant; we use ψ because it will turn out to be the poloidal flux that is constant on a surface. The condition that all lines of magnetic force lie upon that surface $\psi(R)$ is written as

$$\nabla \psi \bullet \mathbf{B} = 0 \qquad\qquad\qquad 1.44$$

because $\nabla\psi$ is the normal to the surface, so the equation says there is no component of B perpendicular to the surface. Now we describe the fields B through the vector potential A, so that

$$B_R = \frac{1}{R}\frac{\partial A_z}{\partial \phi} - \frac{\partial A_\phi}{\partial z}$$

$$B_\phi = \frac{\partial A_R}{\partial z} - \frac{\partial A_z}{\partial R} \qquad\qquad\qquad 1.45$$

$$B_z = \frac{1}{R}\frac{\partial (RA_\phi)}{\partial R} - \frac{1}{R}\frac{\partial A_R}{\partial \phi}$$

For axial symmetry, nothing depends on ϕ (we will also call this toroidal symmetry). Now take

$$\psi(R,z) = RA_\phi \qquad\qquad\qquad 1.46$$

Using Equation 1.45 in 1.46 gives

$$\text{R component:} \frac{\partial(RA_\phi)}{\partial R}\left[\frac{1}{R}\frac{\partial A_z}{\partial \phi} - \frac{\partial A_\phi}{\partial z}\right] = -\left(R\frac{\partial A_\phi}{\partial R} + A_\phi\right)\frac{\partial A_\phi}{\partial z}$$

$$\phi \text{ component:} \frac{1}{R}\frac{\partial(RA_\phi)}{\partial \phi}\left[\frac{\partial A_R}{\partial z} - \frac{\partial A_z}{\partial R}\right] = 0$$

$$z \text{ component}: \frac{\partial(RA_\phi)}{\partial z} \left[\frac{1}{R} \frac{\partial(RA_\phi)}{\partial R} - \frac{1}{R} \frac{\partial A_R}{\partial \phi} \right] = \frac{\partial A_\phi}{\partial z} \left(R \frac{\partial A_\phi}{\partial R} + A_\phi \right) \qquad 1.47$$

where the RHS of each equation represents the result for $\partial/\partial\phi = 0$. Therefore, with the assumed symmetry, the ϕ component is zero and the R component and z component cancel. Therefore our assumed form for the surface (Equation 1.46, $\psi(R,z) = RA_\phi$) ensures that $\nabla \psi \bullet \mathbf{B} = 0$, i.e. it ensures that all field lines lie on that surface where $\psi = RA_\phi$ = constant. In the case of toroidal symmetry the z component of Equation 1.45 gives

$$B_z = \frac{1}{R} \frac{\partial(RA_\phi)}{\partial R} = \frac{1}{R} \frac{\partial(\psi)}{\partial R}$$

$$i.e. \ \psi = \int_0^R B_z R dR = \frac{1}{2\pi} \int_0^R 2\pi B_z R dR \qquad 1.48$$

$$= \frac{1}{2\pi} \int_0^R \int_0^{2\pi} B_z R dR d\phi = \frac{\Psi}{2\pi}$$

where the total poloidal flux Ψ is the integral of the vertical field B_z through the circle we are considering.

An example

I want to consider what the magnetic surfaces look like starting with a single filament in the ϕ direction (a 'toroidal' current), then adding a uniform 'vertical' field in the z direction, and finally adding a filament in the z direction to produce a 'toroidal' field. This is meant to approximate a tokamak equilibrium, but note we are not specifying that the conductors are in equilibrium yet.

Consider a circular filament, as shown in *Figure 1.6*, with current I_ϕ. The field lines lie in a surface (the flux surface) defined by ψ = constant, and we have shown previously that to zero order in the normalized distance ρ/R_0 from the filament

$$\psi = RA_\phi = \frac{\mu_0 I_\phi R_0}{2\pi} \left(\ln\left(\frac{8R_0}{\rho} \right) - 2 \right) = \text{constant} \qquad 1.49$$

where

$$\rho^2 = (R_0 - R)^2 + z^2 \qquad 1.50$$

i.e. the magnetic surfaces are described by circles with ρ = constant.

Far away from the loop we have shown that the field looks like that due to a dipole with moment M:

$$M = \pi R_0^2 I_\phi. \qquad\qquad 1.51$$

Then the equation for the magnetic surfaces becomes

$$\psi = \frac{MR^2}{\left(R^2 + z^2\right)^{\frac{3}{2}}} = \text{constant} \qquad\qquad 1.52$$

Now we add a uniform field B_{z0} in the z direction. This has a vector potential given by

$$A_{\phi 0} = \frac{B_{z0}R}{2} \qquad\qquad 1.53$$

The magnetic surfaces are now given by

$$R\left(A_\phi + A_{\phi 0}\right) = \text{constant} \qquad\qquad 1.54$$

Finally we add a filament up the z axis, which produces a field $\propto 1/R$ in the ϕ direction (a 'toroidal' field. The vector potential due to this filament is

$$A_z = -\frac{\mu_0 I_z}{2\pi}\ln(R) \qquad\qquad 1.55$$

Because this has only a z component, it does not affect the result (Equation 1.54). The results are shown in *Figure 1.14* and *Figure 1.15* for a vertical field (the form used is relevant to that required to maintain a circular tokamak in equilibrium)

$$B_z = \frac{\pm\mu_0 I_\phi}{4\pi R_0}\left(\ln\left(\frac{8R_0}{a}\right) + \Lambda - \frac{1}{2}\right) \qquad\qquad 1.56$$

with $\Lambda = 2$, $R_0 = 1$ m, and a = 0.2 m. In the figures the exact form for A_ϕ from the circular current filament (written in terms of elliptic integrals) is actually used. The positive current I_ϕ produces a field downwards (in the -z direction) at the outer equator (z = 0, R > 1 m). Adding a positive vertical field B_z cancels this field at some point, producing a point where $B_z(z=0) = 0$. This is called an X point; the flux surface through this point is called the separatrix. Note that, with the negative uniform vertical field applied, there is no inner X point. However, if a vertical

field $\propto 1/R$ was applied the more negative B_z at the inner equator would cancel the positive B_z from the filament, and an X point would appear
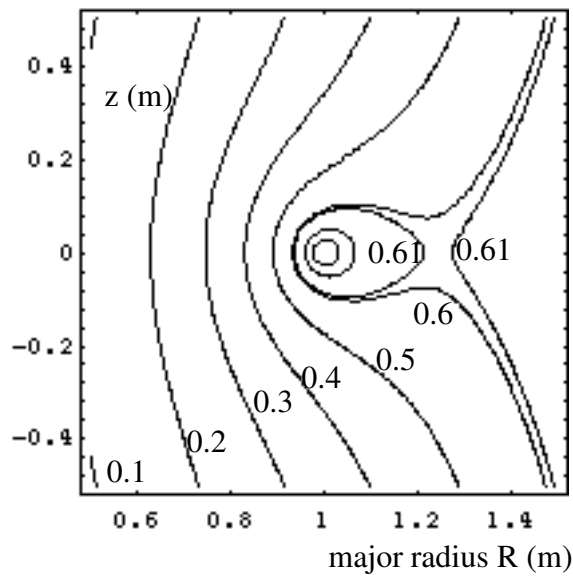
Figure 1.14. Contours of constant flux ψ, with positive B_z.
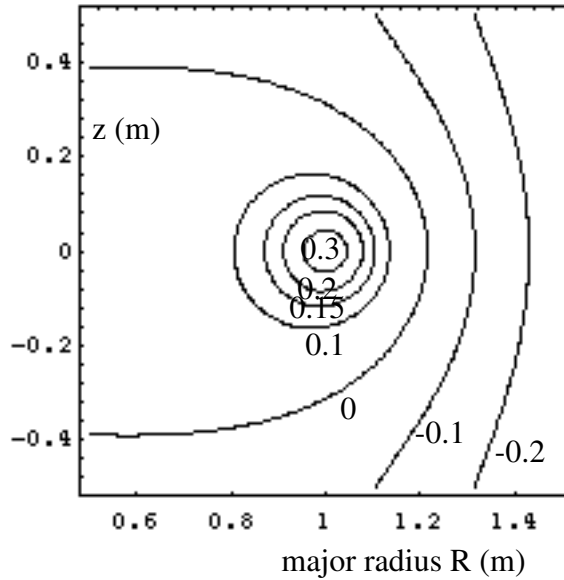
Figure 1.15. Contours of constant flux ψ, with negative B_z.
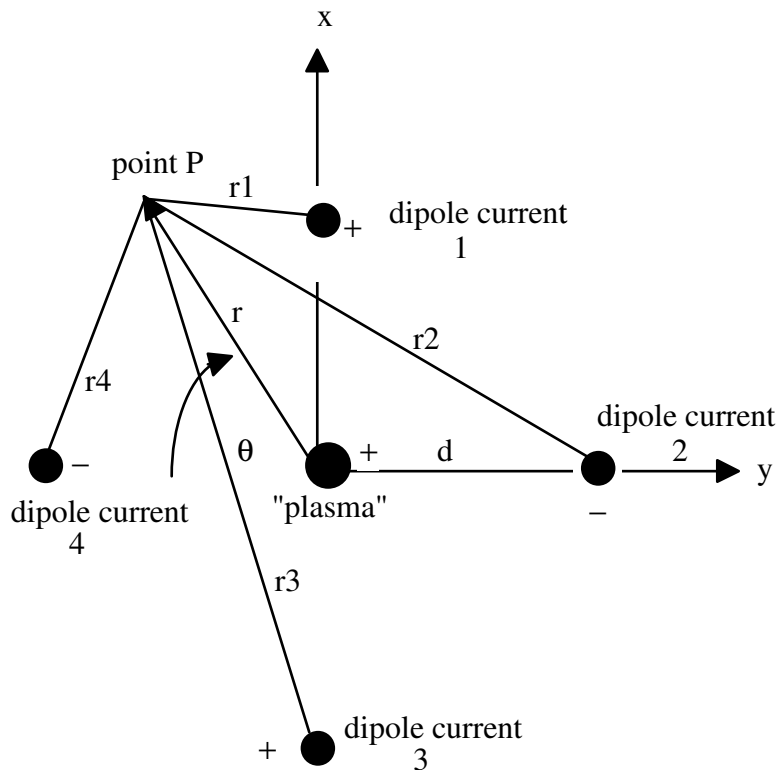
Figure 1.16. The geometry used for calculating the flux surfaces of a straight filament in a quadrupole field. z is into the plane of the figure.

For a second example, consider the field lines and flux surfaces resulting from a quadrupole field applied to a single filamentary current, in straight geometry. In a straight system the field lines will lie in a surface defined by constant vector potential A (i.e. ψ constant, with $R \Rightarrow \infty$). The single ("plasma") filament of current I_{zp} lies at the origin of a rectalinear coordinate system (x,y,z) shown in *Figure 1.16*, where z will approximate the toroidal direction in a toroidal system. The vector potential at P is given by Equation 1.55 as $A_{zp} = -\dfrac{\mu_0 I_{zp}}{2\pi} \ln(r)$, with r the radius from the plasma filament to a point P. There are then four additional filaments, at a distance d from the plasma filament, with currents I_{zq} alternatingly + (into the plane) and - (out of the plane). The ith additional filament (i = 1 to 4) has a vector potential $A_{zqi} = -\dfrac{\mu_0 I_{zq}}{2\pi} \ln(r_i)$ in its own local coordinate system. Transforming to the coordinate system (r,θ) we obtain

$$A_z = \frac{-\mu_0 I_{zp}}{2\pi} \ln(r) + \frac{\mu_0 I_{zq}}{2\pi} \begin{bmatrix} \ln\left(d^2 + r^2 - 2dr\cos(\theta)\right)^{1/2} \\ + \ln\left(d^2 + r^2 + 2dr\cos(\theta)\right)^{1/2} \\ - \ln\left(d^2 + r^2 - 2dr\sin(\theta)\right)^{1/2} \\ - \ln\left(d^2 + r^2 + 2dr\sin(\theta)\right)^{1/2} \end{bmatrix} \qquad 1.57$$

The resulting contours of constant A_z are shown in *Figures 1.17a* through *1.17d* for the ratio I_{zq}/I_{zp} = 1.0 to 2.0. In the examples d = 0.25 m. The equi-distant contours shown are different from frame to frame. Clearly approximately elliptic cross sections are obtained; in tokamaks elliptic surfaces are produced by applying quadrupole fields. A separatrix appears and defines the last closed vector potential surface (a straight circular system is the only one without a separatrix).

We can derive an analytic expression for the shape of a given flux surface. By expanding Equation 1.57 to third order in r/d, we find

$$A_z = -\frac{\mu_0 I_{zp}}{2\pi} \ln(r) - \left(\frac{r}{d}\right)^2 \frac{\mu_0 I_{zq} \cos(2\theta)}{\pi} \qquad 1.58$$

With $I_{zq} = 0$ the surfaces are described by r = constant = a, i.e. a circle. If we assume the surfaces with $I_{zq} \neq 0$ are described by

$$r = a + \Delta_2 \cos(2\theta) \qquad 1.59$$
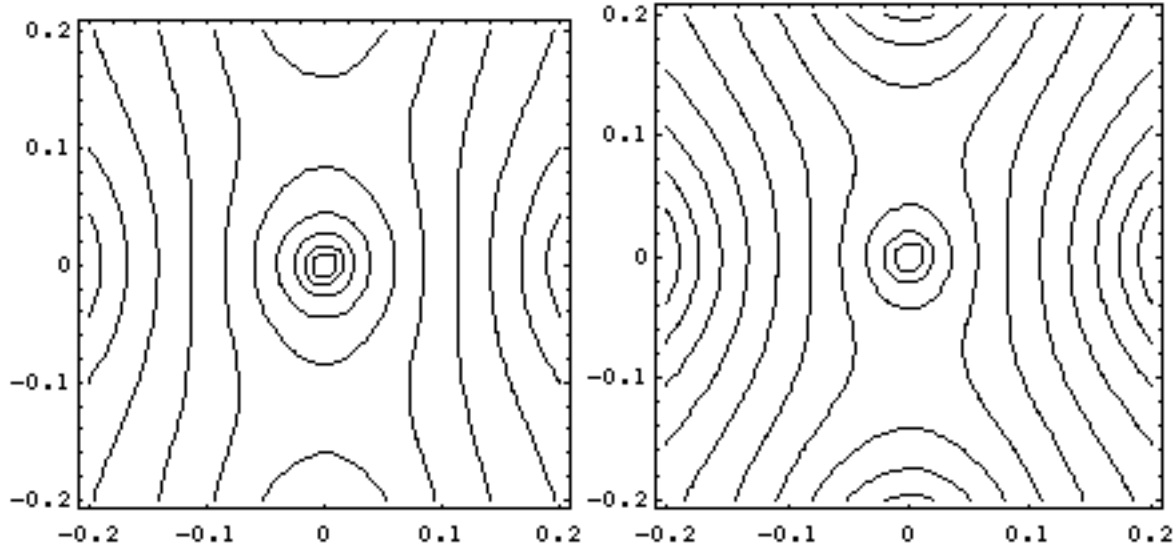
Figure 1.17a. Vector potential contours with $I_{zq}/I_{zp} = 1$. The quadrupole filaments are at ± 0.25 m.

Figure 1.17a. Vector potential contours with $I_{zq}/I_{zp} = 2$. The quadrupole filaments are at ± 0.25 m.

then Equation 1.58 gives, after expanding in Δ/a,

$$-A_z = \frac{\mu_0 I_{zp}}{2\pi}\ln(a) + \left(\frac{\Delta}{a}\right)\frac{\mu_0 I_{zp}}{2\pi}\cos(2\theta) + \left(\frac{a}{d}\right)^2\frac{\mu_0 I_{zq}\cos(2\theta)}{\pi} + \left(\frac{a}{d}\right)^2\left(\frac{\Delta}{a}\right)\frac{2\mu_0 I_{zq}\cos^2(2\theta)}{\pi}$$

$$1.60$$

For $a/d \ll 1$, $\Delta/a \ll 1$ we can ignore the last term ($\propto \cos^2(2\theta)$). Then we ensure that $A_z = const = -\dfrac{\mu_0 I_{zp}}{2\pi}\ln(a)$ by setting the coefficient in front of the $\cos(2\theta)$ to zero, i.e.

$$\frac{\Delta}{a} = 2\left(\frac{I_{zq}}{I_{zp}}\right)\left(\frac{a}{d}\right)^2$$

$$1.61$$

The elongation of the surface is then

$$\frac{height}{width} = \frac{1 + 2\left(\dfrac{I_{zq}}{I_{zp}}\right)\left(\dfrac{a}{d}\right)^2}{1 - 2\left(\dfrac{I_{zq}}{I_{zp}}\right)\left(\dfrac{a}{d}\right)^2} \approx 1 + 4\left(\frac{I_{zq}}{I_{zp}}\right)\left(\frac{a}{d}\right)^2$$

$$1.62$$

Figure 1.18a and *18b* show the computed distortion to a particular surface (A = constant) for d = 0.25, I_{zq}/I_{zp} = 0 and 2.0. With I_{zq}/I_{zp} = 1.0 the value of height to width is measured to be 1.28, as compared to the value of 1.25 derived from Equation 1.62.
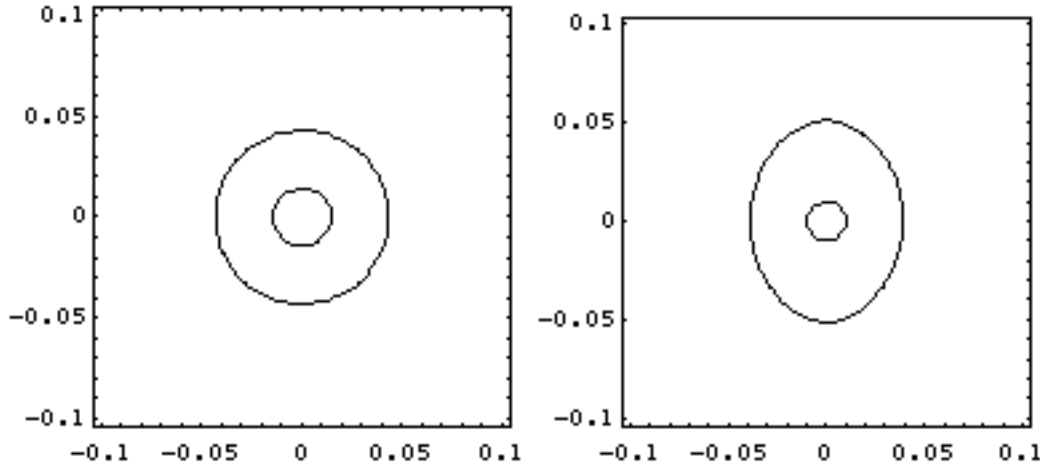
Figure 1.18a. Contours of vector potential with I_{zq}/I_{zp} = 0. The larger contour is taken as a reference in determining the distortion produced by an applied quadrupole field.

Figure 1.18b Contours of vector potential with I_{zq}/I_{zp} = 2. The contours have the same flux values as those shown in *Figure 1.18a*.

Circuit equations

For some applications we will consider the plasma as a lumped series resistance and inductance, coupled to other circuits (including a conducting vacuum vessel) by mutual inductances. *Figure 1.19* shows how this is represented.

The equation for circuit l consisting of a series self inductance L_{ll} and resistance Ω_l, coupled by mutual inductances M_{li} to other circuits i, is

$$1.63$$

The sum over the mutual inductances is for i $\neq$ l because M_{ll} = L_{ll} is brought out separately. If the circuit is closed (short circuited), then ε_l = 0. If the circuit is open, or connected to a high input impedance, then I_l = 0 and ε_l = d/dt($\Sigma M_{l,i}I_i$). The plasma is sometimes represented as one series inductance-resistance circuit, or sometimes as a number of such circuits in parallel, all short circuited together. The vacuum vessel is similarly represented as a number of paralleled resistor-inductor circuits, which can be open circuit (a vessel with an insulating gap) or short

circuited (no insulating gap). For a perfectly conducting plasma the plasma series resistance elements are set to zero, so that the flux enclosed by the plasma loop is conserved. These models are very useful in analyzing axisymmetric stability problems.
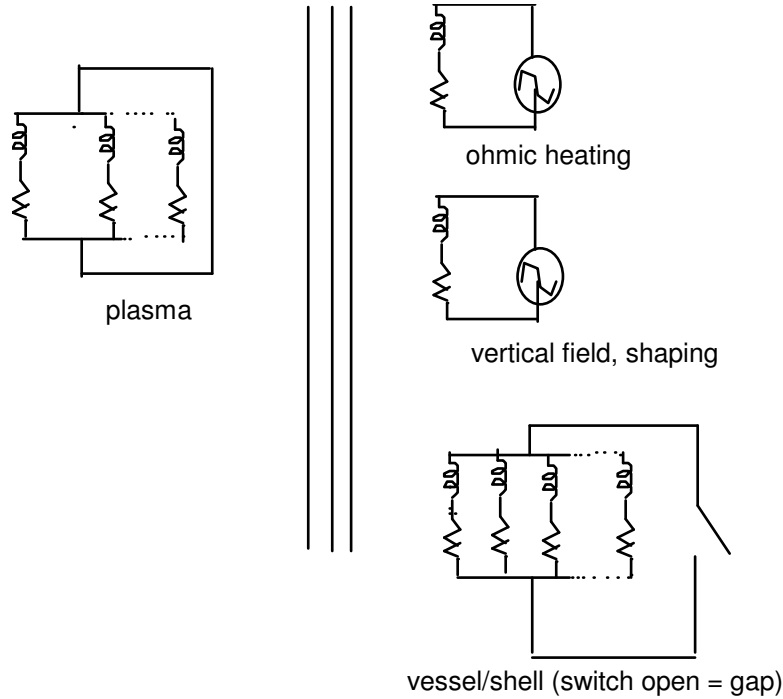
Figure 1.19. Representation of circuits coupling to a plasma.

2. SOME NON STANDARD MEASUREMENT TECHNIQUES

Hall Probe

Other techniques (than pick-up coils) are used to measure magnetic fields. The most common alternative is a Hall probe, shown in *Figure* 2.1. A semiconductor is placed in a field B, and a current I driven perpendicular to B. The current carriers experience a Lorentz force, producing a charge buildup in the direction perpendicular to both B and I. The resulting charge buildup produces an electric field which cancels the magnetic force. This electric field is measured by electrodes. This was iscovered in 1879 in Johns Hopkin University.

Drive j. Charge build up perpendicular to B and j. Measure E.
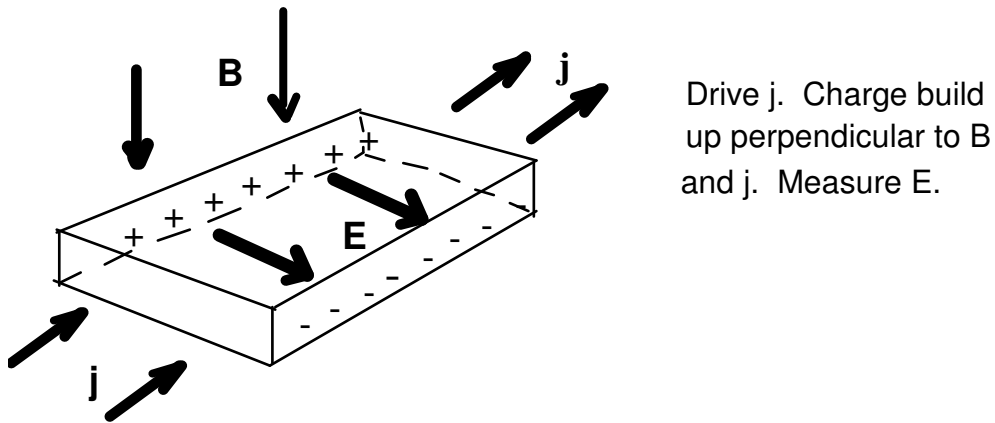
*Figure2.1*a. A Hall probe.
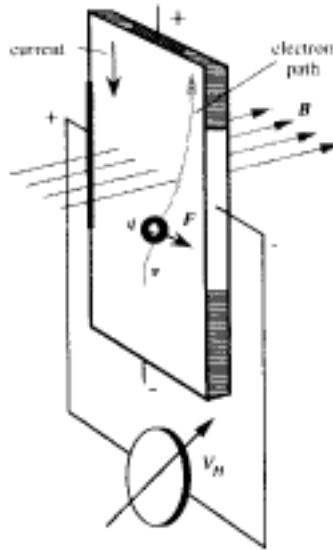
Figure 2.1b. A Hall probe in use

Assume the electrons move inside a flat conductive strip in a magnetic field. Then the output voltage is:

$$V_H = hiB\sin(\alpha) \qquad\qquad 2.1$$

Where i is current, h is efficiency which depends on geometry, temperature, area. Theoretically the overall efficiency depends on the Hall coefficient, the transverse electric potential gradient per unit B field per unit current density.
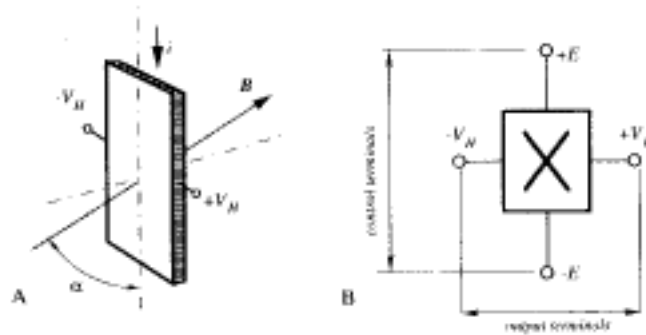
Figure 2.1c. A Hall probe at and angle to the field

Specific problems include: susceptibility to mechanical stress, and temperature (of resistors).

Faraday Effect

It has also been proposed to use the magneto-optic effect (the Faraday effect) in fused silica single mode optical fibers to measure magnetic fields, and the electro-optic (Kerr) effect to measure electric fields. The Faraday effect is the consequence of circular birefringence caused by a longitudinal magnetic field. Circular birefringence causes a rotation F of the plane of linearly polarized light, given by

$$F = V_c \oint_l \mathbf{H} \bullet d\mathbf{l} \qquad\qquad 2.2$$

around a contour l. No time integration is required. The Verdet constant $V_c \approx 5 \times 10^{-6}$ radA^{-1} for silica. Thus the rotation must be now measured. Another approach is to coat a fiber with magnetostrictive material and measure the strain effects, with the fiber as one arm of a Mach Zender interferometer.

The Compass.

Chinese 2634 BC, magnetite suspended on silk.

Flux gates

This is intended for weak fields. A B-H curve below is shown below.
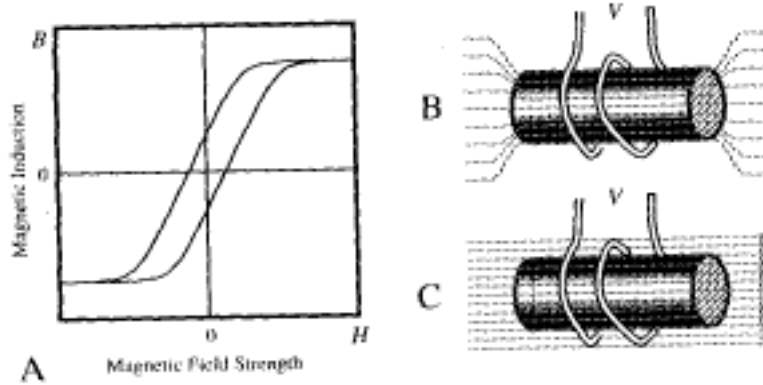
Figure 2.3 a A simple flux gate and the B-H curve

An applied field H to the core induces a magnetic flux $B = mH$. For high B the material saturates and μ is very small. There is hysterisis, and the path is different for increasing and decreasing H. When the core is not saturated the core acts as a low impedance path to lines of magnetic flux in the surrounding space. When the core is saturated the magnetic field lines are no more affected by the core. Each time the core passes from saturated to unsaturated and backwards, there is a change to the magnetic field lines. A pickup coil around the core will generate a spike. Flux lines drawn out of core implies positive spike, lines drawn into core, a negative spike. The amplitude of the spike is proportional to the intensity of the flux vector parallel to the sensing coil. The pulse polarity gives the field direction.

The core must be driven in and out of saturation by a second coil. The excitation current will induce a corresponding current in the sensor coil, but this can be allowed for.
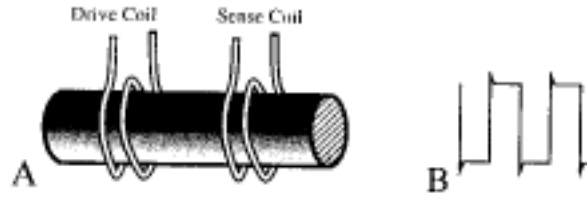
Figure 2.3b. A driven flux gate

A better approach is to position the excitation coil so that it will excite without affecting the sensor coil. i.e. excite the flux at right angles to the axis of the sensor coil. One can use a toroidal core with a drive winding and a cylindrical sensor coil..
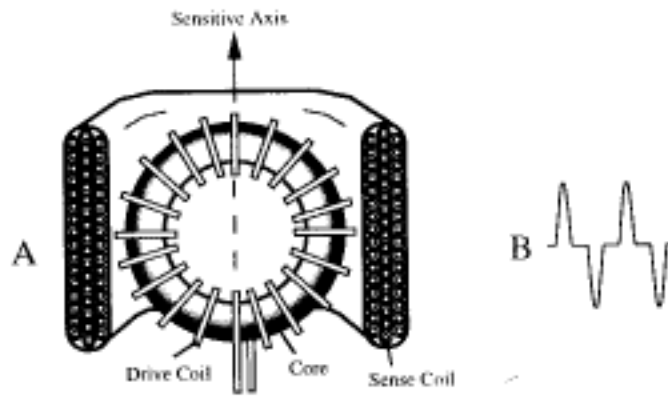
Figure 2.3c: A flux gate with toroidal core with a drive winding and a cylindrical sensor coil

3. GENERAL FIELD CHARACTERIZATION

Fourier components

Suppose we want to characterize the tangential (subscript τ) and normal (subscript n) fields on a circular contour of radius a_l. It is often convenient to express the results as a Fourier series: for the poloidal (θ) and radial (ρ) fields outside a current I we can write

$$B_\omega = B_\tau = \frac{\mu_0 I}{2\pi a_l}\left[1 + \sum_n \lambda_n \cos(n\omega) + \delta_n \sin(n\omega) \right] \qquad\qquad 3.1$$

$$B_\rho = B_n = \frac{\mu_0 I}{2\pi a_l}\left[\sum_n \kappa_n \cos(n\omega) + \mu_n \sin(n\omega) \right] \qquad\qquad 3.2$$

We are working in a coordinate system ρ, ω, ϕ, centered on the contour center-see *Figure 3.1*. Note that it is not uncommon to use a left handed coordinate system.
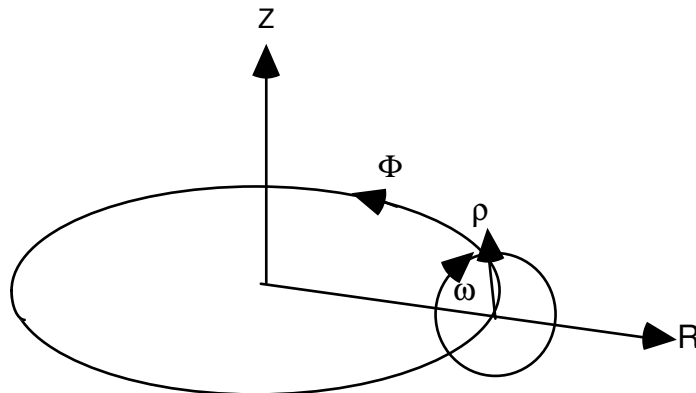
Figure 3.1. Coordinates.

We can measure the components either by performing a Fourier analysis of the data from a set of individual coils measuring $B_n(\omega)$, $B_\tau(\omega)$, or we can construct integral coils which will do the job directly. For example, a "modified Rogowski coil", or "cosine coil", whose winding density (number of turns per unit length) $n_A = n_0\cos(n\omega)$, each turn of area A, will give a signal which, when time integrated, is proportional only to λ_n:

$$\varepsilon = -\frac{d}{dt}\int_S (\mathbf{B}\bullet\mathbf{n}_s dS) = -\frac{d}{dt}\left\{\int_0^{2\pi}(B_\omega(\omega)n_A(\omega)a_l Ad\omega)\right\}$$

$$= -\frac{\mu_0 A n_0}{2\pi}\frac{d}{dt}\left\{I\int_0^{2\pi}\left[\cos(n\omega)\left(1+\sum_n\lambda_n\sin(n\omega)+\mu_n\cos(n\omega)\right)\right]d\omega\right\} \qquad 3.3$$

$$= -\frac{\mu_0 A n_0}{2}\frac{d}{dt}\{I\lambda_n\}$$

The elemental area $dS = n_A A dl$, the unit length $dl = a_l d\omega$, and n_s is the unit normal to the coil area. That is, the only contribution to the space integral comes from the term $\cos^2(n\omega)$, because $\int_0^{2\pi}\cos(n\omega)\cos(m\omega)d\omega = \pi$ if $m = n$, otherwise $= 0$. If the winding density is proportional to $\sin(n\omega)$, the time integrated output is proportional to δ_n. To obtain the coefficients μ_n and κ_n, we must wind a "saddle coil" with n_w turns of width w varying as $\sin(n\omega)$ or $\cos(n\omega)$, so that for a "sin" saddle coil $w(\omega) = w_0\cos(\omega)$, and

$$\varepsilon = -\frac{d}{dt}\left\{\int(B(\omega)n_w w(\omega)a_l d\omega)\right\}$$

$$= -\frac{\mu_0 w_0 n_w}{2}\frac{d}{dt}\{I\mu_n\} \qquad 3.4$$

In this case the elemental area $dS = n_w w dl = n_w w a_l d\omega$, the time integrated output provides the coefficient μ. *Figure 3.2* shows a cosine coil which measures λ_1. Although it is not illustrated, a center return wound inside the Rogowski coil should be used. *Figure 3.3* shows an unfolded "sin saddle coil" measuring μ_1. Of course, we cold also use an array of coils placed on a contour, measuring independent B_τ and B_n at different positions (different ω) and construct the required integrals.
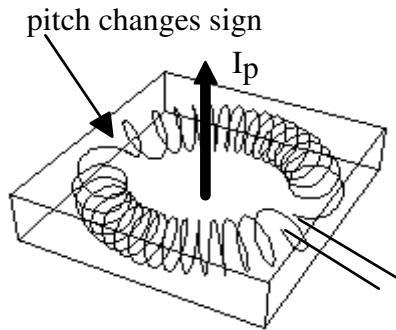
Figure 3.2. A modified Rogowski coil.   Figure 3.3. A saddle coil.
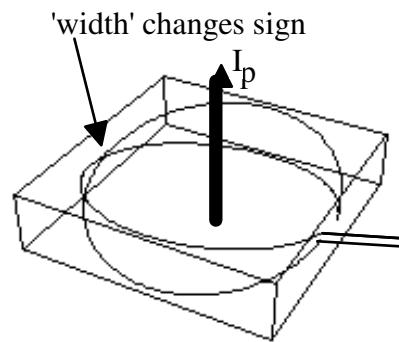
Field components on a rectangle

If we want to characterize the fields on a rectangular contour, we can make use of the fact that an arbitrary function in a plane can be expressed as

$$B(\eta,\xi) = \sum_{m,p} c_{m,p} \xi^m \eta^p \qquad\qquad 3.5$$

with $c_{m,p}$ constant coefficients. Here we are working in a rectalinear coordinate system ξ, η, centered on the contour center, at $R = R_l$, shown in *Figure 3.4*.
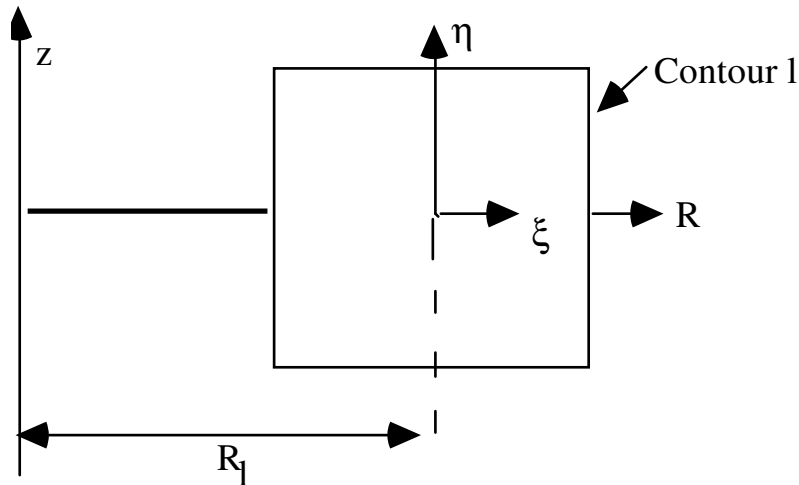
Figure 3.4. The geometry used in describing fields on a rectangle or square.

On a one dimensional contour there will be degeneracy. Suppose we have a "modified Rogowski" coil whose winding density varies as some function $f_p(\eta,\xi)$, so that the time integrated output is proportional to

$$s_{p,\tau} = \oint_l f_p B_\tau dl \qquad\qquad 3.6$$

The subscript τ refers to the tangential (normal) field component on the contour. We could also construct the signal $s_{p,\tau}$ from individual measurements of B_τ around the contour.   Further suppose that we express the tangential field itself in terms of our functions f as

$$B_\tau = \sum_m c_m f_m \qquad\qquad 3.7$$

Then we can write

$$s_{p,\tau} = \sum_m c_m \oint_l f_m f_p \, dl \qquad\qquad 3.8$$

i.e. if we can calculate $\int_l f_m f_p dl$ for our chosen functions f, then we can express the coefficients c_m through the measured parameters $s_{p,\tau}$. In a similar way we can build a saddle coil of width f_p whose time integrated output is then

$$s_{p,n} = \oint_l f_p B_n \, dl \qquad\qquad 3.9$$

Expressing the normal field as

$$B_n = \sum_m d_m f_m \qquad\qquad 3.10$$

we have

$$s_{p,n} = \sum_m d_m \oint_l f_m f_p \, dl \qquad\qquad 3.11$$

Again, assuming we can calculate $\int_l f_m f_p dl$, the coefficients d_m can be expressed in terms of the measured $s_{p,n}$.

We still have to choose the functions f_p. One choice, which is used in 'multipole moments', discussed later, is ρ^p, the pth power of a vector radius on the contour l. This can be expressed in the form of a complex number as

$$\rho = \xi + i\eta \qquad\qquad 3.12$$

e.g. for p = 2 we have

$$\rho^2 = \xi^2 - \eta^2 + i(\xi\eta) \qquad\qquad 3.13$$

If the contour chosen is a square of half width and height a, then this form for the functions f gives

$$\oint_l f_m f_p \, dl = 4a^{(m+p)} \left[\frac{a}{m+1} + \frac{a}{p+1} \right] \text{ if m and p are even} \qquad\qquad 3.14$$

$$\oint_l f_m f_p \, dl = 0 = 0 \text{ otherwise} \qquad\qquad 3.15$$

Then we would have the output from the 'modified Rogowski' coil

$$s_{p,\tau} = \sum_m c_m \oint_l f_m f_p \, dl$$

$$= \sum_m c_m 4a^{(m+p)} \left[\frac{a}{m+1} + \frac{a}{p+1} \right] \quad \text{for m, p even} \qquad\qquad 3.16$$

$$= 0 \quad \text{otherwise} \qquad\qquad 3.17$$

Equations 3.16 and 3.17 show specifically how, by including a finite number of terms (say p_{max} = m_{max} = 5) we will end up with a set of linear equations relating the measured signals to the required constants c_m. We must now solve them to obtain the coefficients c_m as functions of the measured $s_{p,\tau}$; a similar procedure provides the d_m as functions of the signals $s_{p,n}$. The result is not as elegant as the Fourier analysis applicable on a circular contour, where a single coil can be wound to measure each individual Fourier coefficient, but I don't know another way to represent the fields on a square contour. Of course, instead of using these specially wound coils to measure $s_{p,\tau}$ and $s_{p,n}$ directly, the required integrals can always be constructed from individual coil signals of B_τ and B_n around the contour l.

An example of a saddle coil for a particular $f = \eta(1+\xi/R_l)$ is shown in *Figure 3.5*. Here R_l is the major radius of the contour center. These strange looking coils are actually useful for helping determine plasma position
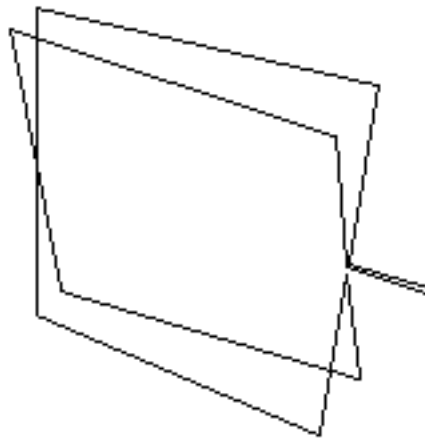
Figure 3.5. A saddle coil suitable for winding on a square vessel

4. PLASMA CURRENT

Rogowski coil

The plasma current is measured by a "Rogowski coil", which is a multi turn solenoid completely enclosing the current to be measured. *Figure 4.1* shows an example, the placement of this coil around the plasma is shown in *Figure 4.2*. The transient plasma current generates a voltage ε which, for a uniform winding density of n_A turns per unit length of area A, is (after applying Faraday's Law)

$$\varepsilon = n_A A \mu_0 \frac{dI}{dt} \qquad\qquad\qquad 4.1$$

from which I_p is deduced after time integration. This is just a special case of our general model for how to measure the fields on a contour. Integration can be performed passively with a resistance-capacitance circuit, with active integrators, or numerically on a computer. In each case there is an associated 'integration time constant' τ_{int}. The Rogowski coil must not be sensitive to other than the wanted field components, so that a center return must be used. The angle between the Rogowski coil and the enclosed current is irrelevant, as is the contour on which the coil is wound.
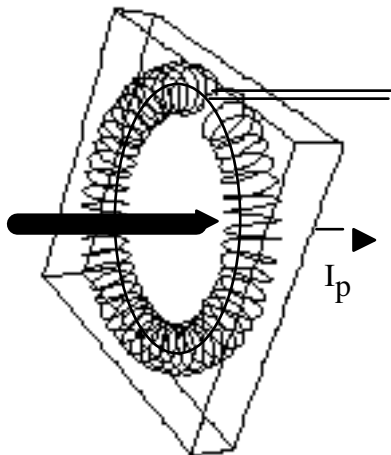
Figure 4.1. A Rogowski coil
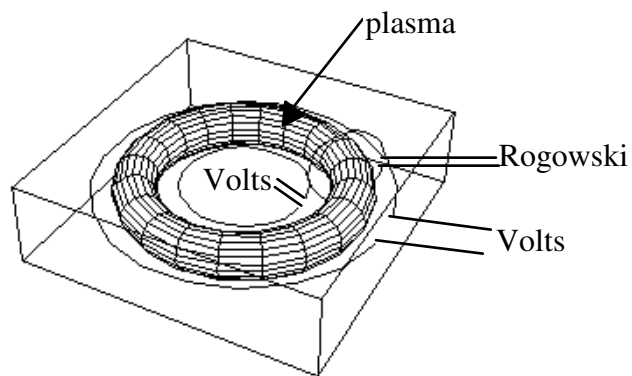
Figure 4.2. Coil placement around plasma

5. LOOP VOLTS, VOLTS per TURN, SURFACE VOLTAGE.

Introduction

The Loop Volts ε_l, also called the Volts per Turn or Surface Voltage, is used in calculating the Ohmic power input to the plasma. It also allows a calculation of the plasma resistivity Ω_p. ε_l is also a useful measure of cleanliness: clean ohmic heated tokamaks usually have $\varepsilon_l \sim 1.5V$.

What we want to measure is the resistive voltage drop across or around a plasma. In a linear machine, this simply done by measuring the potential across the end electrodes with a resistive potential divider. A similar method can be used in a torus with a conducting vacuum vessel which has one or more insulating sections. In an all metal torus the voltage induced in a single turn pickup coil (a volts per turn loop) wound close to the plasma is used, as shown in *Figure 5.1*. However, the interpretation of the output signal is not trivial. Here I want to address two questions. The first is "What does a toroidal loop as shown in *Figure 5.1* tell me?". The second is, "How do I measure the Ohmic power input into a plasma?".

The single volts per turn loop

The voltage across the toroidally wound volts per turn loop (subscript l) is given by:

$$\varepsilon_l = \frac{d}{dt}\left(L_{l,l}I_l\right) + \Omega_l I_l + \sum_j \frac{d}{dt}\left(M_{l,j}I_j\right) + \frac{d}{dt}\left(M_{l,p}I_p\right)$$

5.1

Here subscript j refers to all fixed windings, such as the Ohmic heating, the vertical field, and the shaping winding. The plasma current contribution (subscript p) is brought out separately. We can arrange for the voltage of the loop to be measured with a high input resistance amplifier. Then $I_l \approx 0$, so that the first two terms on the RHS are zero, and

$$\varepsilon_l = \sum_j \frac{d}{dt}\left(M_{l,j}I_j\right) + \frac{d}{dt}\left(M_{l,p}I_p\right)$$

5.2

If this signal is time integrated, then the result is exactly the poloidal flux Ψ, because

$$\varepsilon = \frac{d}{dt}\int_S \left(\mathbf{B}\bullet \mathbf{n}_s dS\right) = \frac{d}{dt}\iint_{R,\phi}\left(B_z R dR d\phi\right)$$
$$= \frac{d}{dt}2\pi\int_0^R B_z R dR = \frac{d\Psi}{dt}$$

5.3

Now consider the voltage ε_p around the plasma. It is connected on itself (a torus) so that:

$$\varepsilon_p = 0 = \frac{d}{dt}\left(L_{p,p}I_p\right) + \mathbf{\Omega}_p I_p + \sum_j \frac{d}{dt}\left(M_{p,j}I_j\right) \qquad 5.4$$

Now remembering the definition of mutual inductance in terms of linked fluxes, we can always write the flux through circuit i due to current I_j in circuit j as the flux through another circuit k due to the current I_j in circuit j plus the incremental flux between the circuits k and i due to the current I_j in circuit j, $\Delta\Psi_{k,i;j}$. Then

$$M_{i,j}I_j = M_{k,j}I_j + \mathbf{\Delta\Psi}_{k,i;j} = M_{j,k}I_j + \mathbf{\Delta\Psi}_{k,i;j} \qquad 5.5$$

Then for example $M_{l,oh}I_{oh} = M_{p,oh}I_{oh} + \Delta\Psi_{p,l;oh}$

Thus we can write

$$\varepsilon_l = \frac{d}{dt}\sum_j\left(M_{p,j}I_j\right) + \frac{d}{dt}\left(M_{l,p}I_p\right) + \frac{d}{dt}\sum_j\left(\mathbf{\Delta\Psi}_{p,l;j}\right) \qquad 5.6$$

Substituting from Equation 5.4 gives

$$\varepsilon_l = -\frac{d}{dt}\left(L_{p,p}I_p\right) - \mathbf{\Omega}_p I_p + \frac{d}{dt}\left(\mathbf{\Psi}_{plasma-loop}\right) \qquad 5.7$$

where $\Delta\Psi_{plasma-loop}$ is now the <u>total</u> flux between the loop and the plasma, provided by all circuits, <u>including the plasma</u> (plasma, ohmic heating, vertical field, shaping). If the plasma current is constant the volts per turn loop tells us the plasma resistance. A more elegant approach to seeing this is to use Poynting's theorem.

Poynting's theorem

Consider a number of non integrated flux loops, i.e. volts per turn loops, measuring $d\Psi/dt$, all placed around the plasma on some contour l, which might be the vacuum vessel. *Figure 5.1* shows the configuration. Note that the emf $\varepsilon = -2\pi RE_\phi$ will not necessarily be the same in each loop, because the contour l is not necessarily on a magnetic surface.

volts per turn

contour

plasma
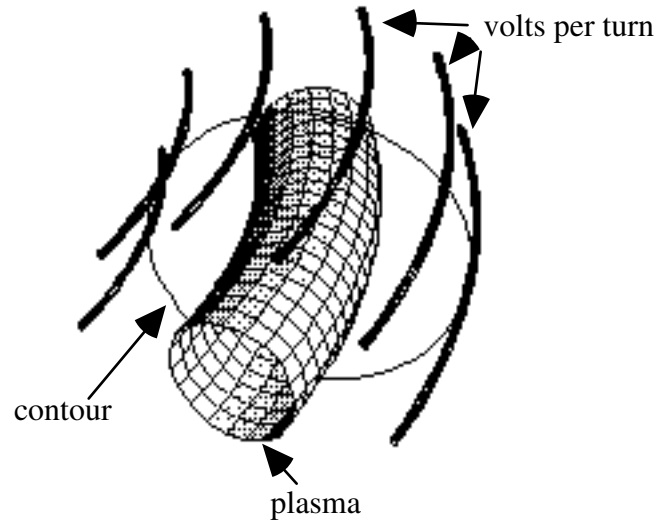
Figure 5.1. A subset of volts per turn coils on a contour l.

To interpret what we are measuring, notice that the poloidal (subscript p) and toroidal fields are not coupled in Maxwell's equations, so that we can write Poynting's theorem for the poloidal fields alone. To remind you, the basic equations needed are

$$\nabla \times \mathbf{B} = \mu \mathbf{j} \qquad\qquad 5.8$$

$$\nabla \times \mathbf{E} = -\frac{\partial \mathbf{B}}{\partial t} \qquad\qquad 5.9$$

Multiplying these by -$\mathbf{E}$ and $\mathbf{B}/\mu$ respectively, adding, and writing the poloidal component, gives (ϕ is the direction the long way around the plasma)

$$\frac{\partial}{\partial t}\left(\frac{B_p^2}{2\mu_0}\right) + \nabla \bullet \left(\mathbf{E} \times \frac{\mathbf{B}_p}{\mu_0}\right) + j_\phi E_\phi = 0 \qquad\qquad 5.10$$

Integrating over the volume V defined by rotating the contour l in the ϕ direction gives

$$\frac{\partial}{\partial t}\left(\frac{L_i I_p^2}{2}\right) + \int_V j_\phi E_\phi dV = \oint_l \varepsilon B_\tau dl \qquad\qquad 5.11$$

Here we have used $\int_V \nabla \bullet (\mathbf{E} \times \mathbf{B}_p) dV = \int_S (\mathbf{E}_\phi \times \mathbf{B}_p) \bullet d\mathbf{S}_\phi = \int_S 2\pi R E_\phi B_p dl$. L_i is defined by $(L_i I_p{}^2)/2$

$= \int (B_p{}^2/(2\mu_0))dV$. Note the integration is to the contour l, not the plasma edge. Therefore the inductance is not just that internal to the plasma, which is usually called l_i. Now use Ohms law $\mathbf{j} \cdot \mathbf{B} = \sigma_\parallel \mathbf{E} \cdot \mathbf{B}$, and assuming $|B_{\phi 0} - B_\phi| \ll B_{\phi 0}$ gives $E_\phi = j_\phi/\sigma_\parallel$. Therefore

$$\frac{\partial}{\partial t}\left(\frac{L_i I_p^2}{2}\right) + \int_V \frac{j_\phi^2}{\sigma_\parallel} dV = I_p \langle \varepsilon \rangle \qquad\qquad 5.12$$

where

$$\langle \varepsilon \rangle = \frac{1}{\mu_0 I_p} \oint_l \varepsilon B_\tau dl \qquad\qquad 5.13$$

What we find, from Equation 5.12, is that the ohmic input power $\int j_\phi^2/\sigma_\parallel dV$ into the plasma must be evaluated knowing the poloidal distribution of both ε and B_τ around the contour l, as well as the inductance L_i within that contour. For example, suppose the contour is a circle of radius a_l, and

$$\varepsilon = \varepsilon_0 \left[1 + \sum_n \varepsilon_n \cos(n\omega) \right] \qquad\qquad 5.14$$

$$B_\tau = \frac{\mu_0 I_p}{2\pi a_l} \left[1 + \sum_n \lambda_n \cos(n\omega) \right] \qquad\qquad 5.15$$

Then we obtain

$$\langle \varepsilon \rangle = \varepsilon_0 \left(1 + \sum_n \lambda_n \varepsilon_n \right) \qquad\qquad 5.16$$

The inductance L_i is given approximately by (i.e. the "straight" circular tokamak)

$$L_i \approx \mu_0 R_p \left[\ln\left(\frac{a_l}{a_p}\right) + \frac{l_i}{2} \right] \qquad\qquad 5.17$$

with a_p, R_p the plasma minor, major radius. The term $\mu_0/(4\pi)l_i$ is the inductance per unit length (toroidally) inside the plasma, and the ln term represents the inductance between the plasma surface ($r = a_p$) and the contour l ($r = a_l$). The approximation given is for a straight circular tokamak coaxial with a circular contour. That part of the inductance between the plasma and the contour is sensitive to plasma position.

Uses of the Volts per turn measurement

We can deduce an average value of the plasma conductivity, $\langle\sigma\rangle$, by writing

$$\frac{2\pi R_p I_p^2}{\pi a_p^2 \langle\sigma\rangle} = \int_V \frac{j_\phi^2}{\sigma_\parallel} dV = I_p \langle\varepsilon\rangle - \frac{\partial}{\partial t}\left(\frac{L_i I_p^2}{2}\right) \tag{5.18}$$

From this we can define a conductivity temperature T_σ. The conductivity deduced by Spitzer for Coulomb collisions is given by (there are corrections for the fact that, in a torus, trapped particles cannot carry current and so σ must be reduced)

$$\sigma = 1.9 \times 10^4 \frac{T_e^{3/2}}{Z_{eff} \ln(\Lambda_s)} \tag{5.19}$$

Then T_σ is defined as that temperature which gives a Spitzer conductivity (with $Z_{eff} = 1$) equal to the average conductivity $\langle\sigma\rangle$, with an approximate value taken for $\ln(\Lambda_s)$. We can also derive an average "skin time", from the formula for the penetration of a field into a conductor of uniform conductivity $\langle\sigma\rangle$:

$$\tau_{skin} = \frac{\pi\mu_0 \sigma a_p^2}{16} \tag{5.20}$$

The definition of energy confinement time for an ohmic heated plasma with major radius R_p, cross sectional area S_ϕ.(here we assume a circular minor radius a_p, so $S_\phi = \pi a_p^2$), total energy content $W = 3\pi R_p \int_{S_\phi} p dS_\phi$, ohmic input power $P_{oh} = I_p^2 \Omega_p$, can we written in terms of the poloidal beta value $\beta_I = 8\pi/(\mu_0 I_p^2)\int_{S_\phi} p dS_\phi$ (discussed later) as

$$\tau_E = \frac{W}{P_{oh}} = \frac{3\mu_0 \beta_I R_p}{8\Omega_p} = \frac{3\mu_0 \beta_I a_p^2 \langle\sigma\rangle}{16} \tau \tag{5.21}$$

Combining equations 5.20 and 5.21 shows that

$$\frac{\tau_E}{\tau_{skin}} \approx \beta_I \tag{5.22}$$

Therefore for ohmic heated plasmas, where typically $\beta_I \approx 0.3$, the currents penetrate approximately 3 times slower than the energy escapes from the plasma.

6. TOKAMAK EQUILIBRIA

6.0. AN INTUITIVE DERIVATION OF TOKAMAK EQUILIBRIUM

Introduction

After having described how to measure the plasma current and loop voltage, the next most important parameter to measure is the plasma position. We will show how we determine both this, and certain integrals of the pressure and field across the plasma cross section (specifically β_I + $l_i/2$), in section 7. The basic idea is that we want an expression for the fields outside the plasma in terms of plasma displacement Δ and (β_I + $l_i/2$). We can only do this by knowing a solution to the plasma equilibrium, i.e. we must solve the Grad Shafranov equation. I deal with this later in this section, but first we can gain a physical picture of tokamak equilibrium by considering the various forces acting on a toroidal plasma. Also note that there are techniques to measure plasma position without recourse to equilibrium solutions, the so called "moments" method. However, the interpretation of this method (i.e. what has been measured) itself requires a knowledge of the equilibrium.

The total energy of our system must be made up of 3 parts,

$$W = W^p + W_1^B + W_2^B \qquad\qquad\qquad 6.0.1$$

where W^P is the energy stored as pressure, W_1^B is the energy stored in toroidal fields (poloidal currents), and W_2^B is the energy stored in poloidal fields (toroidal currents). Once we have calculated expressions for these terms, we can obtain the required forces: the minor radial force $F_a = \partial W/\partial a$, and the major radial force $F_R = \partial W/\partial R$. By setting the net force = 0 we will obtain the conditions necessary for equilibrium. We work with a circular cross sectioned plasma with major radius R and a minor radius a, and a/R << 1. *Figure 6.0.1* shows the geometry. The poloidal coordinate is θ. We use <...> to mean an average over the volume (which is the same as an average over the plasma surface if a/R << 1) and V = $2\pi R\pi a^2$. A positive force is in the "R" or "a" direction (an expansion).
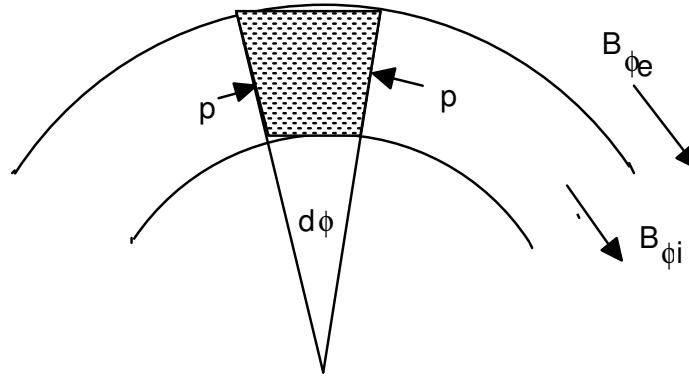
The toroidal fields and pressures p
present in a section of a toroidal
plasma colum. the toroidal angle is
ϕ

Figure 6.0.1. Elemental volume discussed in deriving force balance.

Energy associated with plasma pressure $\underline{W^P}$

The major radial force F_R^p exerted by the plasma pressure in expanding a distance dR is given by F_R^p dR = <p>dV, and the minor radial force F_a^p exerted by the plasma pressure in expanding a distance da is given by F_a^p da = <p>dV. The total energy W^p is given by

$$W^p = \int_V pdV = \langle p \rangle V = \langle p \rangle 2\pi^2 Ra^2 :$$

6.0.2

so that

$$F_a^p = \frac{\partial W^p}{\partial a} = \frac{2V\langle p \rangle}{a}$$

6.0.3

$$F_R^p = \frac{\partial W^p}{\partial R} = \frac{V\langle p \rangle}{R}$$

6.0.4

These forces were computed at constant pressure.

Energy associated with toroidal fields $\underline{W_1}^B$

The energy associated with poloidal currents is written as

$$W_1^B = \frac{L_1 I_1^2}{2} + \frac{L_{1e} I_{1e}^2}{2} + M_1 I_1 I_{1e}$$

6.0.5

Here I_1 is the poloidal current in the plasma, and I_{1e} is the poloidal current in the toroidal field coil (subscript e for external). I_1 is that poloidal current flowing in the plasma edge which produces a toroidal field equal to the <u>difference</u> between the internal toroidal field $B_{\phi i}$ and the external toroidal field $B_{\phi e}$. By definition we have

$$\frac{L_1 I_1^2}{2} = \frac{\left\langle \left(B_{\phi i} - B_{\phi e}\right)^2 \right\rangle V}{2\mu_0}$$

6.0.6

$$M_1 I_1 I_{1e} = \frac{\left(\left\langle B_{\phi i}\right\rangle - B_{\phi e}\right) B_{\phi e} V}{\mu_0}$$

6.0.7

Now the circuits I_1 and I_{1e} are perfectly coupled, so that $L_1 = M_1$. The field $B_1 = \mu_0 I_1/(2\pi R)$, and so

$$M_1 = L_1 = \frac{1}{I_1^2} \int_V \frac{B_1^2}{\mu_0} dV = \mu_0 \left(R - \left(R^2 - a^2\right)^{\!1/2} \right) \approx \frac{\mu_0 a^2}{2R}$$

6.0.8

for skin currents. To get the forces we will need only the functional dependencies, namely

$$\frac{\partial L_1}{\partial a} = \frac{2 L_1}{a}$$
$$\frac{\partial M_1}{\partial a} = \frac{2 M_1}{a}$$

6.0.9

$$\frac{\partial L_1}{\partial R} = -\frac{L_1}{R}$$
$$\frac{\partial M_1}{\partial R} = -\frac{M_1}{R}$$

6.0.10

The forces will be computed at constant current. For example, the part of the force due to $\partial/\partial R(L_1 I_1^2/2)$ is then written as $(I_1^2/2)\partial/\partial R(L_1) = -(I_1^2/2)L/R = -(L_1 I_1^2/2)(1/R)$. Using Equation 6.0.6 this becomes $(I_1^2/2)\partial/\partial R(L_1) = <B_{\phi i}-B_{\phi e})^2>V/(2R\mu_0)$. Doing this for each component in Equation 6.0.5 gives

$$F_{1a}^B = \frac{\partial W_1^B}{\partial a} = \frac{2V}{a}\left(\frac{\left(\langle B_{\phi i}^2 \rangle - B_{\phi e}^2\right)}{2\mu_0}\right)$$
                                                                                        6.0.11

$$F_{1R}^B = \frac{\partial W_1^B}{\partial R} = \frac{V}{R}\left(\frac{\left(B_{\phi e}^2 - \langle B_{\phi i}^2 \rangle\right)}{2\mu_0}\right)$$
                                                                                        6.0.12

There will be no force from the term $L_{1e}I_{1e}^2/2$, because we keep the external currents constant.

Energy associated with poloidal fields $\underline{W_2^B}$

Again we write the energy in the poloidal circuits as

$$W_2^B = \frac{L_2 I_2^2}{2} + \frac{L_{2e} I_{2e}^2}{2} + M_2 I_2 I_{2e}$$
                                                                                        6.0.13

with $I_2 = I_p$ the toroidal plasma current, and I_{2e} the poloidal currents in external windings. These windings are imagined to consist of a set which provides an external vertical field B_z but induces no plasma current, and a set which drives the plasma current but produces no B_z. We will need the radial derivatives (with respect to both major and minor radii) of the self and mutual inductances. All external currents will be kept fixed, so that $\partial(L_{2e})/\partial a = \partial(L_{2e})/\partial R = 0$. Only that winding producing a vertical field is imagined coupled through a mutual inductance to the plasma.

We must make use of the inductance of a current loop:

$$L_2^B = \mu_0 R\left(\ln\left(\frac{8R}{a}\right) - 2 + \frac{l_i}{2}\right)$$
                                                                                        6.0.14

The term l_i accounts for the inductance between the center of the loop and the edge, at $r = a$. We also need the flux $\Psi = M_2 I_{2e}$, the external flux passing through the central aperture, which can be written as

$$\Psi = \int_0^R 2\pi R B_z \, dR$$
                                                                                        6.0.15

Then we have

$$\frac{\partial L_2}{\partial R} = \mu_0\left(\ln\left(\frac{8R}{a}\right) - 1 + \frac{l_1}{2}\right)$$
                                                                                        6.0.16

$$\frac{\partial L_2}{\partial a} = -\frac{\mu_0 R}{a}$$

6.0.17

$$\frac{\partial M_2}{\partial R} = \frac{\partial}{\partial R}\left(\frac{\Psi}{I_{2e}}\right) = \frac{2\pi R B_z}{I_{2e}}$$

6.0.18

$$\frac{\partial M_2}{\partial a} = \frac{\partial}{\partial a}\left(\frac{\Psi}{I_{2e}}\right) = 0$$

6.0.19

Now we can deduce the forces:

$$F_{2a}^B = \frac{\partial W_2^B}{\partial a} = -\frac{2V}{a}\left(\frac{B_{\theta a}^2}{2\mu_0}\right)$$

6.0.20

$$F_{2R}^B = \frac{\partial W_2^B}{\partial R} = \frac{V}{R}\left[\frac{B_{\theta a}^2}{\mu_0}\left(\ln\left(\frac{8R}{a}\right)-1+\frac{l_i}{2}\right)+\frac{2B_z B_{\theta a}R}{\mu_0 a}\right]$$

6.0.21

where

$$B_{\theta a} = \frac{\mu_0 I_2}{2\pi a} = \frac{\mu_0 I_p}{2\pi a}$$

6.0.22

Total forces

We can now add Equations 6.0.3, 6.0.11 and 6.0.20 to get F_a, and Equations 6.0.4, 6.0.12 and 6.0.21 to get F_R:

$$F_a = \frac{2V}{a}\left[-\frac{B_{\theta a}^2}{2\mu_0}+\frac{\left(\langle B_{\phi i}^2\rangle - B_{\phi e}^2\right)}{2\mu_0}+\langle p\rangle\right]$$

6.0.23

$$F_R = \frac{V}{R}\left[\frac{B_{\theta a}^2}{\mu_0}\left(\ln\left(\frac{8R}{a}\right)-1+\frac{l_i}{2}\right)+\frac{2RB_z B_{\theta a}}{\mu_0 a}+\frac{\left(B_{\phi e}^2 - \langle B_{\phi i}^2\rangle\right)}{2\mu_0}+\langle p\rangle\right]$$

6.0.24

with $B_{\theta a} = \frac{\mu_0 I_p}{2\pi a}$. Equilibrium requires $F_a = 0$, so that

$$\langle p\rangle = \left[\frac{B_{\theta a}^2}{2\mu_0}+\frac{\left(B_{\phi e}^2 - \langle B_{\phi i}^2\rangle\right)}{2\mu_0}+\right]$$

6.0.25

Therefore if we can measure the difference in toroidal field with and without (when $B_{\phi i} = B_{\phi e}$) plasma present, we can measure the average plasma pressure. This is discussed later in dealing with "diamagnetism".

The condition $F_R = 0$ specifies the vertical field:

$$B_z = -\frac{aB_{\theta a}}{2R}\left[\ln\left(\frac{8R}{a}\right) - \frac{3}{2} + \frac{l_i}{2} + \frac{2\mu_0 \langle p \rangle}{B_{\theta a}^2}\right]_-$$
$$= -\frac{aB_{\theta a}}{2R}\left[\ln\left(\frac{8R}{a}\right) - \frac{3}{2} + \frac{l_i}{2} + \beta_I\right]$$

<div align="right">6.0.26</div>

This was the field we used in section 1, Field lines and flux surfaces, to plot out the flux surfaces which result from a combined circular filament and a vertical field.

6.1. THE FLUX OUTSIDE A CIRCULAR TOKAMAK

Later we will use the expression for the flux outside a circular tokamak. It can be considered to come from two sources, that from the external maintaining fields ψ_{ext} and that from the plasma itself, ψ_p. In the previous section we derived an expression for the vertical field B_z necessary to maintain a circular equilibrium (Equation 6.0.26). While the major radial term appearing as $\ln\left(\frac{8R}{a}\right)$ in Equation 6.0.26 clearly refers to the geometric center R_g (it comes from the inductance of a plasma with radius a with a geometric center R_g), it is not obvious to what radius the term outside the square brackets refers. It could be either R_g, or the coordinate itself, so that $B_z \propto 1/R$. In the former case, in a right-handed cylindrical coordinate system (R,ϕ,z), the flux would be derived from $\psi \propto R^2$, or in our local coordinate system (ρ,ω,ϕ) based on R_g (See *Figure 1.7*)

$$\psi = k_0 + k_1\cos(\omega) + k_2\cos(2\omega)$$

<div align="right">6.1.1</div>

with k_i a constant. The constant is unimportant, but the $\cos(2\omega)$ term means that such an external field would introduce ellipticity, and we have specifically considered a circular plasma. Therefore we must take $B_z \propto 1/R$, and in the coordinate system (R,ϕ,z) this is derived from a flux

$$\psi_{ext} = \frac{\mu_0 I_p R}{4\pi}\left[\ln\left(\frac{8R_g}{a}\right) + \Lambda - 0.5\right]$$

<div align="right">6.1.2</div>

where $\Lambda = \beta_I + \dfrac{l_i}{2} - 1$. In the local coordinate system (ρ, ω, ϕ) the necessary B_z is then derived from a flux (ignoring the constant of integration)

$$\psi_{ext} = \frac{\mu_0 I_p \rho \cos(\omega)}{4\pi}\left[\ln\left(\frac{8R_g}{a}\right) + \Lambda - 0.5\right] \qquad\qquad 6.1.3$$
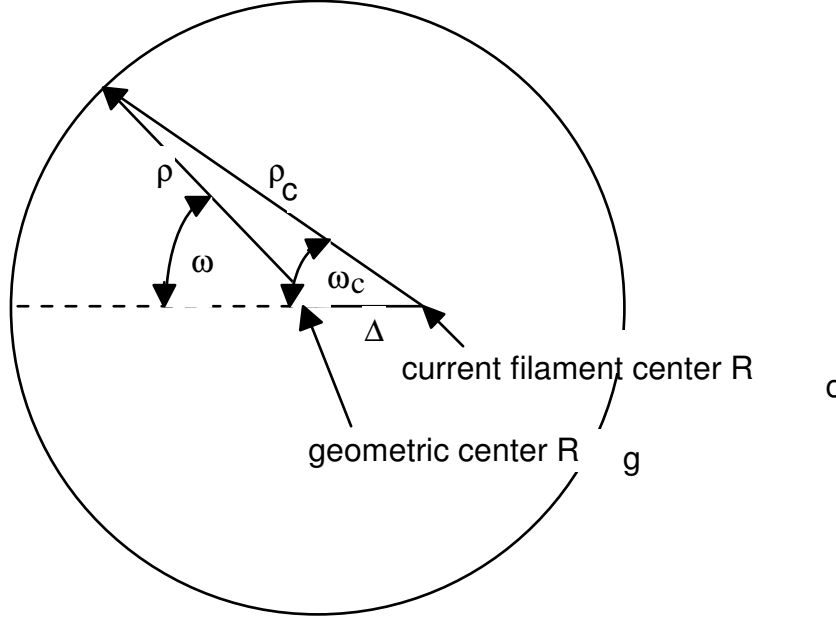
Figure 6.1.1. The geometry used in relating the geometric and current filament centers

Next we come to the flux ψ_p produced by the plasma. Outside the plasma, where there is no current and no pressure, the fields and fluxes we are looking for must be able to be constructed from those due to circular filaments. This will not be true inside the plasma. For a first approximation we will model the flux ψ_p as being due to a single circular filament with current I_p. If we position this filament at a position R_c then in a coordinate system (ρ_c, ω_c, ϕ) based on the filament we have shown that the flux is well represented by

$$\psi_p \approx \frac{\mu_0 I_p R_c}{2\pi}\left[\left(\ln\left(\frac{8R_c}{\rho_c}\right) - 2\right) - \left(\frac{\rho_c}{R_c}\right)\frac{\cos(\omega_c)}{2}\left(\ln\left(\frac{8R_c}{\rho_c}\right) - 1\right)\right] \qquad\qquad 6.1.4$$

However, we have to decide where to place this filament, that is, what to choose for R_c, and how ρ, ρ_c, ω and ω_c are related. Because we have derived ψ_{ext} for a circular cross section (in the calculation of B_z we used inductances for circular current path), we must place the filament so that, in the coordinate system (ρ, ω, ϕ) the surface $\psi_{total} = \psi_{ext} + \psi_p = $ constant is a circle of radius at $\rho = a$.

Suppose we place the filament at a position $R_0 = R_c + \Delta$. From *Figure 6.1.1*, and expanding in the small parameter Δ/r, we then derive that

$$\rho_c^2 = \rho^2 + \Delta^2 - 2\Delta\rho\cos(180 - \omega) \qquad\qquad 6.1.5$$

$$\rho^2 = \rho_c^2 + \Delta^2 - 2\Delta\rho_c\cos(\omega_c) \qquad\qquad 6.1.6$$

from which we have

$$\rho_c \approx \rho\left(1 + \frac{\Delta}{\rho}\cos(\omega)\right) \qquad\qquad 6.1.7$$

and

$$\cos(\omega_c) \approx \cos(\omega)\left(1 - \frac{\Delta}{r}\cos(\omega)\right) + \frac{\Delta}{r} \qquad\qquad 6.1.8$$

Substituting for ρ_c and ω_c in terms of ρ and ω, and using $R_0 = R_c + \Delta$, we obtain an expression for the total flux ψ_{total} (ρ, ω, ϕ) in the coordinate system based on the geometric center. Keeping terms of order Δ/r and $\cos(\omega)$ only (i.e. neglecting elliptic distortions to any surface) we find

$$\psi_{total} = \frac{\mu_0 I_p R_g}{2\pi}\left[\ln\left(\frac{8R_g}{\rho}\right) - 2\right] + \frac{\mu_0 I_p \rho\cos(\omega)}{4\pi}\left[\ln\left(\frac{\rho}{a}\right) + \Lambda + \frac{1}{2} - 2\frac{\Delta R_g}{\rho^2}\right] \qquad 6.1.9$$

To ensure a circular outer contour (at $r = a$) we set the $\cos(\omega)$ term to zero, that is we set

$$\frac{\Delta}{a} = \frac{a}{2R_g}\left(\Lambda + \frac{1}{2}\right) \qquad\qquad 6.1.10$$

Substituting for Δ form Equation 6.1.10 into Equation 6.1.9 gives the final expression for the flux outside a circular tokamak:

$$\psi_{total} = \frac{\mu_0 I_p R_g}{2\pi}\left[\ln\left(\frac{8R_g}{\rho}\right) - 2\right] + \frac{\mu_0 I_p \rho\cos(\omega)}{4\pi}\left[\ln\left(\frac{\rho}{a}\right) + \left(\Lambda + \frac{1}{2}\right)\left(1 - \left(\frac{a}{\rho}\right)^2\right)\right]$$

$$6.1.11$$

6. CIRCULAR EQUILIBRIUM

Derivation of the Grad Shafranov equation

Most analysis of magnetic measurements rely on an understanding of equilibrium. The most general cases are derived from integral equations, which do not constrain the plasma shape, and are discussed later. However, an insight can often be gained by considering the case of a circular, low beta, large aspect ratio ($a/R_p \ll 1$) system. For this we must solve the so called Grad-Shafranov equation. The basic equation for equilibrium is that of pressure balance:

$$\mathbf{j} \times \mathbf{B} = \nabla p \qquad\qquad\qquad 6.1$$

from which $\mathbf{B} \cdot \nabla p = 0$, i.e. there is no pressure gradient along a field line; magnetic flux surfaces are surfaces of constant pressure. Also from 6.1 we have $\mathbf{j} \cdot \nabla p = 0$, so that current lines lie in a magnetic surface. Equation 6.1, together with Maxwell's equations, is all we need.

The conditions for the applicability of equation 6.1 are interesting. It is NOT correct that it only applies to the ideal MHD plasma, which would imply that it is incompatible with diffusive phenomena. In fact it is sufficient that

1) The plasma directed kinetic energy is much smaller than the thermal energy. Inertia is ignored.

2) The gas kinetic pressure is nearly isotropic. This is still possible for a collisionless plasma ($\lambda \gg 2\pi R$) as long as the times considered are long ($t \gg \lambda/v_{th}$, i.e. t $\gg \tau_{ee}$, τ_{ei} with τ_{ee}, τ_{ei} the electron -electron and ion-ion collision times).

3) The local distribution function deviates slightly from a Maxwellian even for a straight system because of the finite Larmor radius r_L: $\delta f \approx r_L . \partial f(r)/\partial r$. This leads to a deviation from pressure isotropy by an amount $\delta p \approx p r_L/a$, with a the minor radius. In toroidal geometry the particles are displaced from a magnetic surfaced by amounts $d \approx r_L q$ for passing particles and $d \approx r_L q \varepsilon^{-1/2}$ for trapped particles (ε is the aspect ratio r/R, q is the safety factor). Then there is a deviation from a local Maxwellian distribution function f by an amount $\delta f/f \approx d/a$, and an associated pressure anisotropy $\delta p/p \approx r_L q/a$. Therefore we should have $r_L q/a \ll 1$. i.e. the plasma can be considered as a gas of Larmor circles produced by charges rotating in a magnetic field.
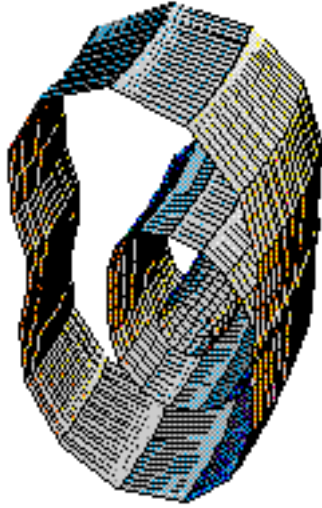
Figure 6.1. Nested flux surfaces.   *Figure 6.2*. Field lines in a surface.
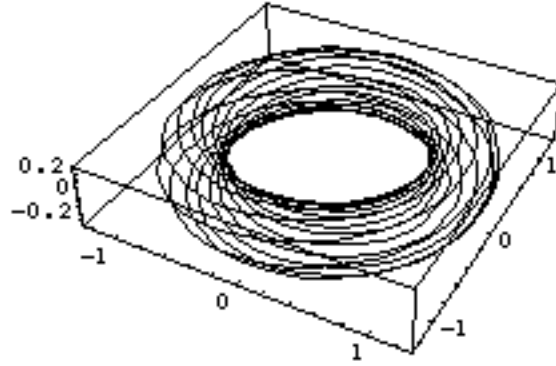
We introduce ψ, the poloidal flux per radian in ϕ. This is proportional to the poloidal flux within each surface; it is constant on a flux surface. *Figure 6.1* shows an example of nested flux surfaces, and *Figure 6.2* shows field lines lying in a flux surface (followed 10 times in the toroidal direction). We will show that the current lies in a flux surface, but current lines do not follow field lines. In *Figure 6.1* the each surface is described by a radius $r = r_0 + \sum_{n=2}^{\infty} \Delta_n \cos(n\omega)$,

where we have also shifted the origin of each surface with respect to each other. The example shown has a circular innermost surface, a mostly elliptic (n = 2) central surface, and an outer surface with a combination of ellipticity (n = 2) and triangularity (n = 3). Note that $\psi = RA_\phi$, where A is the vector potential (note we sometimes use the total flux $\Psi = 2\pi\psi$). In the cylindrical coordinates (R,ϕ,z) of *Figure 1.7* the magnetic fields are derived from

$$B_R = -\frac{1}{R}\frac{\partial \psi}{\partial z}$$ 6.2

$$B_z = \frac{1}{R}\frac{\partial \psi}{\partial R}$$ 6.3

which satisfy $\nabla \cdot \mathbf{B} = 0$. We also introduce a current flux function f, which is related to the poloidal current density so that

$$J_R = -\frac{1}{R}\frac{\partial f}{\partial z}$$ 6.4

$$j_z = \frac{1}{R}\frac{\partial f}{\partial R}$$ 6.5

Now Amperes law $\mu_0\mathbf{j} = \nabla \times \mathbf{B}$ gives

$$j_R = -\frac{1}{\mu_0}\frac{\partial B_\phi}{\partial z}$$ 6.6

$$j_z = \frac{1}{\mu_0 R}\frac{\partial(RB_\phi)}{\partial R}$$ 6.7

so that, comparing Equation 6.4 with Equation 6.6, and Equation 6.5 with Equation 6.7, we have

$$\mu_0 f = RB_\phi$$ 6.8

That is, the function f includes the total current in the windings producing the toroidal field. Since from Equation 6.1. $\mathbf{j}\cdot\nabla p = 0$, using Equations 6.4 and 6.5 for j gives $(\partial f/\partial R)(\partial p/\partial z)$ - $(\partial f/\partial z)(\partial p/\partial R) = 0$, or

$$\nabla f \times \nabla p = 0$$ 6.9

Since p is a function of ψ, i.e. $p = p(\psi)$, we must have $f = f(\psi)$ as well.

Now we want to derive the basic equilibrium equation in terms of ψ. Write Equation 6.1 as

$$\mathbf{j}_p \times \mathbf{e}_\phi B_\phi + j_\phi \mathbf{e}_\phi \times \mathbf{B}_p = \nabla p$$ 6.10

where subscript p means poloidal and $\mathbf{e}_\phi$ is a unit vector in the ϕ direction. Now Equations 6.2. and 6.3 can be written as

$$\mathbf{B}_p = \frac{1}{R}\left(\nabla\psi \times \mathbf{e}_\phi\right)$$ 6.11

and Equations 6.4 and 6.5 can be written as

$$\mathbf{j}_p = \frac{1}{R}\left(\nabla f \times \mathbf{e}_\phi\right)$$ 6.12

Substituting 6.11. and 6.12 into 6.10, (remember $\mathbf{e}_\phi\cdot\nabla\psi = \mathbf{e}_\phi\cdot\nabla f = 0$) gives

$$-\frac{B_\phi}{R}\nabla f + \frac{j_\phi}{R}\nabla\psi = \nabla p$$ 6.13

Writing $\nabla f(\psi) = (df/d\psi)\nabla\psi$ and $\nabla p(\psi) = (dp/d\psi)\nabla\psi$, and substituting into 6.13, gives

$$j_\phi = R\frac{dp}{d\psi} + B_\phi\frac{df}{d\psi} \qquad\qquad 6.14$$

or

$$j_\phi = R\frac{dp}{d\psi} + \frac{\mu_0}{R}f\frac{df}{d\psi} \qquad\qquad 6.15$$

The equilibrium conditions restrict the possible current distributions j_ϕ in the plasma ; instead of a two dimensional distribution $j_\phi(R,z)$ a one dimensional one is obtained, depending on the two profiles $dp/d\psi$ and $fdf/d\psi$.

We can write j_ϕ in terms of ψ using Amperes law, $\mu_0\mathbf{j} = \nabla \times \mathbf{B}$. Substituting from Equations 6.2 and 6.3 for the components of B in the toroidal component j_ϕ gives

$$-\mu_0 Rj_\phi = R\frac{\partial}{\partial R}\left(\frac{1}{R}\frac{\partial\psi}{\partial R}\right) + \frac{\partial^2\psi}{\partial z^2} \qquad\qquad 6.16$$

Substituting for j_ϕ from Equation 6.16 into Equation 6.15 finally gives the Grad Shafranov equation:

$$R\frac{\partial}{\partial R}\left(\frac{1}{R}\frac{\partial\psi}{\partial R}\right) + \frac{\partial^2\psi}{\partial z^2} = -\mu_0 R^2\frac{dp}{d\psi} - \mu_0^2 f\frac{df}{d\psi} \qquad\qquad 6.17$$

In the local coordinates (θ,r,ϕ) of *Figure 6.3*, based on the plasma major radius (the geometric center of the outermost circular surface) R_g this equation becomes:

$$\left[\frac{1}{r}\frac{\partial}{\partial r}\left(r\frac{\partial}{\partial r}\right) + \frac{1}{r^2}\frac{\partial^2}{\partial\theta^2}\right]\psi - \frac{1}{(R_g + r\cos(\theta))}\left[\cos(\theta)\frac{\partial}{\partial r} - \frac{\sin(\theta)}{r}\frac{\partial}{\partial\theta}\right]\psi$$
$$= -\mu_0(R_g + r\cos(\theta))^2\frac{dp}{d\psi} - \mu_0^2 f\frac{df}{d\psi} \qquad\qquad 6.18$$

Note the ordering (θ,r,ϕ) in which the system is right handed. The poloidal angle θ is measured from the outer equator, so that $x = (R + r\cos(\theta))\cos(\phi)$, $y = (R + r\cos(\theta))\sin(\phi)$, and $z = r\sin(\theta)$. The metric coefficients are $h_\theta = r$, $h_r = 1$ and $h_\phi = R + r\cos(\theta)$. If a new variable $\theta_1 = \pi - \theta$ is defined, so θ_1 is measured from the inner equator, then the system (r,θ_1,ϕ) is also right handed. We have mostly used this latter system.
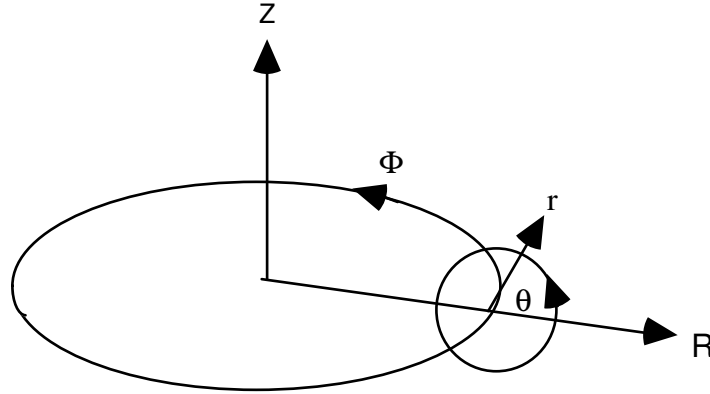
Figure 6.3. Geometry of the local coordinate system used.

Solving the Grad Shafranov equation

In a large aspect ratio expansion let us write

$$\psi = \psi_0(r) + \psi_1(r,\theta) \tag{6.19}$$

where the first term describes a set of concentric circular surfaces, and the second term is the first order correction. Substituting into the general equation (Equation 6.18) gives the zeroeth or leading order equation for ψ_0:

$$\frac{1}{r}\frac{d}{dr}\left(r\frac{d\psi_0}{dr}\right) = -\mu_0 R_g^2 \frac{dp(\psi_0)}{d\psi} - \mu_0^2 f(\psi_0)\frac{df(\psi_0)}{d\psi} \tag{6.20}$$

The first order equation for ψ_1 is rearranged as:

$$\left[\frac{1}{r}\frac{\partial}{\partial r}\left(r\frac{\partial}{\partial r}\right) + \frac{1}{r^2}\frac{\partial^2}{\partial\theta^2}\right]\psi_1 - \frac{\cos(\theta)}{R_g}\frac{d\psi_0}{dr}$$

$$= -\frac{d}{dr}\left(\mu_0 R_g^2\frac{dp(\psi_0)}{d\psi} + \mu_0^2 f(\psi_0)\frac{df(\psi_0)}{d\psi}\right)\frac{dr}{d\psi_0}\psi_1 \tag{6.21}$$

$$-2\mu_0 R_g r\cos(\theta)\frac{dp(\psi_0)}{d\psi}$$

Suppose each surface ψ is displaced a distance $\Delta_1(\psi_0(r))$, so we can write ψ as

$$\psi = \psi_0 + \psi_1 = \psi_0 - \Delta_1(r)\frac{\partial\psi_0}{\partial R} = \psi_0 - \Delta_1(r)\cos(\theta)\frac{\partial\psi_0}{\partial r} \tag{6.22}$$

57

Substituting this form for ψ_1 $(= -\Delta_1(r)\cos(\theta)\partial\psi_0/\partial r)$ into the first order equation, Equation 6.21, gives:

$$\frac{d}{dr}\left(rB_{\theta 0}^2\frac{d\Delta_1}{dr}\right) = \frac{r}{R_g}\left(2\mu_0 r\frac{dp_0}{dr} - B_{\theta 0}^2\right)$$ 6.23

where $B_{\theta 0} = \dfrac{1}{R_g}\dfrac{d\psi_0}{dr}$ has been used.

The solution of this equation gives the horizontal shift Δ_1 of a flux surface away from the geometric axis, as illustrated in *Figure 6.4*. This, together with the solution of Equation. 6.22, gives us what we want. If we wanted to consider non circular surfaces, we could write $r = r_0 + \sum\limits_{n=1}^{\infty}\Delta_n(r)\cos(n\theta)$ for each surface. Then $\psi(r)$ is a constant (by definition), so that $\psi = \psi_0 - \sum\limits_{n=1}^{\infty}\Delta_n(r)\cos(n\theta)\dfrac{d\psi_0}{dr}$.
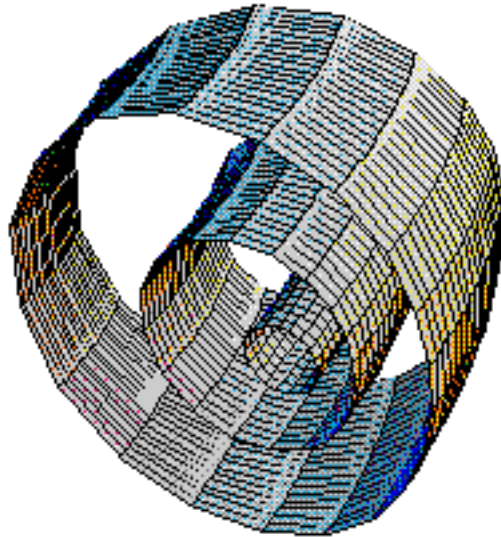
Figure 6.4. Displaced circular flux surfaces.

The poloidal field at the plasma edge

To continue, we need an expression for the boundary field $B_\theta(a)$ from the plasma equilibrium. We will ultimately use this to match the external and internal solutions at the plasma boundary r = a, where B_τ (= B_θ for a circular plasma) must be continuous. Now

$$B_\theta = \frac{1}{R}\frac{d\psi}{dr} = \frac{1}{\left(R_g + r\cos\theta\right)}\frac{d\psi}{dr}$$

6.24

Using Equation 6.22, with $\Delta_1(a) = 0$, gives

$$B_\theta(a) = B_{\theta 0}(a)\left[1 - \left(\frac{a}{R_g} + \left(\frac{d\Delta_1}{dr}\right)_a\right)\cos(\theta)\right]$$

6.25

with $B_{\theta 0}(a)$ the zero order poloidal field at the boundary. Now we need to find an expression for $(d\Delta_1/dr)_a$ in Equation 6.25. Integrating Equation 6.23 (with the condition $d\Delta_1/dr = 0$ at r = 0) gives the displacement of the magnetic surfaces for the zero order pressure distribution $p_0(r)$ and zero order poloidal field $B_{\theta 0}(r)$:

$$\frac{d\Delta_1}{dr} = \frac{2\mu_0}{rR_g B_{\theta 0}^2}\left(r^2 p_0 - \int_0^r\left(2p_0 + \frac{B_{\theta 0}^2}{2\mu_0}\right)rdr\right)$$

6.26

By defining (we will be more careful with definitions later)

$$\beta_I = \frac{8\pi}{\mu_0 I_p^2}\int_{S_{\phi p}} pdS_\phi = \frac{4\mu_0}{a^2 B_{\theta 0}^2(a)}\int_0^a p_0 rdr$$

6.27

for our circular case, and

$$l_i = \frac{4}{\mu_0 R_g I_p^2}\int_{V_p}\frac{B_p^2}{2\mu_0}dV = \frac{4\mu_0}{a^2 B_{\theta 0}^2(a)}\int_0^a \frac{B_\theta^2}{2\mu_0}rdr$$

6.28

where B_p is the poloidal field, $S_{p\phi}$ the plasma cross section in a poloidal plane, and V_p the plasma volume, for our circular case we obtain

$$\left(\frac{d\Delta_1}{dr}\right)_a = -\frac{a}{R_g}\left(\beta_I + \frac{l_i}{2}\right)$$

6.29

Now we can substitute Equation 6.29 into 6.25 and obtain

$$B_\theta(a) = B_{\theta0}(a)\left[1 + \frac{a}{R_g}\Lambda\cos(\theta)\right] \qquad 6.30$$

where

$$\Lambda = \beta_I + \frac{l_i}{2} - 1 \qquad 6.31$$

That is, we now know the distribution of poloidal field at the boundary of a circular plasma including terms of order (a/R).

Simple current distributions

Consider a case where the zero order (circular cylinder) current density is given by

$$j_\phi = j_{\phi0}\left(1 - x^2\right)^\alpha \qquad 6.32$$

with $0 < x = r/a < 1$ representing the normalized minor radius.
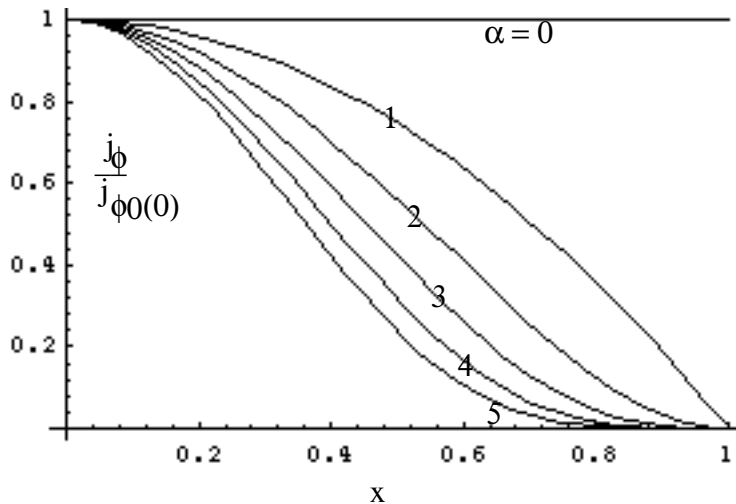
Figure 6.5 The normalized current density distributions $j_\phi/j_{\phi0}(0)$.

Figure 6.5 shows these profiles for integer $\alpha = 0$ through 5 as a function of normalized radius x. The total current J is given by

$$J = \frac{\pi a^2}{1 + \alpha}j_{\phi0} \qquad 6.33$$

so that we can write a normalized current density j_r as

$$j_r = \frac{\pi a^2 j}{J} = (1+\alpha)\left(1-x^2\right)^{\alpha}$$ 6.34

Figure 6.6 shows j_r as a function of x for α between 0 and 5; these curves represent the shape of the current density profiles with the constraint that the total current J is constant.
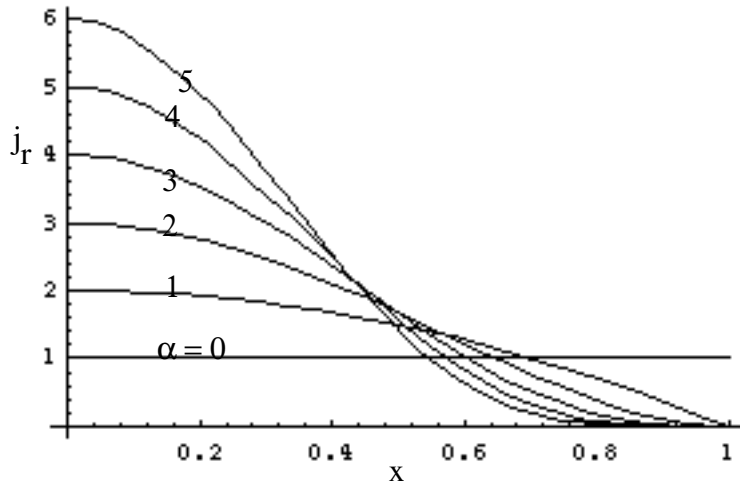
Figure 6.6 The normalized current density distributions $j_r(x)$

The poloidal field B_θ is given by

$$B_\theta = B_{\theta 0}(1)\frac{\left(1-\left(1-x^2\right)^{1+\alpha}\right)}{x}$$ 6.35

with $B_{\theta 0}(1)$ the value at r = a, or x = 1: $B_{\theta 0}(1) = \mu_0 J/(2\pi a)$. The ratio $B_\theta/B_{\theta 0}(1)$ is shown in *Figure 6.7* as a function of x for α between 0 and 5.
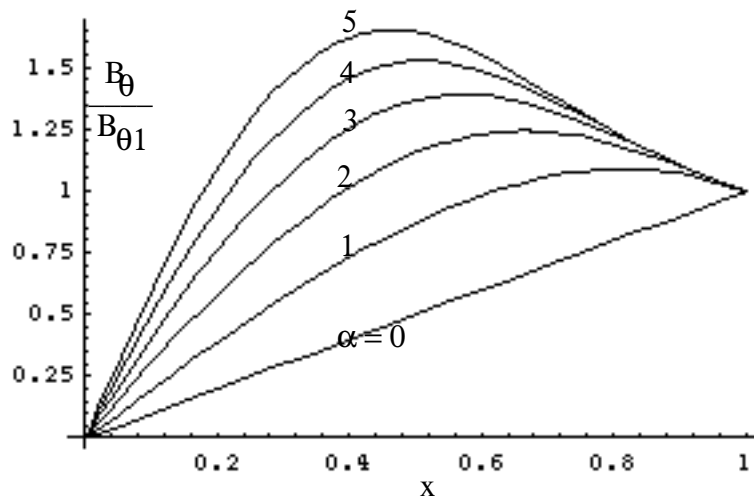
Figure 6.7. The normalized poloidal field distributions $B_\theta/B_{\theta 0}(1)$

61

The "self inductance per unit length" is expressed as

$$l_i = 2\int_0^1 \left(1 - \left(1 - x^2\right)^{1+\alpha}\right)^2 \frac{dx}{x} \qquad\qquad 6.36$$

The solution is written in terms of PolyGamma and EulerGamma functions:

l_i = EulerGamma + 2 PolyGamma[0, 2 + α] - PolyGamma[0, 3 + 2 α]

6.37

However, a polynomial fit in α can also be used:

$$l_i = 0.509619 + 0.462798\alpha - 0.0630876\alpha^2 + 0.00443746\alpha^3 \qquad 6.38$$

Figure 6.8 shows the value of l_i as a function of α for both the exact solution (Equation 6.37) and the polynomial fit (Equation 6.38). The fact that you cannot distinguish the two lines demonstrates that the fit is good.
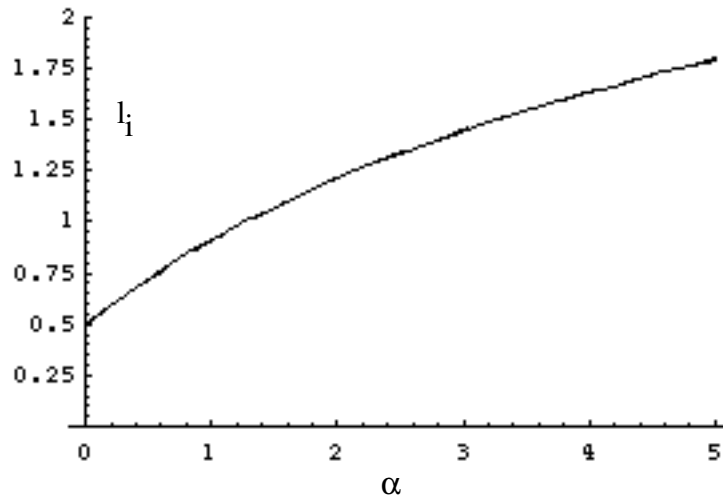
Figure 6.8. The value of l_i as a function of α.

We must determine how to choose the free parameter α. Two ways are suggested. First, if the safety factor (discussed later, but $q = (rB_\phi)/(RB_\theta)$) q(1) at x = 1, (i.e. at r = a) and q(0) at x = 0, (i.e. at r = 0) are known, then

$$\alpha = \frac{q(1)}{q(0)} - 1 \qquad\qquad 6.39$$

We must choose q(0). *Figure 6 .9* shows the resulting α as a function of q(1) for two assumed values of q(0): the long broken line is for q(0) = 0.8, and the short broken line is for q(0) = 1.0. An alternate prescription is to choose α so that the position x_1 of the q = 1 surface is in approximately the correct position. For example, suppose that $x_1 = 1/q(1)$. Then the equation for local safety factor

$$q(x) = q(1)\frac{x^2}{\left(1 - \left(1 - x^2\right)^{1+\alpha}\right)}$$ 6.40

can be solved to give

$$\alpha = \frac{\ln\left|\frac{1 - \frac{1}{q(1)}}{1 - \frac{1}{q(1)^2}}\right|}{\ln\left(1 - \frac{1}{q(1)^2}\right)}$$ 6.41

Figure 6 .9 (solid line) shows the resulting α as a function of q(1).
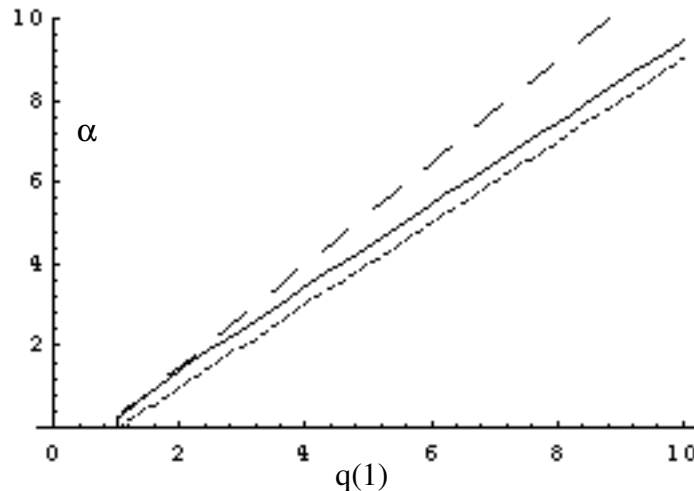
Figure 6.9. The parameter α as a function of q(1), chosen such that 1) solid line: $x_1 = 1/q(1)$, 2) long dashed line q(0) = 0.8, and 3) short dashed line q(0) = 1.0.

We have now uniquely determined α in terms of q(1), and as such there is a unique value of q(0) for each q(a). This is shown in *Figure 6.10*
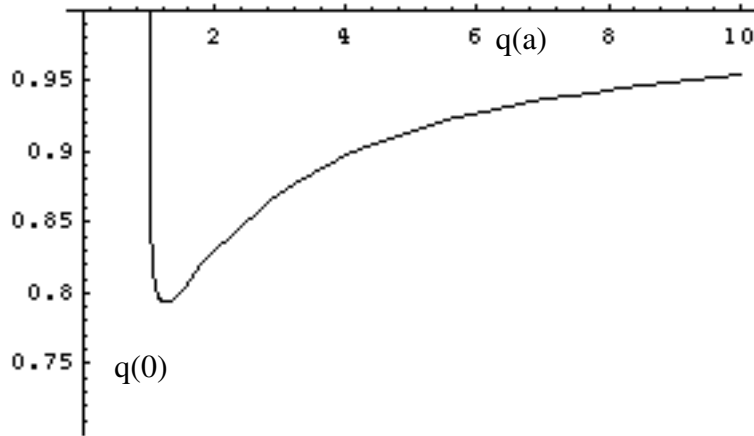
Figure 6.10. The value of q(0) as a function of q(1), with the constraint that $x_1 = 1/q(a)$.

For completeness, *Figure 6.11* shows the various normalized q(x)/q(1) profiles for various values of α.
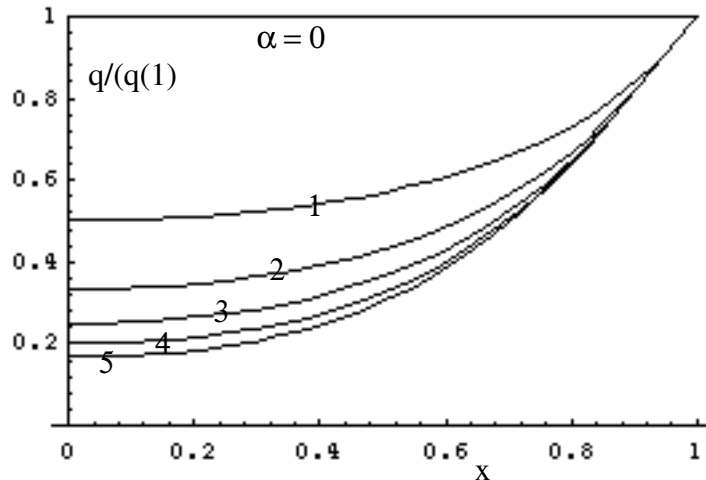
Figure 6.11. Normalized profiles of q for various values of α.

The surface displacements: the Shafranov Shift

If we want to obtain actual values of $\Delta_1(r)$, we have to assume functional forms for the current and pressure distributions, and integrate equation 6.26. We have already discussed a simple current distribution; we must add a simple pressure distribution. Let the zero order pressure be given as

$$p(x) = p_0(0)\left(1 - x^2\right)^{\gamma} \qquad\qquad 6.32$$

so that the poloidal beta value, by definition, is

$$\beta_I = \frac{2\mu_0 p_0(0)}{(1+\gamma)B_{\theta 0}^2(1)}$$ 6.42

Now we can use the normalization x = r/a in equation 6.26 to obtain an expression for the surface displacement:

$$\frac{d\Delta_1}{dx} = -\frac{\varepsilon a}{2}\frac{2x}{\left(1-(1-x^2)^{1+\alpha}\right)^2}$$

$$\left[\beta_I(\gamma+1)x^2(1-x^2)^\gamma - \beta_I\left(1-(1-x^2)^{\gamma+1}\right) - \int_0^x\left(1-(1-x^2)^{1+\alpha}\right)^2\frac{dx}{x}\right]$$ 6.43

Where $\varepsilon = a/R_g$. The Shafranov Shift is defined as the distance between the magnetic and geometric axis: $\Delta_s = \Delta_1(1)$. Using a power series expansion for $\Delta_1(x)$ up to terms x^6 a general expression can be derived:

$$\Delta_s = \frac{\varepsilon a}{2}\left[\frac{1+\frac{2\alpha}{9}+\frac{\alpha^2}{72}}{4} + \frac{\beta_I\gamma(\gamma+1)}{4(1+\alpha)^2}\left\{2+\frac{11\alpha}{9}+\frac{5\alpha^2}{18}+\frac{(\gamma-1)(\gamma-6)}{6}-\frac{4\alpha(\gamma-1)}{9}\right\}\right]$$ 6.44

For the simple case of a flat current profile ($\alpha = 0$, $l_i = 0.5$) and a parabolic pressure profile ($\gamma = 1$) we obtain

$$\Delta_s = \frac{\varepsilon a}{2}\left(\beta_I + \frac{l_i}{2}\right)$$ 6.45

Matching vacuum and plasma solutions

Returning to the field outside the plasma, we must match the vacuum field to the solution for $B_\theta(a)$. The vacuum field is given by the solution to $(\nabla\times\mathbf{B})_\phi = 0$. Expressing B_R and B_Z in terms of ψ (Equations 6.2 and 6.3), $(\nabla\times\mathbf{B})_\phi$ has the form of the LHS of Equation 6.18. This has a solution of the form (for $r \ll R_g$); remember we are outside the plasma:

$$\Psi = 2\pi\psi(r,\theta) = \mu_0 R_g I_p\left(\ln\left(\frac{8R_g}{r}\right)-2\right)$$

$$+\frac{\mu_0 I_p}{2}\left[r\left(\ln\left(\frac{8R_g}{r}\right)-1\right)+\frac{C_1}{r}+C_2r\right]\cos(\theta)$$ 6.46

where the constants C_1 and C_2 are given by the boundary conditions $(\mathbf{B} \cdot \mathbf{n}) = 0$ at the plasma surface $(B_r(a) = 0)$ and the continuity of tangential field at the plasma surface. At infinity ψ takes the form $C_2 r \cos(\theta)$, i.e. this represents the part of ψ from the external sources. The first term on the RHS is the flux from a filament. Substituting 6.46 into 6.24 gives an expression for $B_\theta(a)$, which is matched to the plasma solution equation 6.30 by taking

$$\frac{C_1}{a^2} - C_2 = \ln\left(\frac{8R_g}{a}\right) + 2\Lambda \tag{6.47}$$

Now since $B_r = \dfrac{-1}{rR_g}\dfrac{\partial \psi}{\partial \theta}$ the requirement $B_r(a) = 0$ means that the coefficient of $\cos(\theta)$ in 6.46 is zero at r = a. Therefore we obtain

$$C_1 = a^2(\Lambda + 0.5) \tag{6.48}$$

$$C_2 = -\ln\left(\frac{8R_g}{2}\right) + \Lambda - 0.5 \tag{6.49}$$

Thus we finally obtain an expression for the flux outside the plasma r > a:

$$\psi = \frac{\mu_0 R_g I_p}{2\pi}\left(\ln\left(\frac{8R_g}{r}\right) - 2\right)$$
$$- \frac{\mu_0 r I_p}{4\pi}\left[\left(1 - \frac{a^2}{r^2}\right)\left(\Lambda + \frac{1}{2}\right) + \ln\left(\frac{r}{a}\right)\right]\cos(\theta) \tag{6.50}$$

The field components are given by

$$B_\theta = \frac{1}{R}\frac{\partial \psi}{\partial r}, \quad B_r = -\frac{1}{R_g r}\frac{\partial \psi}{\partial \theta} \tag{6.51}$$

i.e.

$$B_\theta(r,\theta) = -\frac{\mu_0 I_p}{2\pi r} - \frac{\mu_0 I_p}{2\pi R_g}\left[\left(1 + \frac{a_p^2}{r^2}\right)\left(\Lambda + \frac{1}{2}\right) + \ln\left(\frac{r}{a_p}\right) - 1\right]\cos(\theta) \tag{6.52}$$

$$B_r(r,\theta) = -\frac{\mu_0 I_p}{4\pi R_g}\left[\left(1 - \frac{a_p^2}{r^2}\right)\left(\Lambda + \frac{1}{2}\right) + \ln\left(\frac{r}{a_p}\right)\right]\sin(\theta) \tag{6.53}$$

We can also separate the total flux ψ into external (ψ_e) and plasma (ψ_p) parts. At large r, the expression $(\ln(8R_g/r) - 2)$ really approximates an expression which goes to zero. Therefore at large r we have

$$\psi_e = -\frac{\mu_0 I_p}{4\pi}\left(\ln\left(\frac{8R_g}{a}\right) + \Lambda - \frac{1}{2}\right)r\cos(\theta) \qquad\qquad 6.54$$

leaving

$$\psi_p = \frac{\mu_0 R_g I_p}{2\pi}\left(\ln\left(\frac{8R_g}{r}\right) - 2\right)$$
$$-\frac{\mu_0 r I_p}{4\pi}\left[-\ln\left(\frac{8R_g}{r}\right) + 1 - \left(\frac{a}{r}\right)^2\left(\Lambda + \frac{1}{2}\right)\right]\cos(\theta) \qquad\qquad 6.55$$

i.e. the external field at the geometric center $(R = R_g)$ has a component

$$B_z = \frac{1}{R}\frac{\partial\psi_e}{\partial R} = -\frac{\mu_0 I_p}{4\pi R_g}\left(\ln\left(\frac{8R_g}{a}\right) + \Lambda - \frac{1}{2}\right) \qquad\qquad 6.56$$

This is the component of the field which must be produced by external conductors to maintain a tokamak equilibrium.

Figure 6.12 shows contours of the poloidal flux for a plasma with geometric center 0.06 m outside the coordinate center, minor radius $a_p = 0.265$ m, and $\Lambda = 2$. At the inner equator an X point appears, where $\partial\psi/\partial R = 0$. At this point the external vertical field and the poloidal field from the plasma cancel, so that $B_z (= -B_\theta) = 0$. The flux surface through this point is called the separatrix. This X point approaches the plasma surface as β_I increases. As this happens the surfaces are strongly distorted from circular, and the above equations starts break down. *Figure 6.13* shows the poloidal flux $\psi = \Psi/(2\pi)$ in the plane z = 0 for a plasma with minor radius $a_p = 0.2$m, a major geometric radius $R_g = 1$m, current $I = 1/\mu_0$, and $\Lambda = 2$. The external source (vertical field) and plasma components are shown separately. *Figure 6.14* shows the minor radial (B_r) and poloidal (B_θ) field components for this plasma, on a circular contour concentric with the plasma minor radius.
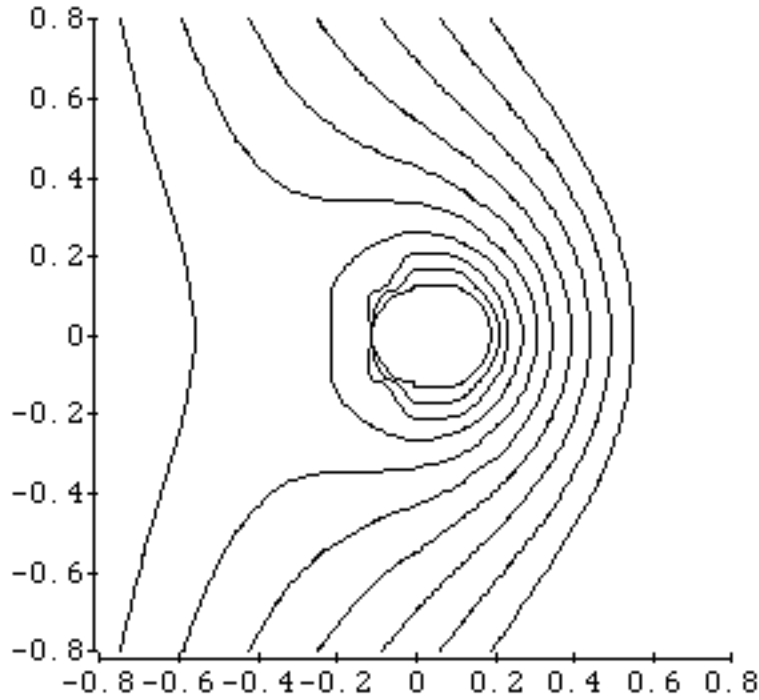
Figure 6.12. Flux contours for a (badly drawn) circular plasma with geometric center 0.06 m outside the coordinate center, minor radius 0.265m, $\Lambda = 2$.
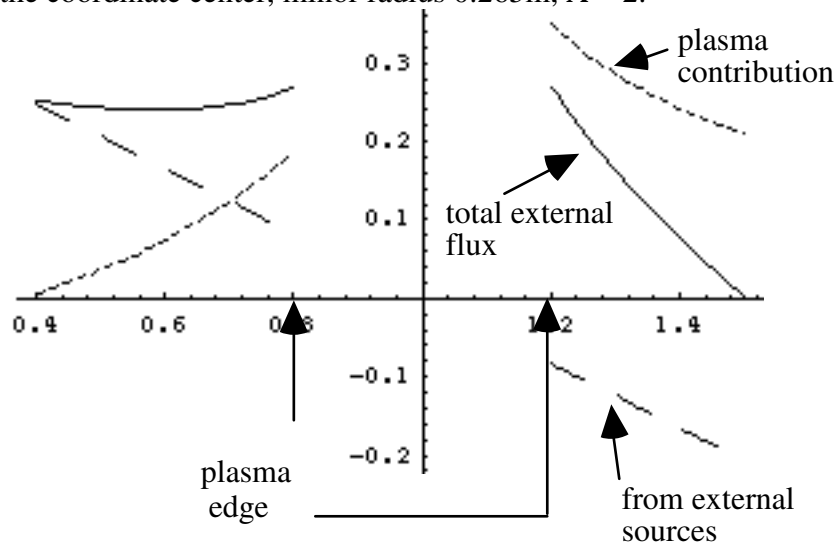
Figure 6.13. The external poloidal flux $\psi = \Psi/(2\pi)$ in the plane z = 0 for a plasma with minor radius $a_p = 0.2$m, a major geometric radius $R_g = 1$m, current $I = 1/\mu_0$, and $\Lambda = 2$.
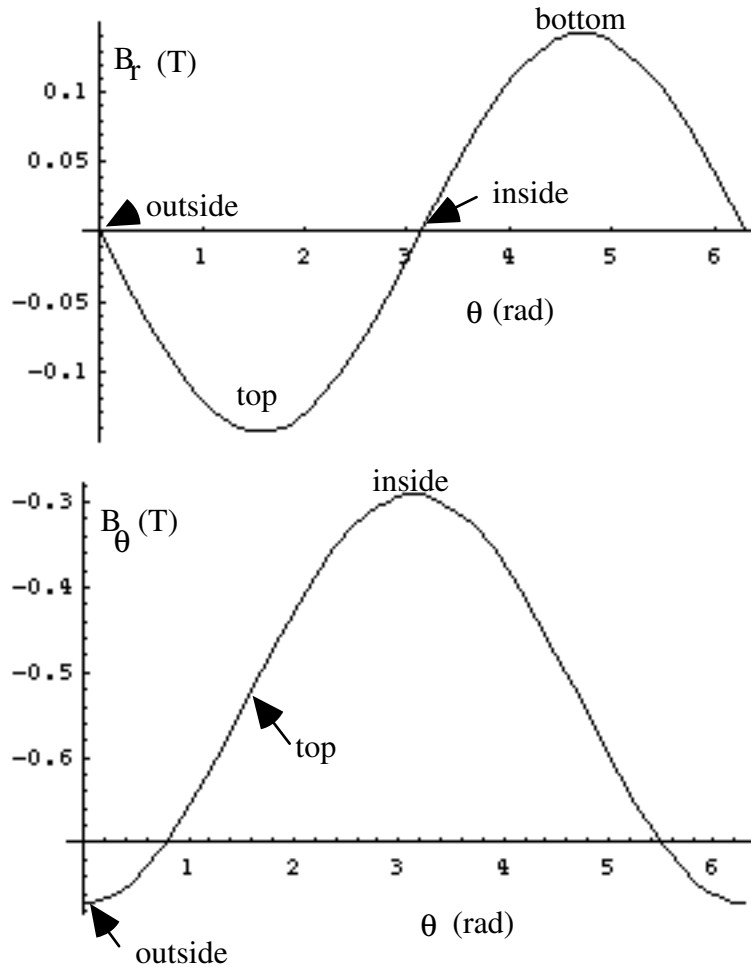
Figure 6.14. The field components B_r and B_θ on a contour with minor radius 0.3m placed outside and concentric with the plasma described in *Figure 6.13*.

More complicated configurations.

It is easy to make non circular cross sectioned plasmas. Adding a quadrupole field produces an elliptic deformation. Adding a hexapole field produces a triangular deformation. There are some analytic expressions available for non circular cross sections, but in general numerical solutions to the basic Grad Shafranov equation must be used.

7. Position and $\beta_I + I_i/2$ for the circular equilibrium

An 'exact' circular equilibrium

Consider the pickup coils shown in *Figure 7.1*. Two coils ($B_{\omega 1}$, $B_{\omega 2}$) measure the poloidal field at the inner and outer equator, each at a distance b from some center at $R = R_l$. A saddle coil measures the difference in flux between the inner and outer equator. Instead of the partial flux loops (i.e. the saddle coil) shown in *Figure. 7.1*, two complete flux loops could be used, as in the plan view of *Figure 7.2*. We want to know what these coils tell us for our circular equilibrium.
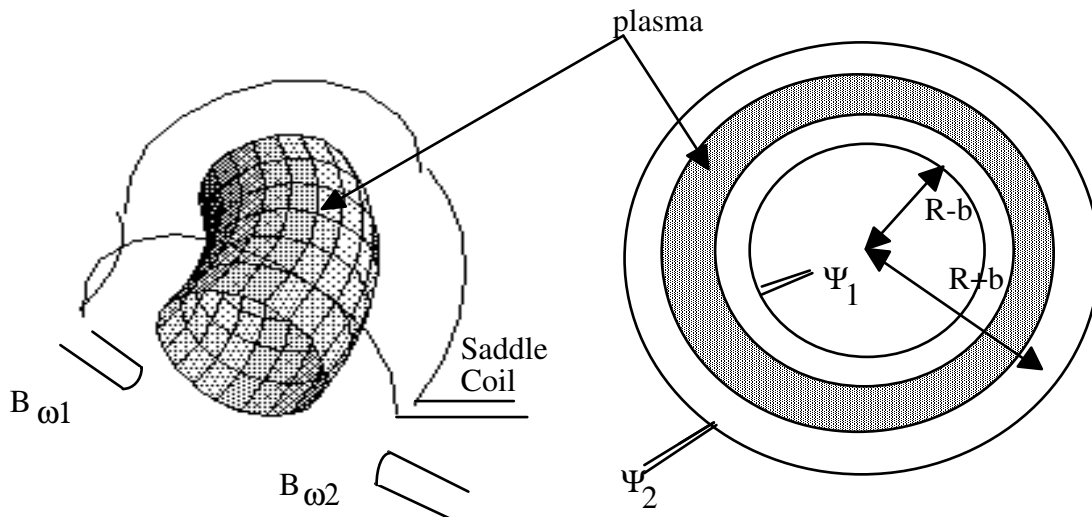
Fig 7.1. Saddle and B_ω coils   Fig 7.2. A plan view of poloidal flux loops

The original equilibrium was derived in a coordinate system (r,θ,ϕ) based on the plasma geometric center R_g. We must translate the results to a coordinate system (ρ,ω,ϕ) based on for example the center of a circular contour centered at $R = R_l$, which might be the vacuum vessel center. Details are seen in *Figure 7.3*.

70
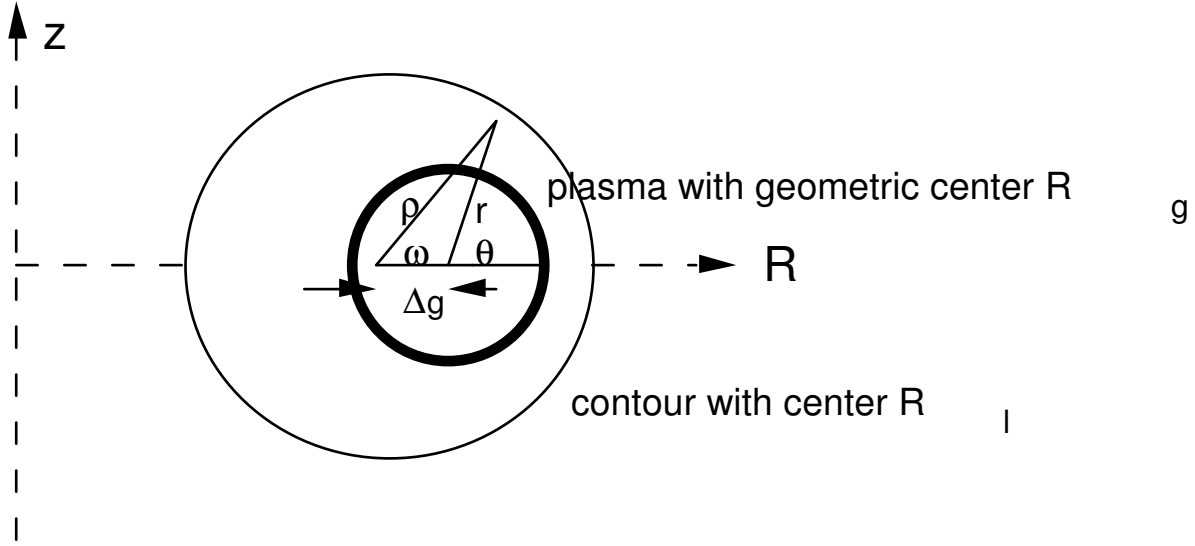
Figure 7.3. The coordinate systems associated with the geometric center R_g, and an external contour center R_l.

Then $R = R_l + \rho\cos(\omega)$, $z = \rho\sin(\omega)$, and let $\Delta_g = R_g - R_l$ be the displacement of the plasma geometric center from the contour center. Remembering that we are only dealing with r > a, the plasma minor radius, and taking $\Delta_g/a_p \ll 1$, we can rewrite Equation 6.50 as

$$\frac{\Psi}{2\pi} = \frac{\mu_0 R_1 I_p}{2\pi}\left(\ln\left(\frac{8R_1}{\rho}\right) - 2\right) - \frac{\mu_0 \rho I_p}{4\pi}\left[\left(1 - \frac{a_p^2}{\rho^2}\right)\left(\Lambda + \frac{1}{2}\right) + \ln\left(\frac{\rho}{a_p}\right) - \frac{2R_1\Delta_g}{\rho^2}\right]\cos(\omega)$$

7.1

The tangential and normal field components on the circular contour are then

$$B_\omega(\rho,\omega) = -\frac{\mu_0 I_p}{2\pi\rho} - \frac{\mu_0 I_p}{4\pi R_1}\left[\left(1 + \frac{a_p^2}{\rho^2}\right)\left(\Lambda + \frac{1}{2}\right) + \ln\left(\frac{\rho}{a_p}\right) - 1 + \frac{2R_1\Delta_g}{\rho^2}\right]\cos(\omega)$$

7.2

$$B_\rho(\rho,\omega) = -\frac{\mu_0 I_p}{4\pi R_1}\left[\left(1 - \frac{a_p^2}{\rho^2}\right)\left(\Lambda + \frac{1}{2}\right) + \ln\left(\frac{\rho}{a_p}\right) - \frac{2R_1\Delta_g}{\rho^2}\right]\sin(\omega)$$			7.3

Now turning to the coil configurations of *Figure 7.1* and *7.2*, the outer coils at $\rho = b$, $\omega = 0$ measure $B_{\omega 2}$, and the inner coils at $\rho = b$, $\omega = \pi$ measure $B_{\omega 1}$. The saddle or flux loops measure the difference in flux between the inner (Ψ_1) and outer (Ψ_2) equator. Define

$$B_\perp = \frac{\Psi_1 - \Psi_2}{4\pi R_1 b} = \frac{\psi_1 - \psi_2}{2R_1 b}$$			7.4

then

$$\frac{B_{\omega 2} - B_{\omega 1}}{2} + B_{\perp} = \frac{\mu_0 I_p}{2\pi R_1} \left[\ln\left(\frac{b}{a_p}\right) + \beta_I + \frac{l_i}{2} - 1 \right]$$ 7.5

and

$$\frac{\Delta_g}{b} = \frac{b}{2R_1} \left[\left(\frac{a_p^2}{b^2}\right) \ln\left(\frac{b}{a_p}\right) + 0.5\left(1 - \frac{a_p^2}{b^2}\right) \right] + \frac{\pi b}{\mu_0 I_p} \left[\frac{(B_{\omega 2} - B_{\omega 1})}{2}\left(1 - \frac{a_p^2}{b^2}\right) - B_{\perp}\left(1 + \frac{a_p^2}{b^2}\right) \right]$$

7.6

Therefore, assuming circular equilibrium, we can obtain the geometric displacement of the plasma from the vessel center, and the parameter $\Lambda = \beta_I + l_i/2 - 1$ if we have an estimate of the plasma radius a_p. To get a_p we must iterate our Equations 7.5 and 7.6, starting with an assumed value (say the limiter radius a_{lim}), and replacing it at step n by the maximum possible radius defined by Δ_g and the specified limiter geometry at step (n-1). Such a procedure is shown below

Īterations to determine magnetic configuration from fields.

1. Set initial guess for plasma minor radius ap = limiter radius. Measure poloidal fields.

2. CalculateΛ andΔ using estimated ap.

3. Calculate plasma geometric center from estimated apΔ, and Λ.

4. Estimate new radius ap from plasma geometric center and limiter locations.
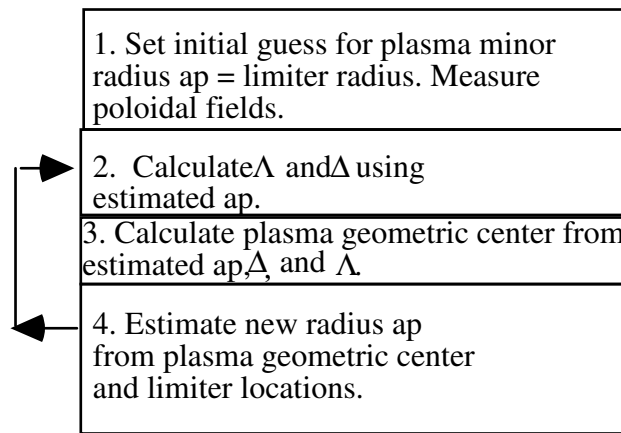
A more sophisticated method is to use a modified Rogowski coil ($nA \propto \cos(\omega)$) to measure the part of $B_{\omega}(\rho,\omega)$ proportional to $\cos(\omega)$, and a saddle coil (width $\propto \sin(\omega)$) to measure that part of $B_{\rho}(\rho,\omega)$ proportional to $\sin(\omega)$. Such coils were shown in *Figures 3.2* and *3.3*. The coefficients measured (after time integration) will be, for a coil on a circular contour of radius ρ,

$$\lambda_1 = -\frac{\rho}{2R_1} \left[\left(1 + \frac{a_p^2}{\rho^2}\right)\left(\Lambda + \frac{1}{2}\right) + \ln\left(\frac{\rho}{a_p}\right) - 1 + \frac{2R_1\Delta_g}{\rho^2} \right]$$ 7.7

$$\mu_1 = -\frac{\rho}{2R_1}\left[\left(1-\frac{a_p^2}{\rho^2}\right)\left(\Lambda+\frac{1}{2}\right)+\ln\left(\frac{\rho}{a_p}\right)-\frac{2R_1\Delta_g}{\rho^2}\right] \qquad 7.8$$

From these two equations we obtain

$$\frac{\rho}{2}(\lambda_1-\mu_1)+\frac{\rho^2}{4R_g}=\Delta_g+\frac{a_p^2}{2R_l}(\Lambda+0.5) \qquad 7.9$$

$$\frac{R_l}{\rho}(\lambda_1+\mu_1)=\Lambda+\log\left(\frac{\rho}{a_p}\right)=\Lambda_T \qquad 7.10$$

from which we can obtain the two unknowns Λ and Δ_g, assuming a_p (which must be determined, together with Λ and Δ_g, by iteration). Note that the term $\ln(r/a)$ represents that part of the inductance between the plasma surface and the coils.

Extension of position measurement to non circular shapes

The previous section showed how, for our circular equilibrium model, the geometric center could be measured. We would like to generalize the method to allow non circular shapes. In fact, the exact same diagnostics can do this, with certain important assumptions about the major radial dependence of the flux Ψ.
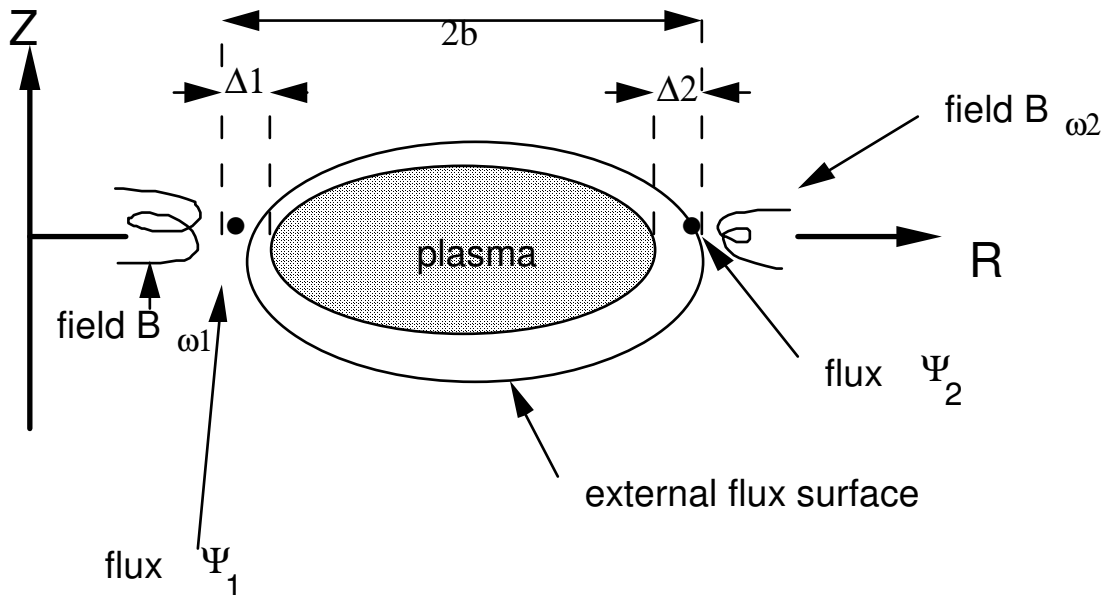
Figure 7.4. Flux loops and poloidal field pick-up coils outside a plasma. There is a coordinate system based on the center $R = R_l$ of the two measuring coils and flux loops

(sensors). The sensors are at a distance b from R_l. The plasma geometric center is displaced Δ_g from R_l.

Consider the situation in *Figure 7.4*. The measurements of flux and field are supposed to be at the same location, either at point 1 (shown at the smaller major radius) or point 2 (larger major radius). If the loops have the same value of flux, then they sit on a flux surface. Using the saddle coil as shown in *Figure 7.1*, if the saddle coil output is zero then the inner and outer toroidal legs are on a flux surface. We expand the flux as

$$\Psi_{plasma} = \Psi_{loop} + \Delta\frac{\partial\Psi}{\partial R}$$

7.11

with Δ the distance between the loop and the plasma surface. This expansion goes badly wrong if there is an X point between the measuring loops and coils and the plasma surface, because in this case there is a point between the measuring loops and the plasma where $\partial\Psi/dR = 0$. Since $B_\omega = 1/(2\pi R)\partial\Psi/\partial\rho$, we can write

$$\Psi_1 = \Psi_{loop} + 2\pi R_1 \Delta_1 B_{\omega 1}$$

7.12

$$\Psi_2 = \Psi_{loop} + 2\pi R_2 \Delta_2 B_{\omega 2}$$

7.13

Now $\Delta_2 = b-a_p-\Delta_g$, $\Delta_1 = b-a_p+\Delta_g$, $R_1 = R_l-b$, $R_2 = R_l+b$, so that Equations 7.12 and 7.13 give

$$\Delta_g = \frac{\Psi_1 - \Psi_2}{2\pi\left[B_{\omega 1}\left(R_1 - b\right) + B_{\omega 2}\left(R_1 + b\right)\right]} - \left(b - a_p\right)$$

7.14

Therefore we can measure Δ_g if we know the plasma minor radius a_p. In limiter geometry a_p is determined by Δ_g and the assumed known limiter geometry, so that as described before iterations are necessary to provide both a_p and Δ_g. If necessary terms in $\partial^2\Psi/\partial R^2$ can be measured using more B_ω coils (two at the inner, and two at the outer, equator). If the plasma is bounded by a separatrix, then the whole expansion is useless anyway, and we must turn to integral relationships discussed later.

Extension of $\beta_I + l_i/2$ measurement to non circular shapes

From our simple circular equilibrium described in section 6, we know that the external field required to maintain a circular low beta plasma is given by Equation 6.49:

$$B_Z = -\frac{\mu_0 I_p}{4\pi R_g}\left[\ln\left(\frac{8R_g}{a_p}\right) + \Lambda - \frac{1}{2}\right]$$

7.15

Therefore if we know all the currents in the external conductors, the plasma current, minor radius and major radius, we can calculate B_Z at the geometric axis $R = R_g$, and obtain a value for $\Lambda = \beta_I + l_i/2 -1$. The result (Equation 7.15) has been found by numerical simulation to be accurate even for non circular discharges. Therefore if we can calculate the maintaining field, and know the plasma minor radius and geometric center, we can calculate $\beta_I + l_i/2$. It becomes difficult to calculate the maintaining field if we have an iron core present; we will discuss this later. However, there are more general techniques which do not explicitly require this calculation of fields from currents, and we also discuss these later.

Non-circular contours.

So far we have only considered poloidal field measurements which can be made on a circular contour. In many cases the simplest contour to use is that of the vacuum vessel, which is often non circular. What do we do then? In section 3 we discussed how fields on a rectangle can be characterized, and suggested that coils wound to measure "moments" might be useful. Specifically, we discussed modified Rogowski coils which would measure

$$s_{p,\tau} = \oint_l f_p B_\tau dl \qquad\qquad 7.16$$

and saddle coils which would measure

$$s_{p,n} = \oint_l f_p B_n dl \qquad\qquad 7.17$$

where the functions f_p were taken to be the pth power of a vector radius on the contour l. The geometry is re drawn in *Figure 7.5*.
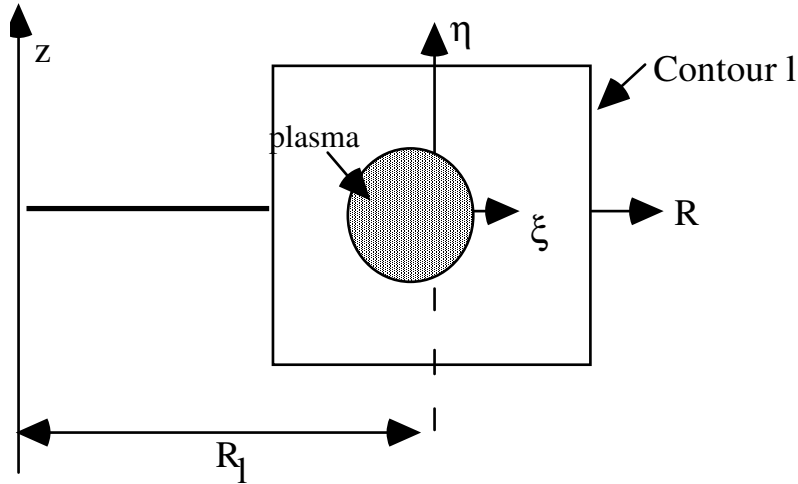
Figure 7.5. Geometry used for a non-circular contour.

An analogy with our cosinusoidally wound Rogowski coil and sinusoidally wound saddle coil would be a modified Rogowski coil measuring the first symmetric (in vertical position) moment

$$s_{1,\tau} = \oint_l \xi B_\tau dl \qquad\qquad 7.18$$

and a saddle coil measuring the first asymmetric (in vertical position) moment

$$\lambda_1 = -\frac{\rho}{2R_1}\left[\left(1+\frac{a_p^2}{\rho^2}\right)\left(\Lambda+\frac{1}{2}\right)+\ln\left(\frac{\rho}{a_p}\right)-1+\frac{2R_1\Delta_g}{\rho^2}\right] \qquad\qquad 7.19$$

To interpret what these coils will measure, we can write an equation for the components B_τ and B_n on our chosen contour (for a rectangular contour they will be either B_η or B_ξ). Because the only variables in the equations for an assumed circular equilibrium are the geometric displacement Δ_g, Λ and minor radius a_p, we must be able to derive expressions for the measured coil outputs $s_{1,\tau}$ and $s_{1,n}$ in terms of these variables. For example, if our contour is a square of half height and half width a, centered at $R = R_l$, we must find

$$s_{1,\tau} = s_{1,\tau}\left(I_p, \Lambda, \Delta_g, a_p, a, R_l\right) \qquad\qquad 7.20$$

$$s_{1,n} = s_{1,n}\left(I_p, \Lambda, \Delta_g, a_p, a, R_l\right) \qquad\qquad 7.21$$

In principle we can then solve Equations 7.20 and 7.21 to give expressions for the required Λ and Δ_g. Iterations will be necessary because we will find a_p entering the final results, which itself is only determined once Δ_g is known.

It may be that the particular geometry of the contour precludes performing the analytic integrals (Equations 7.18 and 7.19, using the analytical representation for the equilibrium fields outside a circular plasma). In this case the problem must be solved numerically. Equations 7.18 and 7.19 are solved numerically for many different Δ_g, Λ, and a_p (we assume the contour geometry does not change!) A regression analysis is then performed, in which solutions of the form

$$\Lambda = f\left(\frac{S_{1n}}{I_p}, \frac{S_{1\tau}}{I_p}, a_p, contour\, geometry\right) \qquad\qquad 7.22$$

$$\Delta_g = f\left(\frac{S_{1n}}{I_p}, \frac{S_{1\tau}}{I_p}, a_p, contour\, geometry\right) \qquad\qquad 7.23$$

are sought.

8. SOME FUNDAMENTAL RELATIONS

Geometry

In section 6 we derived an analytic expression for the flux outside a large aspect ratio ($a/R_g \ll$ 1) circular plasma, which we used in section 7 to interpret magnetic field measurements. Here we want to derive some relationships which are of general use: we shall test them for the analytic equilibrium of section 6.   Use a <u>right handed</u> cylindrical coordinate system (R, ϕ, z), usually symmetric w.r.t. rotations around $R = 0$. Referring to *Figure 8.1*, there is an axisymmetric region V, which completely encloses the plasma. The cross section of V in the poloidal half plane ($\phi = 0$, $R > 0$) is S_ϕ, and the boundaries are S_n and l. dV is the volume element on V, dS_ϕ the area element on S_ϕ, dS_n is the area element on S_n and dl the line element on l. Therefore

$$dV = 2\pi R dS_\phi \qquad\qquad\qquad\qquad 8.1$$

$$dS_n = 2\pi R dl \qquad\qquad\qquad\qquad 8.2$$
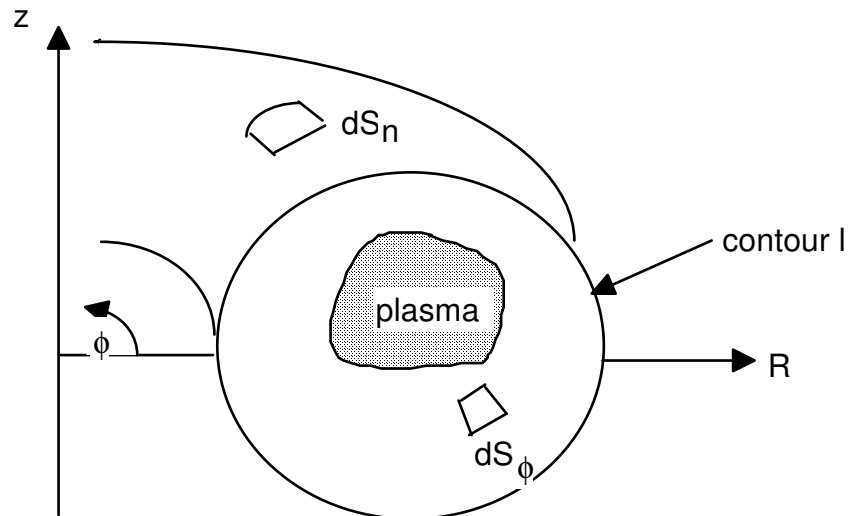
Figure 8.1. Geometry

Normal and tangential derivatives on l are $\partial/\partial n$ and $\partial/\partial\tau$. The positive orientation on l is that S_ϕ lies on the RHS. Note this is DIFFERENT from what was assumed in section 6. The general question is: "How can we derive information on the magnetic field and plasma in V (or S_ϕ) from the fields measured on l?"

Field representation

We shall try and be as general as possible. First we quickly re-derive the equilibrium equation. For the case of axisymmetry, we discussed in section 6 the description of the fields using the form

$$\frac{\Psi}{2\pi} = \frac{\mu_0 R_1 I_p}{2\pi}\left(\ln\left(\frac{8R_1}{\rho}\right) - 2\right) - \frac{\mu_0 \rho I_p}{4\pi}\left[\left(1 - \frac{a_p^2}{\rho^2}\right)\left(\Lambda + \frac{1}{2}\right) + \ln\left(\frac{\rho}{a_p}\right) - \frac{2R_1\Delta_g}{\rho^2}\right]\cos(\omega)$$

8.3

where

$$F = RB_\phi = \mu f \tag{8.4}$$

and $\psi = RA_\phi$

From $\nabla \times \mathbf{H} = \mathbf{j}$, we can also write

$$\mathbf{j} = -\frac{1}{\mu}L^*\psi\nabla\phi + \nabla\left(\frac{F}{\mu}\right) \times \nabla\phi \tag{8.5}$$

where the operator L^* is defined for axisymmetric scalar fields as

$$L^*\psi = \mu R^2 \nabla \bullet \left(\frac{\nabla\psi}{\mu R^2}\right) \tag{8.6}$$

The operator L^* satisfies the equation

$$L^*\psi = -\mu R j_\phi \tag{8.7.}$$

For uniform permeability $\mu = \mu_0$ we have L^* reducing to the operator Δ^*:

$$\Delta^*\psi = R^2 \nabla \bullet \left(\frac{\nabla\psi}{R^2}\right) = R\frac{\partial}{\partial R}\left(\frac{1}{R}\frac{\partial\psi}{\partial R}\right) + \frac{\partial^2\psi}{\partial z^2}\Delta \tag{8.8}$$

That is, Δ^* is the operator on the LHS of the Grad Shafranov equation. We also introduce the operator L:

$$L\psi = \frac{1}{\mu}\nabla \bullet (\mu\nabla\psi) \tag{8.9}$$

which reduces to the Laplacian Δ for uniform permeability. In a current free region we can use the representation $\mathbf{H} = \nabla g$, and $\nabla \cdot \mathbf{B} = 0$ is then equivalent to $Lg = 0$.

Identities

Now we turn to some identities. Green's first identity for L^* is:

$$\int_{S_\phi} \frac{1}{\mu R} \psi L^* \Theta dS_\phi = \oint_l \frac{1}{\mu R} \psi \frac{\partial \Theta}{\partial n} dl - \int_{S_\phi} \frac{1}{\mu R} \nabla \psi \bullet \nabla \Theta dS_\phi \qquad\qquad 8.10$$

Green's second identity (Green's theorem) is:

$$\int_{S_\phi} \frac{1}{\mu R} \left(\psi L^* \Theta - \Theta L^* \psi \right) dS_\phi = \oint_l \frac{1}{\mu R} \left(\psi \frac{\partial \Theta}{\partial n} - \Theta \frac{\partial \psi}{\partial n} \right) dl \qquad\qquad 8.11$$

Both of these are derived by applying the divergence theorem to appropriate expression on V. In particular see Smythe, static and dynamic electricity, page 53 eqn. 3.06(2) for a derivation of Green's theorem, which is, for scalars A, B and E,

$$\int_V \left[A \nabla \bullet (E \nabla B) - B \nabla \bullet (E \nabla A) \right] dV = \int_{S_n} E \left[A \frac{\partial B}{\partial n} - B \frac{\partial A}{\partial n} \right] dS_n \qquad . \qquad\qquad 8.11b$$

Now let the function G(R,R') satisfy the equation $L^* G = \mu R' \delta(R-R')$ in S_ϕ, where G is considered a function of R at fixed R'. No boundary conditions mean that G is specified to within a constant. Then we obtain Green's third identity:

$$\psi(R') = -\int_{S_\phi} G j_\phi dS_\phi + \oint_l \frac{1}{\mu R} \left(\psi \frac{\partial G}{\partial n} - G \frac{\partial \psi}{\partial n} \right) dl \qquad\qquad 8.12$$
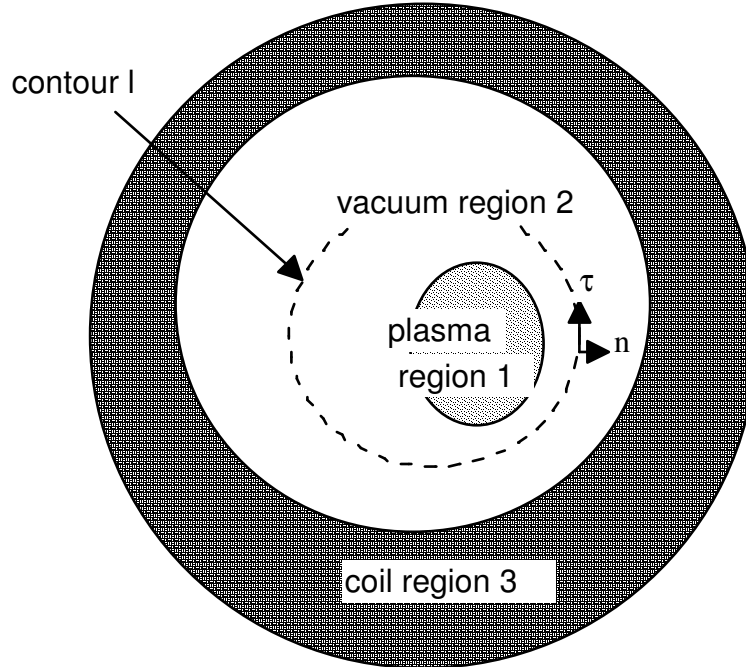
Figure 8.2. The boundaries between the plasma ($S_{\phi plasma}$) region 1, vacuum ($S_{\phi vacuum}$) region 2 and coil ($S_{\phi coil}$) region 3.

Suppose S_ϕ can be split up into three regions, $S_{\phi plasma}$, $S_{\phi vacuum}$ and $S_{\phi coils}$, as shown in *Figure 8.2*. Assume $\mu = \mu_0$ in the plasma and vacuum region. The exterior region (the complement of S_ϕ in the right half plane) is called $S_{\phi ext}$. Then if this external region has only linear magnetic material, we can apply the last equation on the region $S_\phi + S_{\phi ext}$. Choosing the Greens function G_0 so that $G_0(R,R') = 0$ as $|R|$ goes to infinity, and as R goes to 0, we have

$$\psi(R') = - \int_{S_\phi + S_{\phi ext}} G_0 j_\phi dS_\phi \qquad 8.13$$

i.e. $G_0(R,R')$ equals the flux at R' caused by a negative current at position R. Therefore we define

$$\psi_{\mathbf{int}}(R') = - \int_{S_\phi} G_0 j_\phi dS_\phi \qquad 8.14$$

$$\psi_{ext}(R') = \oint_l \frac{1}{\mu R} \left(\psi \frac{\partial G_0}{\partial n} - G_0 \frac{\partial \psi}{\partial n} \right) dl \qquad 8.15$$

and $\psi = \psi_{ext} + \psi_{int}$ from Equation 8.12. We understand ψ_{ext} as the part of the flux caused by currents in the exterior region, and ψ_{int} is that part of the flux associated due to currents in S_ϕ. ψ_{int} is homogeneous in the exterior region, and ψ_{ext} is homogeneous in the interior region.

An analytic expression for G_0 if $\mu = \mu_0$ everywhere is:

$$G_0(R,R') = \frac{\mu_0}{k\pi}\sqrt{RR'}\left[E(k^2) - \left(1 - \frac{k^2}{2}\right)K(k^2)\right]$$

8.16

where

$$k^2 = \frac{4RR'}{\left((R+R')^2 + (z-z')^2\right)}$$

8.17

Ideal MHD

Here we want to note only one important equation, which is a generalization of the "virial" equation. We use Equations 6.1, 1.1 and 1.2. Allow the total equilibrium field to be split up into two parts,

$$\mathbf{B} = \mathbf{B_1} + \mathbf{B_2}$$

8.18

with $\nabla \times \mathbf{B}_2 = 0$. We can choose the partitioning of B in a number of ways. Multiplying $\mathbf{j} \times \mathbf{B} = \nabla p$ by an arbitrary vector $\mathbf{Q}$, we can obtain

$$\int_V\left[\left(p + \frac{B_1^2}{2\mu_0}\right)\nabla \bullet \mathbf{Q} - \frac{\mathbf{B_1} \bullet \nabla \mathbf{Q} \bullet \mathbf{B_1}}{\mu_0}\right]dV$$

$$= \int_{S_n}\left[\left(p + \frac{B_1^2}{2\mu_0}\right)(\mathbf{Q} \bullet \mathbf{n}) - \frac{(\mathbf{B_1} \bullet \mathbf{Q}) \bullet (\mathbf{B_1} \bullet \mathbf{n})}{\mu_0}\right]dS_n - \int_V \mathbf{Q} \bullet (\mathbf{j} \times \mathbf{B_2})dV$$

8.19

with n the normal to the surface S_n. We have made use of the vector identity

$$\mathbf{Q}[\nabla \times \mathbf{B} \bullet \mathbf{B}] = \nabla \bullet \left[(\mathbf{Q} \bullet \mathbf{B})\mathbf{B} - \frac{B^2}{2}\mathbf{Q}\right] + \frac{B^2}{2}\nabla \bullet \mathbf{Q} - \mathbf{B}(\mathbf{B} \bullet \nabla)\mathbf{Q}$$

We shall use equation 8.19 later to derive important integral relationships.

Boundary conditions

Last in this section we turn to boundary conditions. Suppose we have our three regions, as in *Figure 8.2*. Region 1 ($S_{\phi plasma}$) contains all the plasma current. Region 2 ($S_{\phi vacuum}$) contains no source, but contains a contour l on which we make measurements. Region 3 ($S_{\phi coils}$) is outside region 2, extends to infinity, and contains all external currents. To find the plasma boundary we have to know $\psi(R,z)$ in region 2 between the contour on which parameters are measured, and the plasma boundary itself. In principle we can do this knowing either

a) $\partial\psi/\partial n$ (i.e. the tangential field) and either $\partial\psi/\partial\tau$ (the normal field) or ψ on part of l (note specifying $\partial\psi/\partial\tau$ is equivalent to specifying ψ to within an unimportant constant after integration. This is the Cauchy condition. However, there are significant problems with stability to small errors in the measurements. Therefore another useful set of boundary conditions is

b) all currents in region 3, and either $\partial\psi/\partial n$, $\partial\psi/\partial\tau$ or ψ on l. For example, suppose we know the currents and ψ on l. The total fields are then the superposition of the contributions from the external currents in region 3 and the plasma current in region 1:

$$\psi(R,z) = \psi_{plasma} + \psi_{external} \qquad\qquad 8.20$$

$\psi_{external}$ is already specified by specifying the external currents, so we must only determine ψ_{plasma}. Since ψ_{plasma} is homogeneous outside l, it must be completely specified by the condition $\partial\psi_{plasma}/\partial n = 0$ at infinity and either ψ_{plasma} (Dirichlet) or $\partial\psi_{plasma}/\partial n$ on l (Neumann). But condition 2 tells us we already have one of these specified, so that ψ_{plasma} must be determined everywhere outside and on l.

In fact we usually use an apparently over determined problem, for example knowing the external currents, $\partial\psi/\partial n$ and $\partial\psi/\partial\tau$ on l. In fact this is not over determined because we only have the fields at discrete points, and usually the boundary conditions are only applied in a least squares sense.

9. MOMENTS OF THE TOROIDAL CURRENT DENSITY

Let Θ be an arbitrary function satisfying the homogeneous equilibrium equation $L^*\Theta = 0$ in S_ϕ, and let ψ be the poloidal flux function which satisfies $L^*\psi = -\mu R j_\phi$. Apply Green's second identity for the operator L^* (Equation 8.11) to the pair (Θ, ψ): we obtain a fundamental integral equation:

$$\int_{S_\phi} \Theta j_\phi dS_\phi = \int_l \frac{1}{\mu R}\left(\psi \frac{\partial \Theta}{\partial n} - \Theta \frac{\partial \psi}{\partial n} \right) dl \qquad 9.1$$

The moments of the current density (i.e. the integral on the LHS) are expressed in terms of ψ and $\partial\psi/\partial n$ on the boundary. From $L^*\Theta = 0$ we have $\int_l R^{-1}\mu^{-1}(\partial\Theta/\partial n)dl = 0$ so there is no dependence upon the choice of the arbitrary constant in ψ. We introduce together with Θ a conjugate function ξ according to the equation

$$\nabla\left(\frac{\xi}{\mu R} \right) = \frac{\nabla\Theta \times \nabla\phi}{\mu} \qquad 9.2$$

which admits a solution $L^*\Theta = 0$. In cylindrical geometry, Equation 9.2 is

$$\frac{\partial}{\partial R}\left(\frac{\xi}{\mu R} \right) = -\frac{1}{\mu R}\frac{\partial\Theta}{\partial z} \qquad 9.3$$

$$\frac{\partial}{\partial z}\left(\frac{\xi}{\mu R} \right) = -\frac{1}{\mu R}\frac{\partial\Theta}{\partial R} \qquad 9.4$$

The function ξ satisfies $L(R^{-1}\mu^{-1}\xi) = 0$, (remember the operator $L = \mu^{-1}\nabla\cdot(\mu\nabla\psi)$, which reduces to the Laplacian if μ is uniform). Therefore the definition of ξ implies through Equations 9.3 and 9.4 that $-\partial(R^{-1}\mu^{-1}\xi)/\partial\tau = R^{-1}\mu^{-1}\partial\Theta/\partial n$, where $\partial/\partial\tau$ is the partial derivative along l (clockwise on the outer boundary). Now by partial integration we can eliminate ψ from Equation 9.1 and write in terms of $\partial\psi/\partial\tau$:

$$\int_{S_\phi} \Theta j_\phi dS_\phi = \int_l \frac{1}{\mu R}\left(\xi\frac{\partial\psi}{\partial\tau} - \Theta\frac{\partial\psi}{\partial n} \right) dl = \int_l \frac{1}{\mu}\left(\xi B_n + \Theta B_\tau \right) dl \qquad 9.5$$

i.e. the "moments" over the current density can be measured as line integrals of the normal ($B_n = (1/R)\partial\psi/\partial\tau$) and tangential fields ($B_\tau = -(1/R)\partial\psi/\partial n$) along the contour l.

An alternate derivation follows by letting fields **q** and g satisfy the equation $\frac{1}{\mu}(\nabla \times \mathbf{q}) = \nabla\left(\frac{g}{\mu}\right)$,

so that $\nabla \times (\nabla \times \mathbf{q}) = 0$. Then

$$\int_V \mathbf{q} \bullet \mathbf{j} dV = \int_V \mathbf{q} \bullet \left(\nabla \times \frac{\mathbf{B}}{\mu}\right) dV = \int_V \left[\nabla \bullet \left(\frac{\mathbf{B}}{\mu} \times \mathbf{q}\right) + \frac{\mathbf{B}}{\mu} \bullet (\nabla \times \mathbf{q})\right] dV$$

$$= \int_V \left[\nabla \bullet \left(\frac{\mathbf{B}}{\mu} \times \mathbf{q}\right) + \mathbf{B} \bullet \nabla\left(\frac{g}{\mu}\right)\right] dV = \int_{S_n} \left[\left(\frac{\mathbf{B}}{\mu} \times \mathbf{q}\right) \bullet \mathbf{n} + \left(\frac{g}{\mu}\right) \mathbf{B} \bullet \mathbf{n}\right] dS_n$$

9.6

This has not invoked axisymmetry. Letting $\mathbf{q} = \Theta\nabla\phi =$ and $g = R^{-1}\xi$, and using Equations 8.1 and 8.2 gives the previous result (Equation 9.5).

To get the notation used by Shafranov, we let $\mathbf{q} = f\nabla\phi$ (which has a component only in the f direction, $q = f/R$) and consider uniform permeability μ_0. Then we can write an expression for the "multipole moment" Y_m of the toroidal current density

$$Y_m = \frac{1}{I_p} \int_{S_\phi} f_m j_\phi dS_\phi = \frac{1}{\mu_0 I_p} \oint_l (f_m B_\tau + R g_m B_n) dl \qquad 9.7$$

where, from Equations 9.3 and 9.4, (i.e. $\frac{1}{\mu}(\nabla \times \mathbf{q}) = \frac{1}{\mu}\left(\nabla \times \frac{f}{R}\mathbf{e}_\phi\right) = \nabla\left(\frac{g}{\mu}\right)$) f_m and g_m are

various solutions of

$$\frac{\partial g}{\partial R} = -\frac{1}{R}\frac{\partial f}{\partial z} \qquad 9.8$$

$$\frac{\partial g}{\partial z} = \frac{1}{R}\frac{\partial f}{\partial R} \qquad 9.9$$

Remember that $\nabla \times (\nabla \times \mathbf{q}) = 0$, with $\mathbf{q} = f\nabla\phi = \mathbf{e}_\phi f/R$, so the equation for f is

$$\frac{\partial^2 f}{\partial R^2} - \frac{1}{R}\frac{\partial f}{\partial R} + \frac{\partial^2 f}{\partial z^2} = 0 \qquad 9.10$$

That is, f is a solution of the homogeneous equilibrium equation and g is a solution of Laplace's equation. Of course, the trick is to find useful expressions for f_m (equivalent to Θ_m) and g_m.

An important point about the method of multipole moments is that the results obtained are sensitive only to currents flowing within the contour l (including vacuum vessel currents if the measurements are made outside this). Thus either the total equilibrium fields, or just the plasma

fields, can be used. The plasma fields can be calculated if external conductor currents are known. Using just the plasma fields alone may have advantages in terms of requiring fewer moments to accurately describe the data.

10. PLASMA POSITION

Position by multipole moments

Let us apply the concept of multipole moments as described in section 9 to the geometry shown in *Figure 10.1,* using the notation of Shafranov, Equations 9.7 through 9.10. Assume S_ϕ contains only the plasma and vacuum regions so that $\mu = \mu_0$ and $L^* = \Delta^*$. The term $\int dS_\phi$ in Equation 9.7 is over the plasma surface, in a coordinate system centered in the plasma, while the term $\int dl$ is evaluated in a laboratory frame. The two coordinate systems are related by plasma position; therefore Equation 9.7 must provide information on the plasma position.

Figure 10.1. The geometry used in section 10.

There is a contour l, centered on $R = R_l$, with a local rectalinear system (η,ξ), and a second coordinate system based within the plasma, (z,x), centered at $R = R_c$, the plasma current center, defined later. Note that $\xi = x + \Delta_R$, $\eta = z + \Delta_z$, $R_c = R_l + \Delta_R$, and $R = R_c + x = R_l + \xi$. To be convenient, the moments (i.e. the choice of f_m) should, in the large aspect ratio limit $(x^2 + iz^2)/R_p^2 \ll 1$, reduce to a form of the kind

$$(x + iz)^m \qquad\qquad\qquad 10.1$$

with some denominator chosen to get convenient dimensions. We look for solutions of f which are both even (symmetric) in z, and odd (asymmetric) in z. Those suggested up to m = 2 are

symmetric

$f_0 = 1$

$g_0 = 0$

$f_1 = x\left(1 + \dfrac{x}{2R_c}\right)$

$g_1 = \dfrac{z}{R_c}$

$f_2 = x^2\left(1 + \dfrac{x}{2R_c}\right)^2 - z^2\left(1 + \dfrac{x}{R_c}\right)^2$

$g_2 = \dfrac{2xz}{R_c}\left(1 + \dfrac{x}{2R_c}\right) - \dfrac{2z^3}{3R_c^2}$

asymmetric

$f_0 = 0$

$g_0 = -1$

$f_1 = z\left(1 + \dfrac{x}{R_c}\right)^2$

$g_1 = -\dfrac{x}{R_c}\left(1 + \dfrac{x}{2R_c}\right) + \dfrac{z^2}{R_c^2}$

$f_2 = \left[2xz\left(1 + \dfrac{x}{2R_c}\right) - \dfrac{4z^3}{3R_c}\right]\left(1 + \dfrac{x}{R_c}\right)^2$

$g_2 = -\dfrac{x^2}{R_c}\left(1 + \dfrac{x}{2R_c}\right)^2 - \dfrac{z^2}{R_c}\left(1 + \dfrac{4x}{R_c} + \dfrac{2x^2}{R_c^2}\right) - \dfrac{2z^4}{3R_c^3}$

10.2

Because the Y_m are sensitive only to currents flowing within the contour l (including vacuum vessel currents if the measurements are made outside this), either the total equilibrium fields, or just the plasma fields, can be used. The plasma fields can be calculated if external conductor currents are known. Using just the plasma fields alone may have advantages in terms of requiring fewer moments to accurately describe the data.

We define the current center by setting $Y_1 = 0$. Using the symmetric set we obtain

$$\oint_l\left[\left(\xi - \Delta_R + \dfrac{(\xi - \Delta_R)^2}{2R_c}\right)B_\tau + \dfrac{R_1 + \xi}{R_c}\eta B_n\right]dl - \oint_l\left[\dfrac{R_1 + \xi}{R_c}\Delta_z B_n\right]dl = 0 \quad 10.3$$

i.e. the current channel displacement with respect to the center of the contour l is

$$\Delta_R = \Delta_{R0} + \Delta_{R1} - \dfrac{\Delta_{R0}^2}{2R_1} \qquad 10.4$$

$$\Delta_{R0} = \dfrac{1}{\mu_0 I_p}\left[\oint_l(\xi B_\tau + \eta B_n)dl\right] \qquad 10.5$$

$$\Delta_{R1} = \dfrac{1}{\mu_0 I_p}\left[\oint_l\left(\dfrac{\xi^2}{2R_1}B_\tau + \dfrac{\eta\xi}{R_1}B_n\right)dl\right] \qquad 10.6$$

Ignoring the term $\Delta_{R0}^2/(2R_1)$, then Δ_R is constructed from two integrals, namely $\int[\xi + (\xi^2/2R_1)]B_\tau dl$ and $\int[\eta + (\eta\xi/R_1)]B_n dl$. The first integral is measured with a modified Rogowski coil whose winding density times cross sectional area varies as $\xi + \xi^2/(2R_1)$. The second integral is measured with a saddle coil whose width varies as $\eta + \eta\xi/R_1$. Alternatively the integrals can be constructed from discrete local measurements.

Consider as an example a circular contour of radius a_l based on $R = R_l$. Then $\xi = a_l \cos(\omega)$ and $\eta = a_l \sin(\omega)$. These coils measure the fields in the coordinate system (ρ, ω, ϕ) based on the vessel center, and $B_n = B_\rho$, $B_\tau = B_\omega$. Assuming a plasma with no vertical displacement, symmetric about $z = 0$, we can write

$$B_\omega = B_\tau = \frac{\mu_0 I}{2\pi a_l}\left[1 + \sum_n \lambda_n \cos(n\omega)\right] \qquad\qquad 10.7$$

$$B_\rho = B_n = \frac{\mu_0 I}{2\pi a_l}\left[\sum_n \mu_n \sin(n\omega)\right] \qquad\qquad 10.8$$

Substituting these expressions into Equations 10.4 to 10.6 gives

$$\Delta_R \approx \frac{a_l}{2}(\lambda_1 + \mu_1) + \frac{a_l^2}{4R_l}\left(1 + \frac{\lambda_2}{2} + \mu_2\right) - \frac{a_l^2}{8R_l}(\lambda_1 + \mu_1)^2 \qquad\qquad 10.9$$

i.e. for small displacements, $(\lambda_1 + \mu_1) \ll 1$, and a circular plasma $(\lambda_n, \mu_n, = 0$ for $n > 1)$ we have,

$$\Delta_R \approx \frac{a_l}{2}(\lambda_1 + \mu_1) + \frac{a_l^2}{4R_l} \qquad\qquad 10.10$$

i.e. all that is needed to measure the displacement of a nearly circular plasma within a circular contour $(\lambda_n, \mu_n, n \geq 2 = 0)$ is a modified Rogowski coil whose winding density varies as $\cos(\omega)$, and a saddle coil whose width varies as $\sin(\omega)$. This simple coil set gives the correct answer when the constant $a_l^2/(4R_l)$ is allowed for. We already knew this. To allow for significant non-circularity the more general expression (Equations 10.4, 10.5 and 10.6) should be used. We can also derive equations to determine the vertical displacement of an arbitrarily shaped plasma, using the asymmetric components in Equation 10.2.

Application to the large aspect ratio circular tokamak

Let us apply these ideas to the circular equilibrium described in section 6, surrounded by a circular contour on which we have a sinusoidal area Rogowski coil and a cosinusoidal width saddle coil. The equations given in section 6 were in a coordinate system (r, θ, ϕ) based on the plasma geometric center; they were transformed into the vacuum vessel coordinate system in section 7, Equations 7.1, 7.2 and 7.3, allowing for a geometric shift Δ_g.

The output from the integrated saddle coil with n_w layers of width $w(\omega) = w_0\sin(\omega)$ and integrator time constant τ_{int} is

$$\varepsilon_{\mu 1} = \frac{n_w w_0 a_l}{\tau_{int}} \int_0^{2\pi} B_\rho(\omega)\sin(\omega)d\omega = \frac{n_w w_0 \mu_0 I_p}{\tau_{int}} \frac{\mu_1}{2} \qquad 10.11$$

Using the expression for B_ρ from Equation 7.3 we get

$$\mu_1 = \frac{\Delta_g}{a_l} - \frac{a_l}{2R_l}\left[\ln\left(\frac{a_l}{a_p}\right) + \left(\Lambda + \frac{1}{2}\right)\left(1 - \frac{a_p^2}{a_l^2}\right)\right] \qquad 10.12$$

The output from the integrated 'modified Rogowski coil each turn of area A, with $n_0\cos(\omega)$ turns per unit length, is.

$$\varepsilon_{\lambda 1} = \frac{n_0 A a_l}{\tau_{int}} \int_0^{2\pi} B_\omega(\omega)\cos(\omega)d\omega = \frac{n_0 A \mu_0 I_p}{\tau_{int}} \frac{\lambda_1}{2} \qquad 10.13$$

Using the expression for B_ω from Equation 7.2 we obtain

$$\lambda_1 = -\frac{\Delta_g}{a_l} - \frac{a_l}{2R_l}\left[\ln\left(\frac{a_l}{a_p}\right) + \left(\Lambda + \frac{1}{2}\right)\left(1 + \frac{a_p^2}{a_l^2}\right) - 1\right]$$

$$= -\frac{a_l}{R_l}\left[\Lambda + \ln\left(\frac{a_l}{a_p}\right)\right] - \mu_1 \qquad 10.14$$

Before we can substitute these expressions (Equations 10.13 and 10.14) into Equation 10.10, we must recognize that our equilibrium fields were evaluated in a left handed coordinate system, while this section we have worked in a right handed system. Sorting this out we find $\lambda_1 \Rightarrow -\lambda_1$, and $\mu_1 \Rightarrow \mu_1$, so that

$$\Delta_R - \Delta_g = \frac{a_p^2}{2R_l}\left(\Lambda + \frac{1}{2}\right) \qquad 10.15$$

This is the difference between the geometric center Δ_g and the current center Δ_R of a circular plasma, under the present approximations. We also note that, after sorting out the coordinates, subtracting the outputs from our coils gives

$$\lambda_1 - \mu_1 = \frac{a_l}{R_l}\left(\Lambda + \ln\left(\frac{a_l}{a_p}\right)\right) \qquad 10.16$$

that is, we can measure

$$\beta_I + \frac{l_i}{2} = \Lambda + 1 = 1 + \frac{R_l}{a_l}(\lambda_1 - \mu_1) - \ln\left(\frac{a_l}{a_p}\right)$$ 10.17

Combining Equations 10.15 and 10.16, we see that we can measure the current center, the geometric center, and Λ, using our modified Rogowski and saddle coils.

11. PLASMA SHAPE

Using higher order moments we can obtain information on the plasma shape. Y_2 determines ellipticity and Y_3 determines triangularity. Using equations 9.7 and 10.2, we obtain:

$$Y_2 = \left(1 - \frac{2\Delta_R}{R_1}\right)\frac{\left(s_3^\tau + s_4^n\right)}{s_0^\tau} + \Delta_z^2 - \left(1 - \frac{\Delta_R}{R_1}\right)\Delta_R^2 \qquad\qquad 11.1$$

where

$$s_3^\tau = \oint_1 \left[\xi^2\left(1 + \frac{\xi}{R_1}\right) - \eta^2\left(1 + \frac{2\xi}{R_1}\right)\right]\mathbf{B}_\tau dl \qquad\qquad 11.2$$

$$s_4^n = \oint_1 \left[2\xi\eta\left(1 + \frac{3\xi}{2R_1} - \frac{\eta^2}{3R_1\xi}\right)\right]\mathbf{B}_n dl \qquad\qquad 11.3$$

$$s_0^\tau = \oint_1 \mathbf{B}_\tau dl = \mu_0 I_p \qquad\qquad 11.4$$

That is, with the Rogowski coil measuring I_p (i.e. $s_0{}^\tau$) and either modified Rogowski and saddle coils, or single point measurements of B_n and B_τ suitably combined, we can construct Y_2. If we want to use modified Rogowski and saddle coils, then to obtain I_p, Δ_R and Y_2 takes a total of 5 coils. For a circular contour, and ignoring toroidal effects, Equation 11.1 is written as

$$Y_2 = -\Delta_R^2 + \Delta_z^2 + \frac{a_1^2}{2}\left(\lambda_2 + \mu_2\right) \qquad\qquad 11.5$$

That is, neglecting toroidal effects we need only λ_2 and μ_2, in addition to Δ_R and I_p.

To interpret the moments it is necessary to assume a plasma current distribution; because the moment is an integral of the current density over the surface S_ϕ there is no unique solution for the boundary shape. As an example, consider a uniform current density and a surface described by an ellipse with minor and major half width and half height a and b, so that $\left(\frac{x}{a}\right)^2 + \left(\frac{z}{b}\right)^2 = 1$. Then for $k = \frac{b}{a} - 1$, k << 1, and ignoring toroidal effects, we have

$$Y_2 \approx -\frac{ka^2}{2} \qquad\qquad 11.6$$

In a similar manner, if the surface is described by a function which includes both elongation and triangularity, namely

$$\left(\frac{x}{a}\right)^2 + \left(\frac{z}{b}\right)^2 + \frac{2\gamma x}{a}\left(\left(\frac{x}{a}\right)^2 - 3\left(\frac{z}{b}\right)^2\right) = 1 \qquad\qquad 11.7$$

then ignoring toroidicity (i.e. x/R_l and z/R_l <<1, we have for a flat current distribution

$$Y_3 \approx -a^3\gamma \qquad\qquad 11.8$$

12. MOMENTS OF PLASMA PRESSURE

The Virial Equation

Here we consider certain integral relations which allow us to determine information on the energy density within S_ϕ. The techniques described to determine plasma position, and more generally plasma shape, needed only Maxwell's equations. Now we add the constraint of equilibrium. Generally we apply these results to $S_\phi = S_{\phi plasma} + S_{\phi vacuum}$: even simpler relations are obtained by identifying S_ϕ with $S_{\phi plasma}$.

From a previously derived integral equation (Equation 8.19), we can obtain some very useful relationships. First, take $\mathbf{B}_2 = 0$ (i.e. all the fields are described by $\mathbf{B} = \mathbf{B}_1$), and let the arbitrary vector $\mathbf{Q}$ be the polar vector ($\mathbf{r} = R\mathbf{e}_R + z\mathbf{e}_Z$.). Then Equation 8.19 becomes the "virial theorem":

$$\int_V \left(3p + \frac{B^2}{2\mu_0} \right) dV = \int_{S_n} \left[\left(p + \frac{B^2}{2\mu_0} \right) (\mathbf{r} \bullet \mathbf{n}) - \frac{(\mathbf{r} \bullet \mathbf{B})(\mathbf{B} \bullet \mathbf{n})}{\mu_0} \right] dS_n \qquad 12.1$$

Note that if B were the self plasma field, and there was no other field, then the surface integral on the RHS approaches zero as the surface (where p = 0) approaches infinity, because B(self) $\propto$ R^{-3}. This contradicts the positive definiteness of the LHS volume integral, showing that equilibrium by self fields alone is impossible.

Now restricting to toroidal symmetry, $\partial/\partial\phi = 0$. Therefore the poloidal (subscript p) and toroidal (subscript ϕ) fields satisfy

$$\mathbf{B} = \mathbf{B}_p + \mathbf{B}_\phi$$
$$\mathbf{B}_p \bullet \mathbf{B}_\phi = 0 \qquad\qquad 12.2$$

Next assume that the surface S_n is outside the plasma, where $\nabla \times \mathbf{B} = 0$, and that the vectors $\mathbf{Q}$ and $\mathbf{B}_2$ are purely poloidal (i.e. there is no toroidal component of $\mathbf{B}_2$);

$$\mathbf{Q} = Q_R\mathbf{e}_R + Q_z\mathbf{e}_z$$
$$\mathbf{B}_2 = B_{2R}\mathbf{e}_R + B_{2z}\mathbf{e}_z \qquad\qquad 12.3$$

Noting that the toroidal field outside the plasma is given by $B_{\phi e} = \text{const}/R$, then we have

$$\int_{S_n} B_{\phi e}^2 (\mathbf{Q} \bullet \mathbf{n}) dS_n = \int_V B_{\phi e}^2 \left(\nabla \bullet \mathbf{Q} - \frac{2\mathbf{Q} \bullet \mathbf{e}_R}{R} \right) dV \qquad 12.4$$

and

$$\mathbf{B}_1 \bullet \mathbf{B}_1 \bullet \nabla \mathbf{Q} = \mathbf{B}_{p1} \bullet \mathbf{B}_{p1} \bullet \nabla \mathbf{Q} + \frac{B_{\phi e}^2 \mathbf{Q} \bullet \mathbf{e}_R}{R} \qquad 12.5$$

Using these, we can express Equation 8.19 so that the toroidal field enters only as $B_\phi^2 - B_{\phi e}^2$ on the LHS:

$$\int_V \left[\left(p + \frac{B_{p1}^2}{2\mu_0} \right) \nabla \bullet \mathbf{Q} + \frac{B_\phi^2 - B_{\phi e}^2}{2\mu_0} \left(\nabla \bullet \mathbf{Q} - 2 \frac{\mathbf{Q} \bullet \mathbf{e}_R}{R} \right) - \frac{\mathbf{B}_{p1} \bullet \nabla \mathbf{Q} \bullet \mathbf{B}_{p1}}{\mu_0} \right] dV$$

$$= \int_{S_n} \left[\left(p + \frac{B_{p1}^2}{2\mu_0} \right) (\mathbf{Q} \bullet \mathbf{n}) - \frac{(\mathbf{B}_{p1} \bullet \mathbf{Q})(\mathbf{B}_{p1} \bullet \mathbf{n})}{\mu_0} \right] dS_n - \int_V \left[\mathbf{j} \bullet (\mathbf{B}_{p2} \times \mathbf{Q}) \right] dV \qquad 12.6$$

Now let

$$P = p + \frac{B_\phi^2 - B_{\phi e}^2}{2\mu_0} \qquad 12.7$$

$$T = p + \left(\frac{B_{p1}^2 + B_{\phi e}^2 - B_\phi^2}{2\mu_0} \right) \qquad 12.8$$

(Remember B_1 is the poloidal field). Then the integrand on the LHS of Equation 12.6 can be written as (from now on drop the subscript p for poloidal)

$$[\ldots] = P \left(\frac{\partial Q_R}{\partial R} + \frac{\partial Q_z}{\partial z} \right) + \frac{T}{R} Q_R + \frac{B_{1R}^2 - B_{1z}^2}{2\mu_0} \left(\frac{\partial Q_z}{\partial z} - \frac{\partial Q_R}{\partial R} \right) - \frac{B_{1R} B_{1z}}{\mu_0} \left(\frac{\partial Q_R}{\partial z} + \frac{\partial Q_z}{\partial R} \right) \qquad 12.9$$

Now we have to chose something for Q. Let

$$u = R - R_{ch} + iz = \rho e^{i\omega} \qquad 12.10$$

with R_{ch} some characteristic radius, a fixed point within the plasma cross section. Then

$$\rho^2 = (R - R_{ch})^2 + z^2 \qquad 12.11$$

Now with this notation let

$$Q_R = F(u)$$
$$Q_z = -iF(u) \qquad 12.12$$

so that the last two terms in Equation 12.9 are zero. Next take

$$F(u) = u^{m+1}$$
12.13

Finally we can rewrite Equation 12.6 in the form

$$\int_V \left[2(m+1)Pu^m + \frac{T}{R} u^{m+1} \right] dV$$

$$= \int_{S_n} \left[\left(p + \frac{B_1^2}{2\mu_0} \right) (\mathbf{n}_R - i\mathbf{n}_z) - \frac{(B_{1R} - B_{1z})(\mathbf{B}_1 \bullet \mathbf{n})}{\mu_0} \right] u^{m+1} dS_n - \int_V \left[\mathbf{j} \bullet (\mathbf{B}_2 \times \mathbf{Q}) \right] dV$$

12.14

Surprisingly, this is useful. We now consider the results when we take different values of m.

m = -1, B₂ = Bₑₓₜ

Take B_2 as the externally supplied maintaining field and B_1 the plasma self field. For large volumes the surface integral approached zero, and we have

$$-\int_V \frac{T}{R} dV = \int_V j_\phi B_{z,ext} dV$$
12.15

or equivalently

$$\int_{S_\phi} j_\phi B_{z,ext} R dS_\phi = -\int_{S_\phi} \left[p + \left(\frac{B_{p1}^2 + B_{\phi e}^2 - B_\phi^2}{2\mu_0} \right) \right] dS_\phi$$
12.16

Suppose (low toroidicity) that $\rho/R_{ch} \ll 1$. Then the R dependence of T appears in the form R - R_{ch}, so that $dT/dR = -dT/dR_{ch}$. Now because $T/R = \nabla \cdot T\mathbf{e}_R - dT/dR$ (if $\rho/R_{ch} \ll 1$) we have, with $T = 0$ at infinity:

$$\int_V \frac{T}{R} dV = -\int_V \frac{\partial T}{\partial R} dV \approx \frac{\partial}{\partial R_{ch}} \left(\int T dV \right)$$
12.17

Now introduce some definitions:

$$B_\perp = -\frac{1}{2\pi R_{ch} I_p} \int_V j_\phi B_{z,ext} dV$$
12.18

$$R_T = \frac{\int_{S_\phi} TR dS_\phi}{\int_{S_\phi} T dS_\phi}$$

12.19

$$L_{pt} = \frac{8\pi}{\mu_0 I_p^2} \int_V \frac{B_{p1}^2}{2\mu_0} dV$$

12.20

$$\beta_I = \frac{8\pi}{\mu_0 I_p^2} \int_{S_\phi} p dS_\phi$$

12.21

$$\mu_I = -\frac{8\pi}{\mu_0 I_p^2} \int_{S_\phi} \left(\frac{B_\phi^2 - B_{\phi e}^2}{2\mu_0} \right) dS_\phi$$

12.22

Note that $\mu_0 L_{pt}/(4\pi)$ is a total inductance, and the usual "inductance per unit length times $4\pi/\mu_0$" is given as

$$L_p = \frac{4}{\mu_0 R_{ch} I_p^2} \int_V \frac{B_p^2}{2\mu_0} dV$$

12.23

Now we can write Equation 12.16 as

$$B_\perp = \frac{\mu_0 I_p}{8\pi R_{ch}} \left[\beta_I + \mu_I + \frac{\partial}{\partial R_{ch}} \left(R_{ch} L_p \right) \right]$$

12.24

This is a generalization of the external vertical field needed to maintain a plasma, allowing for non circularity.

m = 0, B₂ = 0

Now Equation 12.14 gives an integral expression along the minor radius:

$$\int_V P dV + \frac{(R_T - R_{ch})}{2R_T} \int_V T dV$$

$$= 0.5 \int_{S_n} \left[\frac{(B_{\tau1}^2 - B_{n1}^2)}{2\mu_0} \mathbf{n} \bullet \mathbf{e}_\rho - \frac{B_{\tau1} B_{n1}}{\mu_0} \tau \bullet \mathbf{e}_\rho \right] dS_n - 0.5 \int_V j_\phi \left[B_{z2}(R - R_{ch}) - B_{R2} z \right] dV$$

12.25

If we assume that $|R-R_{ch}| \ll R_{ch}$, then the term with $(R_T-R_{ch})/(2R_T)$ can be omitted, and the LHS is independent of the choice of S_n. Therefore the RHS must also be independent of S_n. Then we can write (with $|R-R_{ch}| \ll R_{ch}$)

$$\int_V PdV = \frac{\mu_0 R_{ch} I_p^2}{4} s_1 \qquad\qquad 12.26$$

where s_1 must be independent of the choice of B_2. In particular, taking $B_2 = 0$, Equation 12.25 can be written, using the definitions above, as

$$\beta_I = \mu_I + s_1 \qquad\qquad 12.27$$

where

$$s_1 = \frac{1}{\mu_0^2 R_{ch} I_p^2} \int_{S_n} \left[\left(B_\tau^2 - B_n^2\right)\rho\mathbf{n}\bullet\mathbf{e}_\rho - 2B_\tau B_n \rho\tau\bullet\mathbf{e}_\rho \right] dS_n \qquad\qquad 12.28$$

The difference between s_1 and 1 is due to non circularity.

In fact, the constraint $R-R_{ch}| \ll R_{ch}$, but not $(R_T-R_{ch})/(2R_T)$, can be relaxed by redefining β_{Iv} and μ_{Iv} as volume integrals: see Equations 12.31 and 12.32 below.

m = -1, B$_2$ = 0

Now we obtain another important integral relationship, assuming $|R-R_{ch}| \ll R_{ch}$, namely

$$\beta_I + \frac{L_p}{2} = \frac{s_1}{2} + s_2 \qquad\qquad 12.29$$

where

$$s_2 = \frac{1}{\mu_0^2 I_p^2} \int_{S_n} \left[\left(B_\tau^2 - B_n^2\right)\mathbf{n}\bullet\mathbf{e}_\varsigma - 2B_\tau B_n \tau\bullet\mathbf{e}_\varsigma \right] dS_n \qquad\qquad 12.30$$

and $\zeta = R - R_{ch}$.

In fact, the approximation $|R-R_{ch}| \ll R_{ch}$ is not necessary if β and μ are redefined as volume integrals, namely

$$2\pi R_{ch}\beta_{IV} = \frac{8\pi}{\mu_0 I_p^2} \int_V pdV \qquad\qquad 12.31$$

$$2\pi R_{ch}\mu_{IV} = -\frac{8\pi}{\mu_0 I_p^2}\int_V \frac{\left(B_\phi^2 - B_{\phi e}^2\right)}{2\mu_0}dV \qquad\qquad 12.32$$

13. $\beta_I + l_i/2$

Solution

In the previous section, Equation 12.29, we showed that we could express the parameter $\beta_I + L_p/2$ through the integral equation

$$\beta_I + \frac{L_p}{2} = \frac{s_1}{2} + s_2 \qquad\qquad 13.1$$

where s_1 and s_2 are two integrals of the fields over dS_n, which we will be able to measure as contour integrals, namely

$$
\begin{aligned}
s_1 &= \frac{1}{\mu_0^2 R_{ch} I_p^2} \int_{S_n} \left[\left(B_\tau^2 - B_n^2\right)\rho\, \mathbf{n} \bullet \mathbf{e}_\rho - 2 B_\tau B_n \rho \boldsymbol{\tau} \bullet \mathbf{e}_\rho \right] dS_n \\
&= \frac{2\pi}{\mu_0^2 R_{ch} I_p^2} \int_l \left[\left(B_\tau^2 - B_n^2\right)\rho\, \mathbf{n} \bullet \mathbf{e}_\rho - 2 B_\tau B_n \rho \boldsymbol{\tau} \bullet \mathbf{e}_\rho \right] R\,dl
\end{aligned}
\qquad 13.2
$$

$$
\begin{aligned}
s_2 &= \frac{1}{\mu_0^2 I_p^2} \int_{S_n} \left[\left(B_\tau^2 - B_n^2\right)\mathbf{n} \bullet \mathbf{e}_\varsigma - 2 B_\tau B_n \boldsymbol{\tau} \bullet \mathbf{e}_\varsigma \right] dS_n \\
&= \frac{2\pi}{\mu_0^2 I_p^2} \int_l \left[\left(B_\tau^2 - B_n^2\right)\mathbf{n} \bullet \mathbf{e}_\varsigma - 2 B_\tau B_n \boldsymbol{\tau} \bullet \mathbf{e}_\varsigma \right] R\,dl
\end{aligned}
\qquad 13.3
$$

Equation 13.1 was good for toroidal geometry if volume definitions β_{IV} and μ_{IV} were used. Note that $dS_n = 2\pi R dl$, so that s_1 and s_2 can be written as contour integrals around l. Unfortunately they involve the squares of fields, and so we cannot design simple modified Rogowski and saddle coils to make the measurements. Instead we must measure B_n and B_τ at discrete points along the contour, and then construct the required integrals. All we have to do is construct the integrals s_1 and s_2 from measured B_n and B_τ.

Suppose we are measuring fields on a circular contour of radius a_l, centered at $R = R_l = R_{ch}$; that is we identify our characteristic radius with the center of the contour l. Then in the vessel coordinates we have $\boldsymbol{\tau} \bullet \mathbf{e}_\rho = 0$, $\mathbf{n} \bullet \mathbf{e}_\rho = 1$, $\mathbf{n} \bullet \mathbf{e}_\zeta = \cos(\omega)$, $\boldsymbol{\tau} \bullet \mathbf{e}_\zeta = -\sin(\omega)$, and $dS_n = 2\pi R_l[1+(a_l/R_l)\cos(\omega)]a_l d\omega$. If the fields can be expanded as in Equations 10.7 and 10.8, and keeping only the terms λ_1 and μ_1 (i.e. a circular plasma), we obtain

$$s_1 = 1$$

$$s_2 = \frac{R_l}{a_l}(\lambda_1 + \mu_1)$$

13.4

i.e., substituting 13.4 into 13.1:

$$\beta_I + \frac{L_p}{2} = 1 + \frac{R_l}{a_l}(\lambda_1 + \mu_1)$$

13.5

Let us apply this equation to the displaced analytic equilibrium discussed in sections 6 and 9. The Rogowski coil with cosinusoidal varying winding density, and the saddle coil with sinusoidal varying width, tell us λ_1 and μ_1. First there is a mess with right and left handed coordinate systems to unravel. Doing this then $\mu \Rightarrow -\mu$ in Equation 13.5. Now Equation. 10.16 already tells us that

$$\lambda_1 - \mu_1 = \frac{a_l}{R_l}\left[\ln\left(\frac{a_l}{a_p}\right) + \beta_I + \frac{l_i}{2} - 1 \right]$$

13.6

Therefore comparing Equations 13.5 and 13.6 we must have (allowing $\mu \Rightarrow -\mu$ in Equation 13.5) that

$$\frac{l_i}{2} + \ln\left(\frac{a_l}{a_p}\right) = \frac{L_p}{2}$$

13.7

This is exactly what we expect, because the total inductance to a radius a_l is given by:

$$L_{total} = 2\pi R\left(\frac{\mu_0}{4\pi}\right) L_p = \mu_0 R\left[\ln\left(\frac{a_l}{a_p}\right) + \frac{l_i}{2} \right]$$

13.8

Separation of β_I and l_i

If we have $\beta_I + l_i/2$ from the poloidal field measurements just described, and β_I from diamagnetic measurements (see later) then obviously we can separate β_I and l_i. If no diamagnetic measurement is available, two possibilities exist. For non circular plasmas, there is a third integral relationship, which I have not derived, which gives in terms of a measurable line integral the parameter $\int_V (2p + B_z^2/\mu_0)dV$. When V is the plasma volume, this is related to $2\beta_I + L_p$. If the volume averages $<B_z^2>$ and $<B_p2>$ are different, as is the case for non circular discharges, then this measurement allows the separation.

For near circular plasmas, we must estimate L_p separately. For example, for the simple circular low beta equilibrium of section 6, we can take a model current distribution $j_{\phi 0}(r) = j_0(1-(r/a)^2)^\alpha$. Then $l_i = L_p-\ln(a_l/a_p)$, with l_i given as a function of $\alpha = (q_a/q_0 -1)$. By assuming $q_0 = 1$ we can then estimate l_i, and make the separation.

Comments on the definition of poloidal beta

We must be careful with the definition of "poloidal beta". So far we have used Equation 12.21, namely

$$\beta_I = \frac{8\pi}{\mu_0 I_p^2} \int_{S_\phi} p S_\phi \qquad\qquad 13.9$$

We could replace β_I by β_p (the poloidal beta), which characterizes the ratio of plasma pressure to the pressure of the magnetic field for an arbitrary shaped cross section. It should be introduced so that the pressure balance, Equation 12.27, is replaced by

$$\beta_p = 1 + \mu_p \qquad\qquad 13.10$$

so that $\beta_p = 1$ for $\mu_p = 0$.

14. DIAMAGNETISM

Comments

Next we turn to the toroidal flux and its measurement. Before plasma initiation this is simply given by $\oint_l B_\phi dl = \mu_0 \int_S j_z dS$, i.e. $2\pi R B_\phi = \mu_0 I_z$, where we have applied Amperes law to a contour in the toroidal direction, encircling the inner vertical legs of the toroidal field coils (i.e. $I_z = i_z n_t n_c$, with i_z the current from the generator, n_c the number of assumed series coils, and n_t the assumed series number of turns in each coil).

Microscopic picture for a square profile plasma in a cylinder

During formation inside a magnetic field the plasma particles acquire a magnetic moment m:

$$m = Area_{orbit} I_{orbit} = \pi \left(\frac{v}{\omega}\right)^2 \left(\frac{q\omega}{2\pi}\right) \qquad 14.1$$

Since $\omega = qB/m_e$, we have

$$m = \frac{m_e v^2}{2B} \qquad 14.2$$

adding up to a total magnetic moment

$$M = nmS_\phi \qquad 14.3$$

per unit length of column with cross section S_ϕ and a number density of n Supposing cylindrical geometry the elementary currents cancel within the homogeneous column, leaving only an azimuthal surface "magnetization' current density j_s:

$$j_s = nm = \frac{nk_b T}{B} = \frac{p_\perp}{B} \qquad 14.4$$

where $p_\perp = nk_b(T_e + T_i)_\perp$, k_b is Boltzmann's constant. The toroidal field will be modified.

The associated flux from this surface current can be calculated:

$$\Delta\Phi = \pi a_p^2 \Delta B_\phi = \pi a_p^2 \frac{\mu_0}{2\pi R} I = \pi a_p^2 \frac{\mu_0}{2\pi R} 2\pi R j_s$$

$$= \pi a_p^2 \frac{\mu_0}{2\pi R} 2\pi R \frac{p_\perp}{B_\phi} = \pi a_p^2 \mu_0 \frac{p_\perp}{B_\phi}$$

Using the definition of β_I, discussed much more a little later, we then have

$$\Delta\Phi = \frac{\mu_0^2 I_p^2 \beta_I}{8\pi B_\phi}$$

Macroscopic picture

Let us consider a toroidal device with no toroidal current plasma current, i.e. a stellarator, in which the necessary rotational transform is produced only by external conductors. Starting with the radial pressure balance, with $p_\perp = 0$ at the plasma edge, and approximating the torus by a long cylinder, then

$$\frac{dp_\perp}{dr} = j_\theta B_\phi \qquad\qquad 14.5$$

integrating over the minor radius ($r = 0$ to a_p) gives

$$p_\perp = -B_\phi \int_r^{a_p} j_\theta(r')dr' \qquad\qquad 14.6$$

and

$$\langle p_\perp \rangle = \frac{1}{\pi a_p^2}\int_0^{a_p} 2\pi p_\perp r dr = -\frac{B_\phi}{\pi a_p^2}\int_0^{a_p} 2\pi r dr \int_r^{a_p} j_\theta(r')dr'$$

$$= -\frac{B_\phi}{\pi a_p^2}\int_0^{a_p} \pi r^2 j_\theta(r)dr = -B_\phi \int_0^{a_p} \frac{S(r)}{\pi a_p^2} j_\theta(r)dr$$

14.7

Then $j_{se} = \int_0^{a_p} S(r)/(\pi a_p^2) j_\theta(r)dr$ is the effective surface current density at the plasma edge as a consequence of the finite plasma pressure.

Paramagnetic and diamagnetic flux

Outside the plasma the toroidal field has the form $B_{\phi e} = B_{\phi 0}(R_0/R)$, with $B_{\phi 0}$ the value at a fixed radius R_0. This toroidal field, together with the poloidal field, takes part in balancing the plasma pressure.

We need an equation relating fields to pressure. Substituting $\nabla \times \mathbf{B} = \mu_0 \mathbf{j}$ into $\nabla p = \mathbf{j} \times \mathbf{B}$ yields (using $\mathbf{B} \times (\nabla \times \mathbf{B}) = \dfrac{\nabla \mathbf{B}^2}{2} - (\mathbf{B} \bullet \nabla)\mathbf{B}$)

$$\nabla\left(p + \frac{B^2}{2\mu_0}\right) = (\mathbf{B} \bullet \nabla)\frac{\mathbf{B}}{\mu_0}$$

For a straight axially symmetric system $(\partial/\partial z = 0)$ we obtain

$$\frac{\partial}{\partial r}\left(p + \frac{B_z^2 + B_\theta^2}{2\mu_0}\right) = -\frac{B_\theta^2}{r\mu_0}$$

Multiplying each side by r^2, letting $u = r^2$, $du = 2rdr$, $dv = \partial/\partial r(.)$, $v = (..)$, we obtain by integrating by parts ($\int u\,dv = uv - \int v\,du$)

$$r^2\left(p + \frac{B_z^2 + B_\theta^2}{2\mu_0}\right)\Bigg|_0^a - \int_0^a\left(p + \frac{B_z^2 + B_\theta^2}{2\mu_0}\right)2rdr = -\int_0^a \frac{B_\theta^2}{\mu_0}rdr$$

i.e.,

$$\left(p + \frac{B_z^2 + B_\theta^2}{2\mu_0}\right)_{r=a} = \frac{1}{\pi a^2}\int_0^a\left(p + \frac{B_z^2}{2\mu_0}\right)2\pi rdr$$

That is, ignoring curvature and equating B_z with B_ϕ, the pressure balance constraint is

$$2\mu_0\langle p \rangle = B_{\theta a}^2 + B_{\phi e}^2 - \langle B_\phi^2 \rangle \tag{14.8}$$

where B_ϕ is the toroidal field inside the plasma, $B_{\phi e}$ is the toroidal field outside the plasma, <..> means an average over the plasma radius, and we have assumed $p = 0$ at the boundary (i.e. at $r = a$). That is, for a given plasma current I_p and pressure <p>, the difference ($B_{\phi e}^2$ - <B_ϕ^2>) adjusts itself to ensure pressure balance. This happens because of a poloidally flowing current, either diamagnetic or paramagnetic, in the plasma, as we derived in equations 14.4 and 14.17. In a tokamak we have $B_{\phi e}^2 \gg B_{\phi e}^2$ - <B_ϕ^2>, so that if the cross section is circular with radius a_p,

$$B_{\phi e}^2 - \langle B_\phi^2 \rangle \approx 2B_{\phi e}\langle B_{\phi e} - B_\phi \rangle = \frac{2B_{\phi e}\delta\Phi}{\pi a_p^2} \qquad\qquad 14.9$$

where

$$\delta\Phi = \pi a_p^2 \langle B_{\phi e} - B_\phi \rangle \qquad\qquad 14.10$$

is the diamagnetic flux of the longitudinal (toroidal) field. We will discus its measurement later; it is the difference in toroidal flux in the plasma column when the plasma is initiated. Defining

$$\beta_I = \frac{8\pi}{\mu_0 I_p^2} \int_{S_\phi} p \, dS_\phi$$

i.e. $\quad \beta_I = \dfrac{2\mu_0 \langle p \rangle}{B_{\theta a}^2} \qquad\qquad$ for a circular cross section $\qquad\qquad 14.11$

with $B_{\theta a} = \dfrac{\mu_0 I_p}{2\pi a_p}$ the poloidal field at the plasma edge, we can write

$$\beta_I = 1 + \frac{8\pi B_{\phi e}\delta\Phi}{\mu_0^2 I_p^2} \qquad\qquad 14.12$$

From this equation we write the net flux difference $\delta\Phi = (\mu_0 I_p)^2/(8\pi B_{\phi e}).(\beta_I - 1)$ as the sum of the paramagnetic flux $\delta\Phi_p$:

$$\delta\Phi_p = -\frac{\mu_0^2 I_p^2}{8\pi B_{\phi e}} \qquad\qquad 14.13$$

due to the poloidal component of the force free plasma current, and the diamagnetic flux $\delta\Phi_d$:

$$\delta\Phi_d = -\delta\Phi_p \beta_I \qquad\qquad 14.14$$

due to the poloidal currents providing pressure balance for the finite pressure.

Toroidal, non circular geometry

In a torus curvature must be accounted for: Corrections with coefficients (a/R) appear in the RHS of the equation for β_I. For $\beta_I \ll R/a$ the corrections are small, and it should be noted only that for $B_{\phi e}$ the value on a line $R = R_g$, the plasma center, should be used. We will derive that below. Also, we must now be rather careful with definitions.

We derived, in section 13, a general expression relating β_I to poloidal field measurements and the diamagnetic measurements. This derivation allowed for both toroidicity and non circularity, and gave in terms of <u>volume</u> integrals (equations. 12.31, 12.32, 12.27, 12.28)

$$\beta_{IV} = \mu_I + s_1 \qquad\qquad 14.15$$

$$\mu_{IV} = -\frac{4}{\mu_0 R_{ch} I_p^2} \int_V \frac{\left(B_\phi^2 - B_{\phi e}^2\right)}{2\mu_0} dV \qquad\qquad 14.16$$

$$\beta_{IV} = \frac{4}{\mu_0 R_{ch} I_p^2} \int_V p\, dV \qquad\qquad 14.17$$

The measurable integral $s_1 = 1$ for a circular discharge. Remember that R_{ch} was a characteristic major radius of the plasma. Because we can write $|B_{\phi e}-B_\phi| \ll B_{\phi 0}$, the diamagnetic parameter can be expressed through the experimentally determined flux (the measurement is discussed later)

$$\delta\Phi = \int_{S_\phi} \left(B_{\phi e} - B_\phi\right) dS_\phi \qquad\qquad 14.18$$

By substituting $(B_{\phi e}^2 - B_\phi^2) \approx 2B_\phi(B_{\phi e}-B_\phi)$, and writing

$$B_{\phi e} = \frac{B_{\phi 0} R_{ch}}{R} \qquad\qquad 14.19$$

then we have

$$\mu_{IV} = \frac{8\pi B_{\phi 0} \delta\Phi}{\mu_0^2 I_p^2} \qquad\qquad 14.20$$

That is, in toroidal geometry and for an arbitrary shaped cross section, measuring $\delta\Phi$ and the integral s_1 gives us a good measure of β_{IV}, the volume defined current beta. Note that the field $B_{\phi 0}$ is the external field at the characteristic plasma major radius, which we can take as $R_{ch} \approx R_g$..

The meaning of β_I

We can understand β_I by integrating by parts Equation 14.11 to give (for a circular cross section), and assuming p at $r = a_p = 0$, we have

$$\beta_I = \frac{8\pi}{\mu_0 I_p^2} \int\limits_0^{2\pi}\int\limits_0^{a_p} pr\,dr\,d\theta = \frac{8\pi}{\mu_0 I_p^2} \int\limits_0^{a_p} 2pr\,dr$$

$$= \frac{8\pi^2}{\mu_0 I_p^2} \left[\left| pr^2 \right|_0^{a_p} - \int\limits_0^{a_p} r^2 \frac{dp}{dr} dr \right] = -\frac{8\pi^2}{\mu_0 I_p^2} \int\limits_0^{a_p} r^2 \frac{dp}{dr} dr$$

14.21

Here we have integrated by parts, with u = p, du = (dp/dr)dr, v = r^2, dv = 2rdr. Next we use the approximate pressure balance equation (dp/dr = $j_\theta B_\phi$ - $j_\phi B_\theta$, we will work in a RH coordinate system). We substitute for j_θ and j_ϕ in terms of B_ϕ and B_θ (from $\mu_0 \mathbf{j} = \nabla \times \mathbf{B}$), i.e. $\mu_0 j_\theta = -\dfrac{\partial B_\phi}{\partial r}$, $\mu_0 j_\phi = \dfrac{1}{r}\dfrac{\partial(rB_\theta)}{\partial r}$, we obtain

$$\frac{dp}{dr} + \frac{d}{dr}\left(\frac{B_\phi^2}{2\mu_0}\right) + \frac{B_\theta}{\mu_0 r}\frac{d}{dr}(rB_\theta) = 0$$

14.22

Substituting for dp/dr from equation. 14.22 into equation. 14.21 gives

$$\beta_I = \frac{4\pi^2}{\mu_0^2 I_p^2}\left[\int\limits_0^{a_p} \frac{d\left(B_\phi^2\right)}{dr} r^2 dr + \int\limits_0^{a_p} 2B_\theta r \frac{d(rB_\theta)}{dr} dr \right]$$

$$= \frac{1}{a_p^2 B_{\theta a}^2}\left[\int\limits_0^{a_p} \frac{d\left(B_\phi^2\right)}{dr} r^2 dr + \left| (rB_\theta)^2 \right|_0^{a_p} \right]$$

14.23

$$= 1 + \frac{1}{a_p^2 B_{\theta a}^2} \int\limits_0^{a_p} \frac{d\left(B_\phi^2\right)}{dr} r^2 dr$$

If $(dB_\phi^2/dr) > 0$ then $\beta_I > 1$, and if $(dB_\phi^2/dr) < 0$ then $\beta_I < 1$. *Figure 14.1* shows this schematically. A reduced B_ϕ (diamagnetic) inside the plasma is associated with $\beta_I > 1$. The normal ohmic heating case, with $\beta_I \approx 0.3$ has an increased B_ϕ inside the plasma (paramagnetic). The figures are not well drawn, because we must have that $B_\phi R$ is constant on a flux surface.
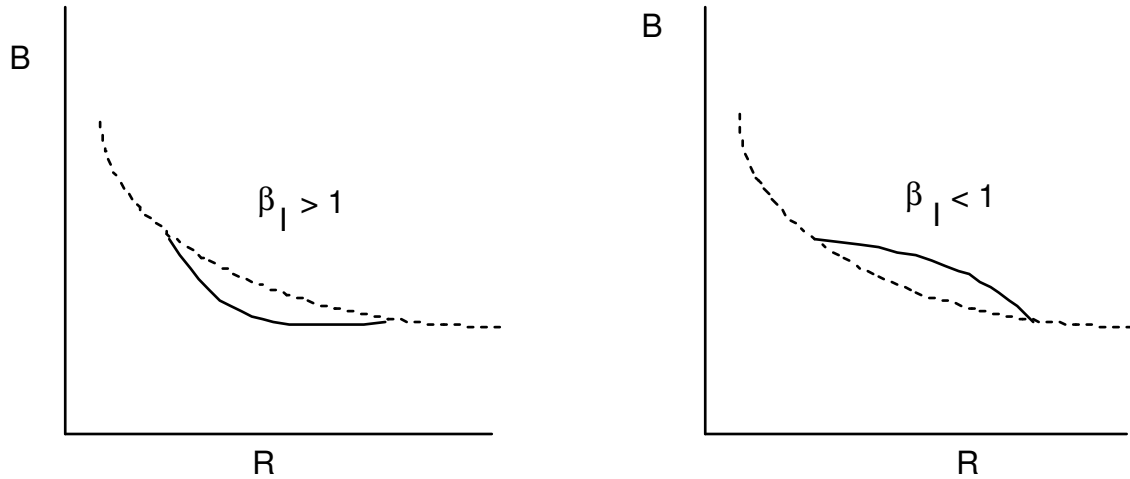
Figure 14.1. The toroidal field with different values of β_I.
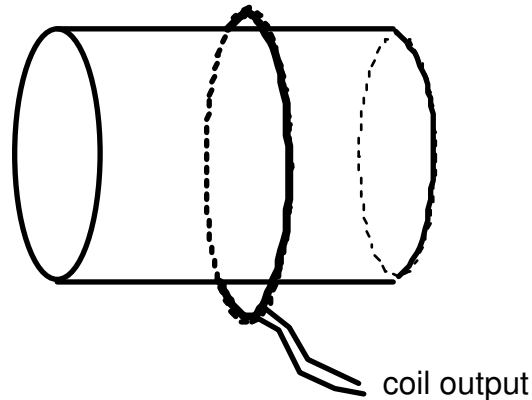
Measurements

coil output

Figure 14.2. A simple loop to measure toroidal flux.

To measure $\delta\Phi$ it is usual to use a wire wrapped around the vacuum vessel, as in *Figure 14.2*. The voltage output from the coil is integrated to give a signal proportional to the enclosed flux. For most cases $\delta\Phi$ is small, typically $\sim$ 1mWb, which must be compared to a typical vacuum flux $\Phi_v = 1$Wb enclosed by the same loop.   Therefore we have to use techniques which allow measurements to better than 1 part in 10^4 to get 10% accuracy in values of β_I. This is done using compensating coils.
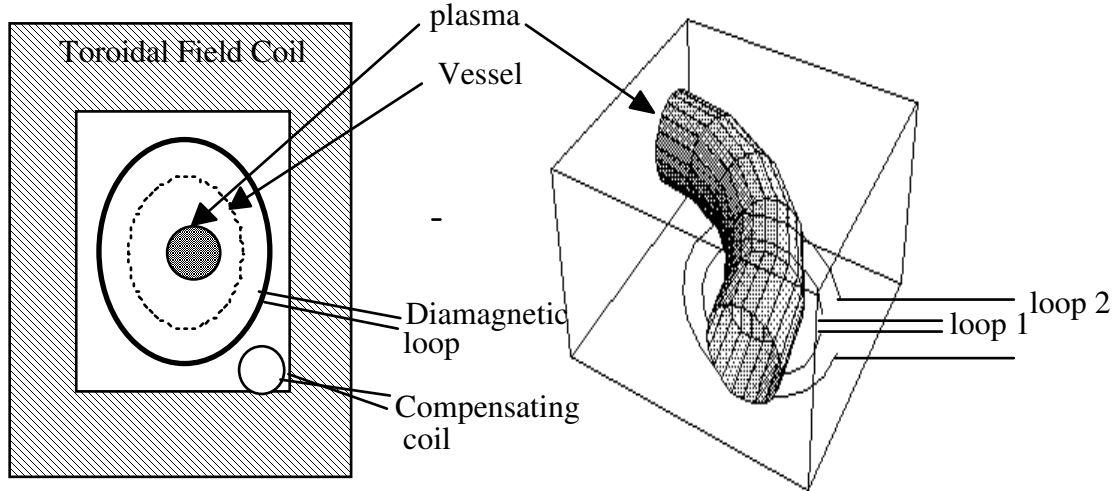
Fig 14.3. Diamagnetic loop
and compensating coil

Fig 14.4. Two concentric diamagnetic loops

Figure 14.3 shows a typical set up for the 'diamagnetic loop', a single turn coil around the vessel, and a compensating coil.   The idea is to make the vacuum signal from the two coils as near identical as possible, so that a simple summing (or subtraction) circuit can be employed.   A compensating and balancing circuit is then employed, as for example is shown in *Figure 14.5*. The vacuum common mode flux is canceled using the summing integrator, so that the balance is determined only by the effective areas and the resistors.   The product of resistance and capacitance (RC) is adjusted using 'toroidal field only' shots (no plasma). By opening the switch after the toroidal field (TF) has 'flat topped' much of the common mode is also rejected.   Of course, to balance the system during the toroidal field only shots the switch is opened to consider toroidal field ramp up.   The circuit shown also allows for phase difference between the two signals to be compensated.
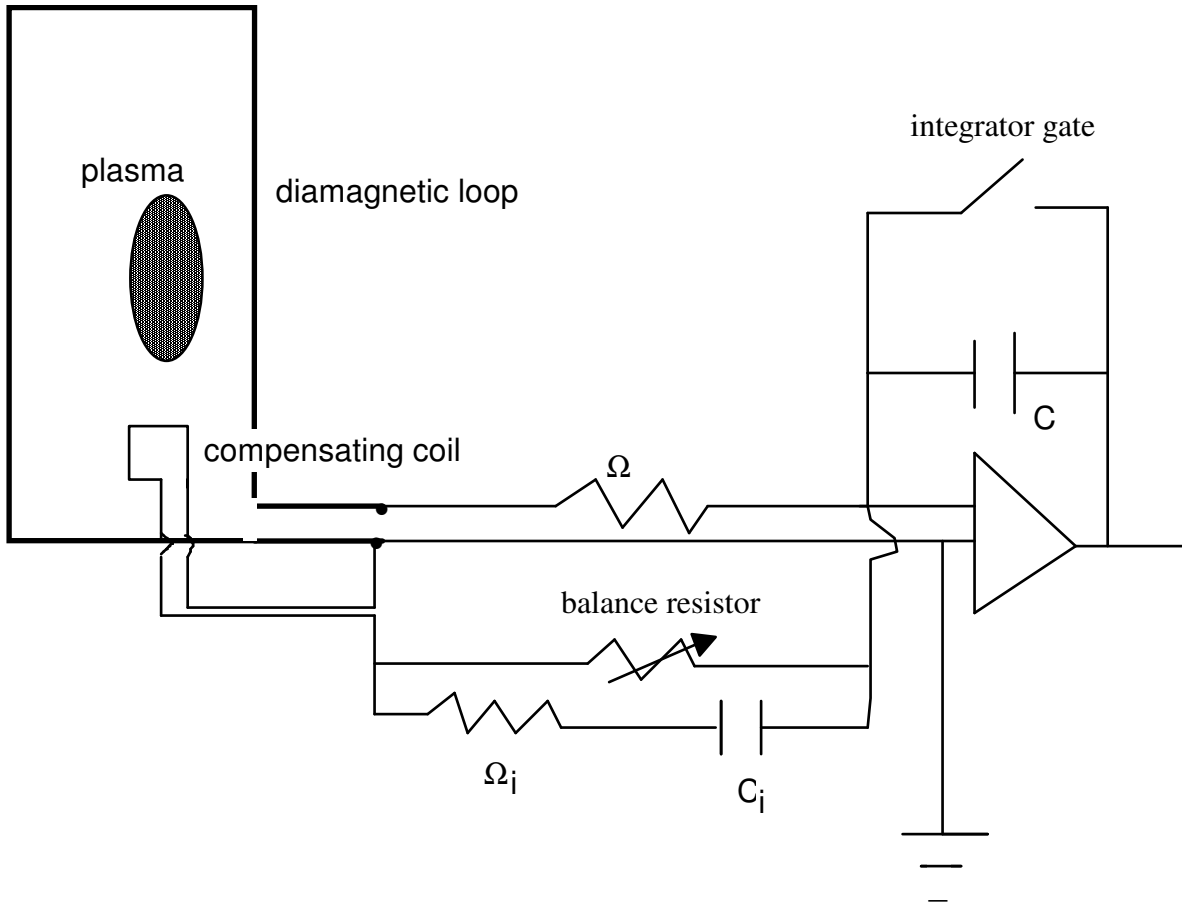
Figure 14.5. A diamagnetic coil compensating system

An alternative technique is to wrap two simple toroidal flux loops around the vessel, but at different minor radii. Such a configuration is shown in *Figure 14.4.* Let two concentric loops have radii b_1 and b_2, and let R_l be the major radius of the loops. Then, remembering that $B_{\phi e} = B_{\phi 0} R_l / R$, we have after time integration

$$\Phi(b_i) = 2\pi R_1 B_{\phi 0}\left[R_1 - \left(R_1^2 - b_i^2\right)^{\frac{1}{2}} \right] + \delta\Phi \qquad\qquad 14.24$$

$$\Phi(b_i) = 2\pi R_1 B_{\phi 0}\left[R_1 - \left(R_1^2 - b_i^2\right)^{\frac{1}{2}} \right] + \delta\Phi \qquad\qquad 14.25$$

$$\delta\Phi = \Phi(b_1) - k\left(\Phi(b_2) - \Phi(b_1)\right), \qquad k = \frac{b_1^2}{b_2^2 - b_1^2}\frac{\sqrt{R_1^2 - b_1^2} + \sqrt{R_1^2 - b_2^2}}{R_1 + \sqrt{R_1^2 + b_1^2}} \qquad 14.26$$

From these two signals we can calculate $\delta\Phi$. The subtractions are performed electronically (i.e. analog); the constant k is determined experimentally so that $\delta\Phi$ is zero without plasma (toroidal field only).

In reality there are problems. One in particular is caused by the discreteness of the toroidal field system, and the current redistribution in the toroidal field coils during a shot. When the toroidal field current is initiated, the current flows at the inner edge of the conductors to minimize the linked flux. As the pulse proceeds, the current redistributes and approximates a uniform distribution (not exactly because of repulsion of current channels). The time for this redistribution to occur is approximately the radial penetration time of the poloidal current into the conductor of radial extent w: $\tau \approx \pi\mu_0\sigma w^2/16$, typically 200 ms. If the toroidal field system was a perfect toroidal solenoid this redistribution would leave the fields unaffected. However, because of the discrete number of toroidal fields, there is now a time varying toroidal field ripple. The size of the changing field ripple depends on where a pickup coil is placed: therefore two coils linking the same steady state flux can link different transient fluxes. It is best to place the coils between the toroidal field coils, where the redistribution effect is smallest.

Another problem is due to poloidal eddy currents in any conducting vacuum vessel. This produces a non zero change in the toroidally averaged B_ϕ, not just a local ripple. Therefore it couples strongly to the pickup loops. Compensation for both the effects discussed has been performed successfully using software, by simulating redistribution and eddy currents as simple circuits, coupled to both the primary B_ϕ coil current and a secondary pickup coil.

Further problems occur if the loops are not exactly positioned, so that they couple to the poloidal fields produced by the primary, vertical field and shaping windings. That any such effects exist can be checked for by firing discharges with positive (+) and negative (-) B_ϕ. Let $\Delta\Phi_p$ be the signal caused by poloidal field coupling, $\Delta\Phi(+)$ the signal obtained with positive B_ϕ, and $\Delta\Phi(-)$ the signal obtained with negative B_ϕ. While the toroidal field coupling effects will change sign with reversing B_ϕ, any poloidal field effects will not. Therefore

$$\Delta\Phi(+) - \Delta\Phi(-) = 2\left(\delta\Phi + \Delta\Phi_p\right) \qquad\qquad 14.27$$

$$\Delta\Phi(+) + \Delta\Phi(-) = 2\Delta\Phi_p \qquad\qquad 14.28$$

Any finite $\Delta\Phi_p$ can be correct for using a circuit model again, with the coupling between any winding (including vacuum vessel) and the pickup coil written in terms of mutual inductances.

15. FULL EQUILIBRIUM RECONSTRUCTION

The problem under discussion is how to reconstruct as much as is possible about the equilibrium from external measurements. In particular, if we knew everything about the fields outside the plasma, what could we uniquely determine? Could we separate β_I and l_i? (In principle yes for toroidal systems). Could we go further and actually uniquely determine the plasma current distribution of a toroidal plasma (I don't know)?

If we want to allow measurements of $dp(\psi)/d\psi$ and $FdF(\psi)/d\psi$ we must have redundancy beyond that required to solve the equilibrium equation with a known current density profile. We see immediately a problem in straight geometry, because with straight circular cross sections the magnetic measurements must be consistent with a solution that has concentric circular surfaces. In this case the measurements are consistent with any profile function which gives the correct total plasma current, so there is an infinite degeneracy.

In practice the mathematical subtleties of what can and cannot in principle be determined are not discussed. Instead the usual technique for equilibrium reconstruction is to choose a parameterization for j_ϕ, with a restricted number of free parameters. These free parameters are chosen to minimize the chi squared error or cost function between some measured and computed parameter, for example the poloidal field component on some contour. Obviously we need some boundary conditions, as discussed in section 8. Information available might consist of the flux ψ on a contour, the fields B_n and B_τ on a contour, and currents in conductors, the total current, and if lucky the diamagnetism. Typical parameterizations are

$$j_\phi = \left[a\beta \frac{R}{R_0} + (1-\beta)\frac{R_0}{R} \right] g(\delta\psi) \qquad\qquad 15.1$$

$$j_\phi = \left(\alpha_1 \delta\psi + \alpha_2 \delta\psi^2 + \alpha_3 \delta\psi^3 \right)R + \left(b_1 \delta\psi \right)R^{-1} \qquad\qquad 15.2$$

with $\delta\psi = (\psi - \psi_{boundary})(\psi_{mag\ axis} - \psi_{boundary})$. In each case the term proportional to R represent the part of j_ϕ proportional to $dp/d\psi$, and the part of j_ϕ proportional to R^{-1} is proportional to $FdF/d\psi$. R_o is some characteristic radius. The assumed function g might be of the form $g(\delta\psi, \gamma) = \exp(-\gamma^2(1-\delta\psi)^2$, $d\psi^\gamma$ or $\delta\psi + \gamma\delta\psi^2$. If in equation 15.1 the function $g(\delta\psi)$ is 1, then the description of j_ϕ is called quasi uniform: for a circular outer boundary there is an exact analytic solution of the equilibrium equation.

The general results show that, given only poloidal field magnetic measurements (i.e. no diamagnetic signal), then β_I and l_i can only be separated for significantly non circular equilibria. From our discussions of $\beta_I+l_i/2$, we know we can measure $\beta_I+L_i/2$ exactly anyway. If we have reconstructed the plasma surface then we can evaluate the integrals s_1 and s_2 on that plasma surface, and then $L_i = l_i$. For circular equilibria it is found that only the sum $\beta_I + l_i/2$ can be found. Of course, adding a diamagnetic measurement allows the separation for any shape, as we have seen. Also adding a pressure profile form, or the pressure on axis, is enough to allow separation even for circular discharges. It is generally found that a distortion of the shape to $b/a \sim$ 1.3 is needed to make the separation.

A significant problem is that, having made specific assumptions about the form of the current density profile, we do not know how general our results are.

16. FAST SURFACE RECONSTRUCTION

Here we want to investigate 'fast' methods of determining the plasma boundary, and fields on that boundary. If we can do this, then we can exactly derive parameters such as $\beta_I + l_i/2$, and q, on the boundary, as well as parameterizing the boundary shape itself. Here we specifically do not want to obtain any information on fields and fluxes inside the plasma boundary.

In the vacuum region $S_{\phi vacuum}$ bounded by the contour l_{plasma} and l, the flux function satisfies the homogeneous equation $L^*\psi = 0$. A solution for this equation which agrees with boundary conditions on l, and that is valid in a region containing $S_{\phi vacuum}$, must then be valid on the plasma boundary itself.

In general we choose to approximate ψ by a series solution

$$\psi \approx \psi_{est} = \psi^0 + \sum_{j=1}^{N} c_j \chi_j \qquad\qquad 16.1$$

With ψ^0 any known terms, and the basis functions all satisfy the homogeneous equilibrium equation on some region $S_{\phi 0}$ which includes the vacuum region $S_{\phi vacuum}$. Following the discussion in section 8 we can write $\psi = \psi_{ext} + \psi_{int}$ from Equations 8.12 through 8.15. Usually we take an interior solution ψ_{int} associated with current distributions inside S_ϕ, and an exterior part ψ_{ext} associated with currents in the exterior region $S_{\phi ext}$. For example ψ_{ext} may be known from measured currents in external conductors, or calculated directly from the measurements using Green's functions. Various representations for the plasma current have been used;

> an expansion in toroidal eigenfunctions,

> discrete current filaments,

> single layer potential on a control surface,

To date no purely analytic answers are available; generally the coefficients in an expansion, of position or currents in filaments, are altered numerically to provide a minimum "chi squared" between some measured and computed fields or fluxes. For example, suppose the actual measurements are represented by q_i, with i running from 1 to M. There is a response matrix Q such that

$$q_{est,i} = q_{est,i}^0 + \sum_{j=1}^{N} c_j Q_{ij} \qquad\qquad 16.2$$

where $q_{est,i}$ is the value expected for q_i when Equation 15.1 holds. $q_{est}{}^0{}_{,i}$ is associated with ψ^o, and the known Q_{ij} is associated with χ_j. Then the usual least squares approach will determine the coefficients c_j to minimize the function

$$\sum_{i=1}^{M} \frac{\left(q_i - q_{est,i}\right)^2}{\sigma_i^2} \qquad\qquad 16.3$$

With σ_i the standard error of the ith measurement. This procedure may not be stable, in which case some numerical damping is added

One technique which avoids the iterations necessary to match the measured and predicted field components is as follows. From the measured fields construct the multipole moments Y_m using the techniques outlined in sections 9 and 10. Then m toroidal filaments with current (I_p/m) can be positioned to give the same moments Y_m as those measured. Because we have analytic forms for the Y_m produced by discrete current filaments (the integral $Y_m = \int j_\phi f_m dS_\phi$ only takes a finite value at the filament location) we can derive analytic expressions for the filament positions in terms of the measured Y_m's, thus avoiding the need for the iterative procedure. Just as discussed above, we then use toroidal filaments with known currents for external windings, the m filaments for the plasma, and plot the flux contours immediately. Solutions up to the plasma boundary are as exact as our set of moments allows. I am not sure how unique the solution is, or to what extent I should consider taking more than m filaments. We have still to ask if our solution is unique: that is, do the m moments uniquely specify the fields on the contour l?

An example of such a procedure is shown in *Figure 16.1a. Figure 16.1b* shows a full equilibrium reconstruction with $j_\phi(r)$ iterated until a good fit between measured and computed moments was obtained. Clearly the 3 filament approximation, with the filaments chosen to give the measured moments Y_1, Y_2 and Y_3, gives a good description of the outer surface.

In principle we should be able to extend the "moments with filaments" method of finding the plasma shape to the use of an analytic representation for the current density. Indeed, we did this in section 11 to find a relationship between the second moment Y_2 and ellipticity. However, there we made an arbitrary choice that the current density be flat. In fact we should specify that j_ϕ satisfy the Grad Shafranov equation: this problem is considerably more complicated. However, if solved, we should be able to obtain analytic relationships between the measured moments and the plasma shape. We would still have to parameterize the form for j_ϕ: this would be restricted by, for example, a knowledge of the ratio of q on axis to q at the edge.
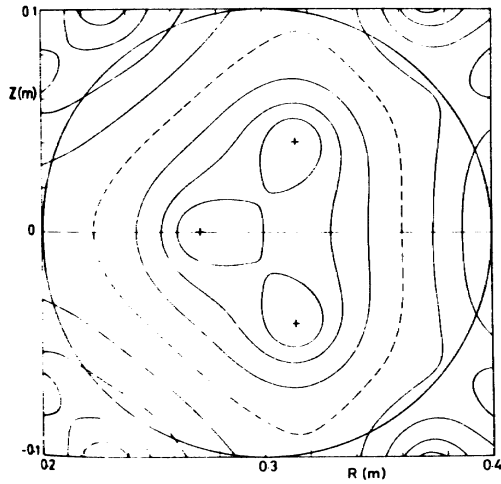
. *Flux surfaces, computed for a three-filament plasma current, with the experimentally measured moments. The broken line represents the plasma surface, the circle the vacuum vessel around which the line intergrals were measured.*
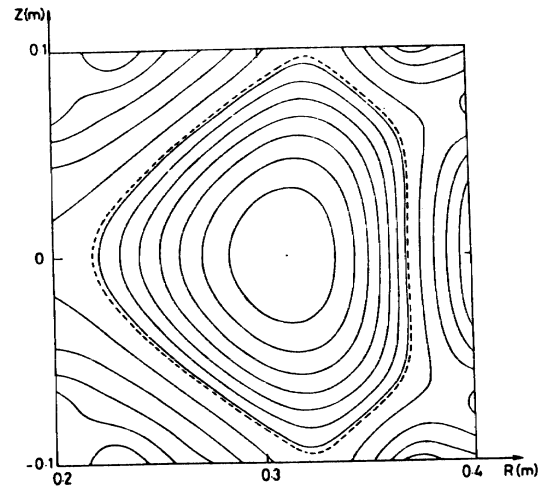
Flux surfaces predicted by a free-boundary equilibrium calculation. Flux-independent current, with poloidal beta = 0.5, gives moments similar to those measured

Fi

gure 16.1a. External surface reconstruction *Figure 16.1b.* External and internal surface reconstruction

17. FLUCTUATING FIELDS

(MIRNOV OSCILLATIONS and TURBULENCE)

Mirnov Oscillations

In tokamaks it is expected that magnetic islands play a role in determining transport. Their structure is approximately of the form $\exp(i(m\theta+n\phi))$, and they are located at surfaces where $q = m/n$, a ratio of integers. This is illustrated in *Figure 17.0*.
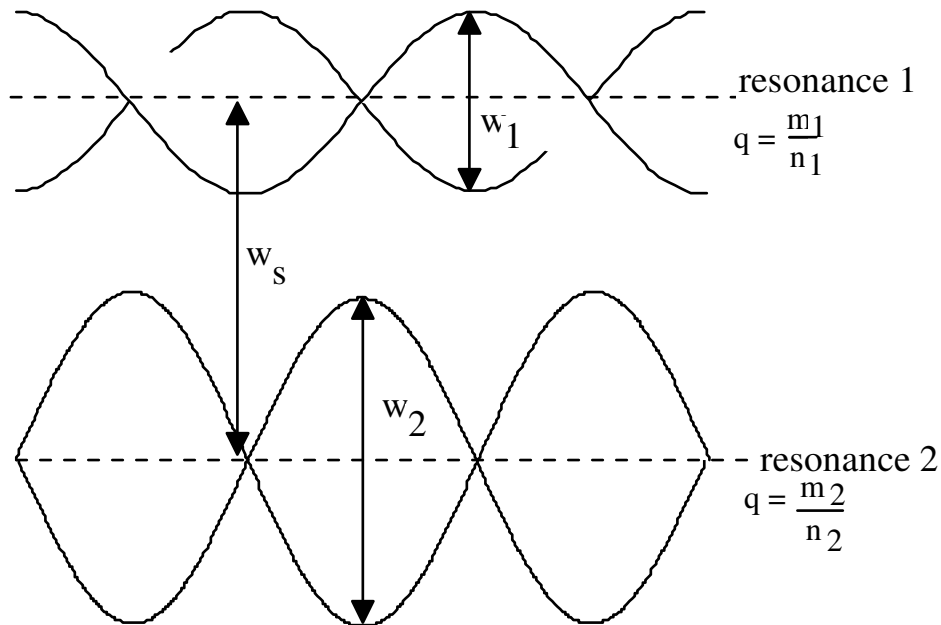

Figure 17.0. The envelopes of two adjacent magnetic islands.

In terms of the Fourier coefficients of the radial component of perturbing field $b_{r,mn}$ at the resonant surface r_{mn} (where $q = m/m$), the island full width w is given by:

$$w_i = 2\sqrt{\frac{4q^2|b_{rmn}|R}{mB_\phi\frac{\partial q}{\partial r}}}$$

17.1

Note that if the current distribution is uniform, (so $\partial q/\partial r=0$) and a resonance exists, this predicts that an infinitesimally small perturbing field will destroy the circular flux surfaces completely. Mirnov first studied their presence using b_θ loops, actually measuring $\partial b_\theta/\partial t$ outside the plasma (B denotes total fields, while b denotes just the oscillating part). Because the coils are outside the plasma they do not measure the field strength at the integer q surface where the perturbation is

resonant, so that we cannot immediately calculate the magnetic island width using Equation 17.1. Other problems to cope with include how to determine the poloidal (m) mode number from a set of coils measuring b_θ if they are not on a circular contour, so that a simple Fourier analysis is not possible, and toroidal effects.

If the field perturbation is b, then outside the circular plasma at some radius $r > a_p$ we have

$$\nabla \bullet \mathbf{b} = \frac{\partial b_r}{\partial r} + \frac{im}{r} b_\theta + \frac{in}{R} b_\phi = 0 \qquad\qquad 17.2$$

$$(\nabla \times \mathbf{b}) \bullet \mathbf{e}_r = \frac{im}{r} b_\phi - \frac{in}{R} b_\theta \qquad\qquad 17.3$$

Form the second equation we have

$$\frac{b_\theta}{b_\phi} = \frac{mR}{nr} \qquad\qquad 17.4$$

which for low m, n is $>>1$, i.e. $b_\theta >> b_\phi$. Therefore with Equation 17.2 we determine that the most important contributions to measure are b_r and b_θ, not b_ϕ. If we are measuring just inside a conducting wall (e.g. the vessel) then $b_r \approx 0$, so that only b_θ should be monitored (but note the conducting wall also affects the value of b_θ: it can also affect the instability which produces b_θ itself).
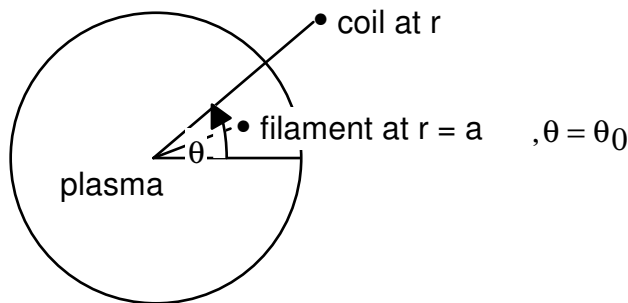

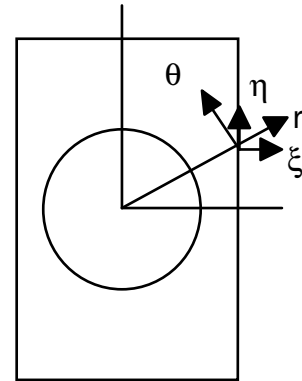*Figure 17.1a*   *Figure 17.1b*

A common representation of the fluctuations is as current filaments aligned along the field lines. Initially let us consider the fields produced in a straight cylinder by a current filament (current I) aligned along the cylinder, located at poloidal angle $\theta = \theta_0$, at $r = a$ (see *Figure 17.1*). Then.

$$b_\theta = \frac{\mu_0 I}{2\pi} \frac{(r - a\cos(\theta - \theta_0))}{(a^2 + r^2 - 2ar\cos(\theta - \theta_0))} \qquad\qquad 17.5$$

$$b_r = -\frac{\mu_0 I}{2\pi} \frac{a\sin(\theta - \theta_0)}{\left(a^2 + r^2 - 2ar\cos(\theta - \theta_0)\right)}$$

17.6

These can be rewritten by expanding the denominator into [r - a exp(i(θ−θ0))].[r - a.exp(-i(θ−θ0))]. For example:

$$b_\theta = \frac{\mu_0 I}{4\pi}\left[\frac{1}{\left(r - ae^{i(\theta - \theta_0)}\right)} + \frac{1}{\left(r - ae^{-i(\theta - \theta_0)}\right)}\right]$$

17.7

These new expressions can be expanded in powers of (r/a), so that

	r < a **inside filament**	**r > a** **outside filament**
b$_\theta$	$-\dfrac{\mu_0 I}{2\pi r}\sum\limits_{n=1}^{\infty}\left(\dfrac{r}{a}\right)^n\cos(n(\theta - \theta_0))$	$\dfrac{\mu_0 I}{2\pi r}\sum\limits_{n=0}^{\infty}\left(\dfrac{a}{r}\right)^n\cos(n(\theta - \theta_0))$
b$_r$	$-\dfrac{\mu_0 I}{2\pi r}\sum\limits_{n=1}^{\infty}\left(\dfrac{r}{a}\right)^n\sin(n(\theta - \theta_0))$	$-\dfrac{\mu_0 I}{2\pi r}\sum\limits_{n=0}^{\infty}\left(\dfrac{a}{r}\right)^n\sin(n(\theta - \theta_0))$

17.8

i.e. we have the fields as a Fourier series. A certain sum of the coefficients allows us to look only at the current inside the cylinder, while ignoring external currents:

$$r\int_0^{2\pi} b_\theta(\theta)\cos(m\theta)d\theta - r\int_0^{2\pi} b_r(\theta)\sin(m\theta)d\theta = \mu_0 I\left(\frac{a}{r}\right)^m\cos(m\theta_0) \text{ if a < r (outside)}$$

$$r\int_0^{2\pi} b_\theta(\theta)\cos(m\theta)d\theta - r\int_0^{2\pi} b_r(\theta)\sin(m\theta)d\theta = 0 \text{ if a > r (inside)}$$

$$r\int_0^{2\pi} b_\theta(\theta)\sin(m\theta)d\theta + r\int_0^{2\pi} b_r(\theta)\cos(m\theta)d\theta = \mu_0 I\left(\frac{a}{r}\right)^m\sin(m\theta_0) \text{ if a < r (outside)}$$

$$r\int_0^{2\pi} b_\theta(\theta)\sin(m\theta)d\theta + r\int_0^{2\pi} b_r(\theta)\cos(m\theta)d\theta = 0 \text{ if a > r (inside)}$$

17.9

Consider just the m = 1 component . These equations tell us that, in straight geometry the sum of a modified Rogowski coil with winding density proportional to cos(θ), and saddle coil with width proportional to sin(θ), tells us the horizontal position. A modified Rogowski coil with winding

density proportional to sin(θ), and saddle coil with width proportional to cos(θ), tells us the vertical position. Actually we already new this; section 9 tells us how to do better and correct for toroidal effects as well. Note if the Mirnov coils are mounted just inside a conducting vessel then $b_r = 0$, and the second terms are zero.

Now we must consider a general distribution j(r,θ) instead of the line current at r = a. Then using complex notation, and assuming a conducting vessel where $b_r = 0$:

$$r\int_0^{2\pi} b_\theta(\theta)e^{im\theta}d\theta = \mu_0\int_0^r dr'\left(\frac{r'}{r}\right)^m \int_0^{2\pi} r'\,d\theta j(r',\theta)e^{im\theta} \qquad 17.10$$

thus relating moments of the external field to moments of the current density. Rogowski coils with winding density cos(mθ) and sin(mθ) would directly measure the LHS of this equation (again we knew this from section 9). Now we see a problem: the LHS is an integral over θ while the RHS is an integral over r' and θ. Without some assumptions we cannot work back from the externally measured fields to the currents at the surface. This is exactly the same problem that we came across in dealing with reconstructing the plasma shape from the multipole moments without invoking equilibrium: varying the assumed j_ϕ distribution gives different plasma shapes.

A typical assumption is

$$j(r,\theta) = j_0(r) + \sum_{m,n} j_{mn} e^{i(m\theta+n\phi-\omega_{mn}t)} \delta(r-r_{mn}) \qquad 17.11$$

with $j_0(r)$ the equilibrium current, r_{mn} the radius of the resonant surface, $\delta(r-r_{mn})$ the delta function restricting the currents to r = r_{mn}. The perturbed field measured at r, produced by the current perturbation j_{mn} at r_{mn}, is

$$b_\theta(r,\theta,\phi) = \mu_0 j_{mn} r_{mn}\left(\frac{r_{mn}}{r}\right)^{m+1} e^{i(m\theta+n\phi-\omega_{mn}t)} \text{ for r > } r_{mn} \qquad 17.12$$

Here we have introduced a frequency f = ω/(2π) into the problem: the filaments are rotating. If we want to consider b_r and b_θ, and work in real space, then

$$b_\theta = \frac{\mu_0 j_{mn} r_{mn}}{2}\left(\frac{r_{mn}}{r}\right)^{m+1} \cos(m\theta+n\phi-\omega_{mn}t) \qquad 17.13$$

$$b_r = -\frac{\mu_0 j_{mn} r_{mn}}{2}\left(\frac{r_{mn}}{r}\right)^{m+1} \sin(m\theta+n\phi-\omega_{mn}t) \qquad 17.14$$

Often we will write an expression for the Fourier coefficients of the field at the resonant surface, $b_{mn}(r = r_{mn}) = \mu_0 j_{mn} r_{mn} / 2$. Note if we were working on a rectangular vessel we would measure for example b_η (see *Figure 10.1*):

$$b_\eta = b_\theta \cos(\theta) + b_r \sin(\theta) = b_{mn}\left(\frac{r_{mn}}{r}\right)^{m+1} \cos\big((m+1)\theta + n\phi - \omega_{mn}t\big) \qquad 17.15$$

i.e. we see that working with a rectangular contour the phase varies as $(m+1)\theta$, instead of $m\theta$ when working with a circular contour.

Now in toroidal geometry there are complications. We must consider that

a) j_{mn} produces a stronger field at the inner equator

b) the perturbation are displaced because of a Shafranov shift

c) the pitch of the field lines is no longer constant

We will now derive the toroidal corrections for a case where we are considering surface current perturbations for our model equilibrium of section 6. We start with the field line equation for the total equilibrium fields, evaluated at a radius $r = a_p$, the plasma minor radius:

$$\frac{ad\theta}{B_\theta} = \frac{Rd\phi}{B_\phi} \qquad 17.16$$

With

$$R = R_g + a\cos(\theta) \qquad 17.17$$

$$B_\phi = \frac{B_{\phi0}(R = R_g)}{\left(1 + \frac{a}{R_g}\cos(\theta)\right)} \qquad 17.18$$

$$B_{\theta a} = \frac{\mu_0 I_p}{2\pi a}\left(1 + \frac{a}{R_g}\Lambda\cos(\theta)\right) \qquad 17.19$$
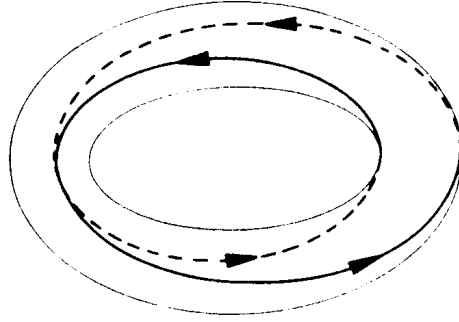
$$\Lambda = \beta_I + \frac{l_i}{2} - 1 \qquad 17.20$$

Figure 17.2. Field lines around a torus, for the case q = 2.

We can derive what is sometimes called q_{mhd}, sometimes q_I. This is the number of toroidal field revolutions a field line must be followed to make one poloidal revolution. *Figure 17.2* shows the field lines for the case where q = 2. Generally we have

$$q_{MHD} = \frac{1}{2\pi} \int_0^{2\pi} \frac{aB_\phi}{RB_\theta} d\theta \qquad\qquad 17.21$$

Keeping $(a/R)^2$ terms gives

$$q_{MHD} = \frac{2\pi a^2 B_{\phi 0}}{\mu_0 I_p R_g}\left[1 + \left(\frac{a}{R_g}\right)^2\left(1 + 0.5\left(\beta_I + \frac{l_i}{2}\right)^2\right)\right]$$

$$= q_{circ}\left[1 + \left(\frac{a}{R_g}\right)^2\left(1 + 0.5\left(\beta_I + \frac{l_i}{2}\right)^2\right)\right] \qquad\qquad 17.22$$

The toroidal angle covered when a field line is followed around a poloidal angle of θ is

$$\phi = \int \frac{aB_\phi}{RB_\theta} d\theta = q_{circ}\int\left[\left(1 + \left(\frac{a}{R_g}\right)\cos(\theta)\right)^{-2}\left(1 + \left(\frac{a}{R_g}\right)\Lambda\cos(\theta)\right)^{-1}\right]d\theta$$

$$= q_{circ}\left[\theta - \frac{a}{R_g}(2 + \Lambda)\sin(\theta)\right] \qquad\qquad 17.23$$

where we have written q_{circ} for the value in a straight cylinder. In this straight cylinder we would have the toroidal angle ϕ covered in following a field line a given poloidal angle θ given by Equation 17.23 with $a/R_g = 0$, i.e. $\phi = q_{circ}\theta$. Now we see that, in transferring to toroidal geometry, we must replace the poloidal angle θ by θ^*, where

$$\theta^* = \frac{\phi}{q_{MHD}} = \theta - \frac{a}{R_g}\left(\beta_I + \frac{l_i}{2} + 1\right)\sin(\theta) \qquad\qquad 17.24$$

i.e. the perturbing fields must have the form (for $r_{mn} \approx a$)

$$b_\theta = b_{mn}\left(\frac{r_{mn}}{r}\right)^{m+1}\cos\left(m\theta^* + n\phi - \omega_{mn}t\right) \qquad\qquad 17.25$$

Figure 17.3 illustrates the field line trajectories in (ϕ,θ) space. Here we have assumed that $q_{MHD}(r) = q_0 + (q_a - q_0)\left(\frac{r}{a}\right)^\alpha$, with q_0 the value at r = 0, q_a the value at r = a (the plasma edge). This allows us to express $r = a\left(\frac{q_{MHD}(r) - q_0}{q_a - q_0}\right)^{\frac{1}{\alpha}}$. In the figure we show examples for a = 0.25 m, R_g = 1 m, q_0 = 0.9, q_a = 3.2, β_I = 0.5, l_i = 0.9. The solid lines are for q_{MHD} = 3.2 (the plasma edge), and the broken lines for q_{MHD} = 2. The shear in the q profile is apparent.
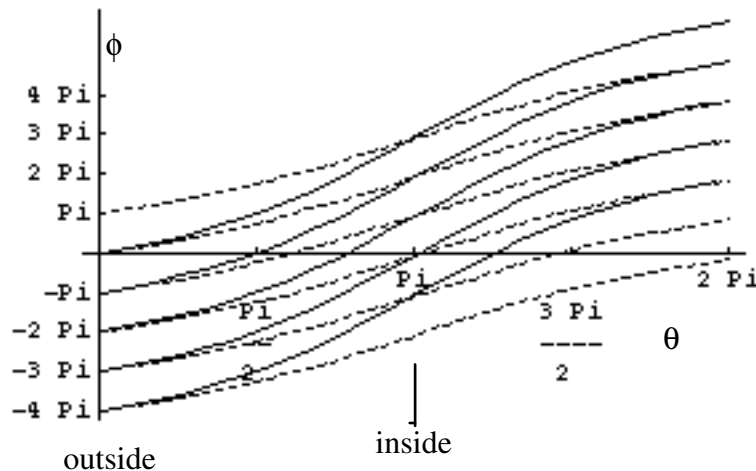

Figure 17.3. The trajectory of field lines in ϕ, θ space for q = 2 (broken lines) and q = 3.2 (solid lines).

Analysis techniques

With a set of Mirnov coils spanning a poloidal cross section of a low beta, circular cross section tokamak, we can take a Fourier transform in θ to obtain the amplitude of each component $\cos(m\theta + n\phi - \omega_{mn}t)$. If we have a rectangular vessel, then we have shown that the relevant expression is $\cos(m\theta + \theta + n\phi - \omega_{mn}t)$. This has been done both computationally, and using analog multiplexing. We should allow for the toroidal corrections discussed above when performing this Fourier analysis; so that θ is replaced by θ^*. *Figure 17.4* shows the placement of the coils

around a circular vessel. Both poloidal and toroidal arrays are required to determine poloidal (m) and toroidal (n) mode numbers.
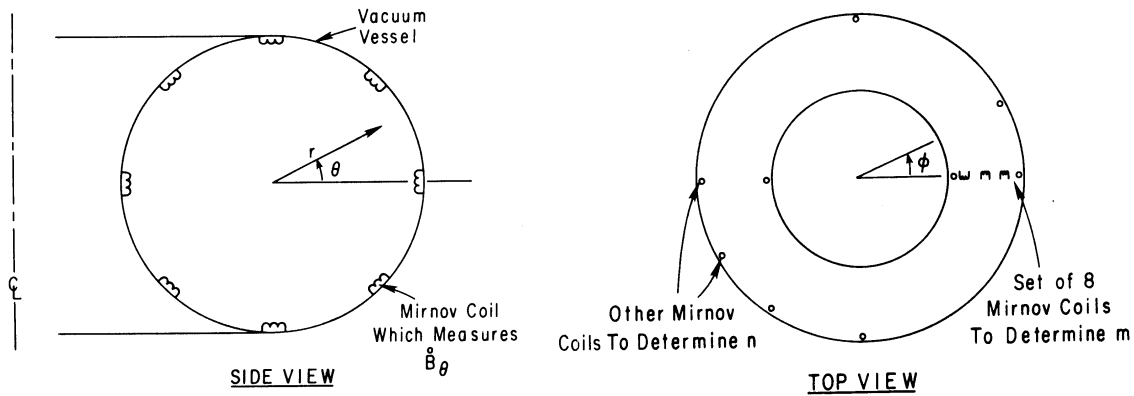

Figure 17.4. The placement of Mirnov coils (magnetic pick-up coils) around a vessel

Figure 17.5 shows an example of data obtained from PBX, a machine with a non circular vessel but operated with a circular plasma. Coils 1 through 5 are located on a vertical line at the outer equator, with coil 1 the lowest. Coils 6 through 10 are located on a vertical line at the inner equator, with coil 6 the highest. Coils 11 through 14 are elsewhere; but in particular coil 12 is at the outer equator ($\theta = 0$) while coil 13 is at the inner equator ($\theta = \pi$). Data is shown for a period of 10 ms. The scale in volts is shown on the right hand side. A peak first appears on coil 1, and then progresses to coil 5. An outside to inside asymmetry (coil 12 to coil 13) is evident.
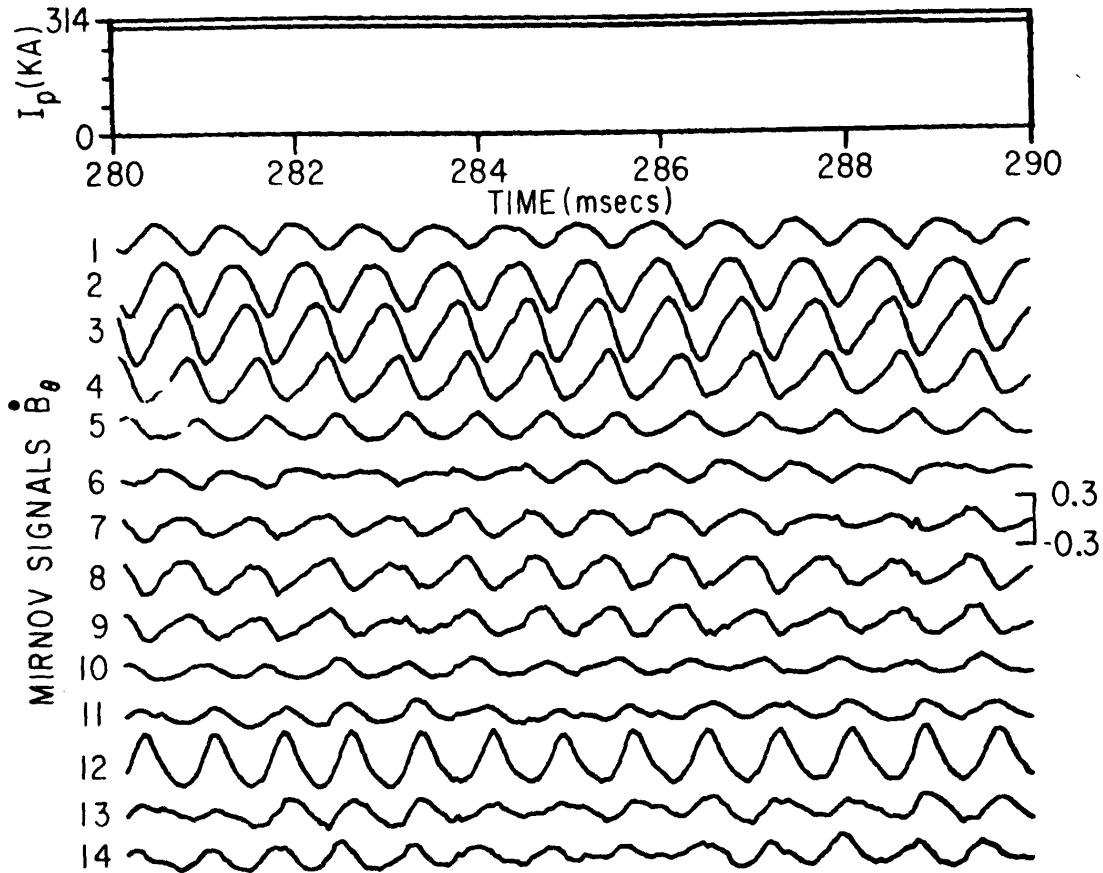
Figure 17.5. Data from PBX.

Another technique is to look in the frequency domain. Suppose we have coils placed both poloidally and toroidally around the plasma. Then the relationship between the phases of different signals identifies m and n without the amplitudes being known. By looking in the frequency domain we can reject noise, and other modes at frequencies other than ω_{mn}. Taking a rectangular vessel as an example (we measure b_η), then the fundamental component of the ith coil signal will be of the form

$$S_i = A_i \cos(\omega_{mn}t - \delta_i)$$ 17.26

with ω_{mn} identified from power spectra. The relative phase shift δ_i will be, for the m,n mode,

$$\delta_i = m\left[\theta_i - \frac{r_{mn}}{R_g}\left(1+\beta_I+\frac{l_i}{2}\right)\sin(\theta_i)\right] + \theta_i + n\phi_i + \delta_0 + 2\pi k_i$$ 17.27

where (θ_i,ϕ_i) locates the ith coil, δ_0+2pk_i expresses the multi-valued phase property. If we were in a circular vessel, then the phase shift would be

126

$$\delta_i = m\left[\theta_i - \frac{r_{mn}}{R_g}\left(1 + \beta_I + \frac{l_i}{2}\right)\sin(\theta_i)\right] + n\phi_i + \delta_0 + 2\pi k_i \qquad 17.28$$

By performing a best fit of the measured phase with this expression gives m and n. For example plotting δ_i-$n\phi_i$ against θ_i (to remove the toroidal effects) should give a line of slope m+1. An example is shown in *Figure 17.6,* data from PBX. The best fit to the data was obtained using m = 2, n = 1.
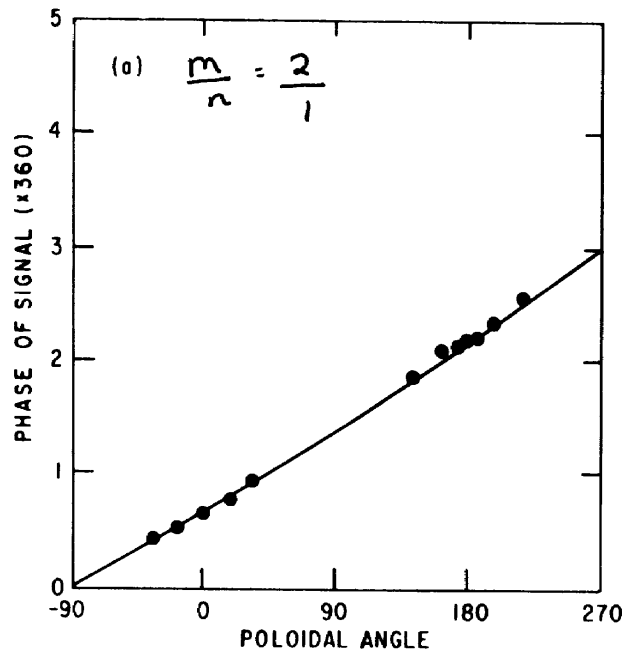

Figure 17.6. The phase of the experimental data shown in Figure 17.5, together with the phase given by equation 17.28. with m = 2, n = 1

Turbulence

Magnetic coils outside the plasma measure not only the low m,n "Mirnov" oscillations (tearing modes), but also higher frequency, higher mode number fluctuations. Many m, n modes are possible; *Figure 17.7* shows an example where 1 ≤ m ≤ 40, and 1 ≤ n ≤ 12 are considered. Each point represents a possible mode combination, the dark area shows those possible when q_a = 3.2 , q_0 = 1, and constraints to m are applied (in this case 6 ≤ m ≤ 12).
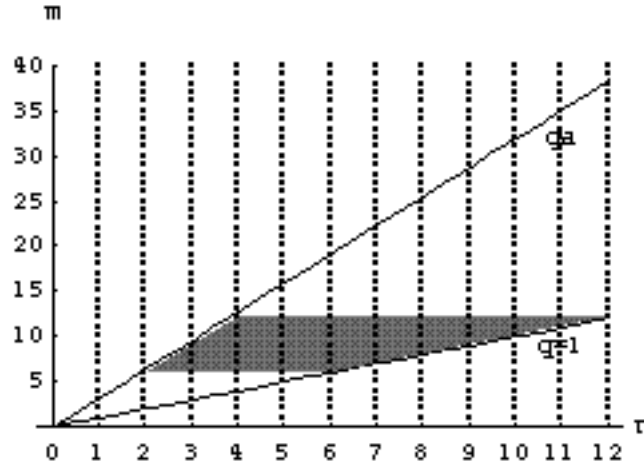
Figure 17.7. The (m,n) space, with the limits imposed by $q_0 = 1$ and $q_a = 3.2$. The darker shaded area represents the space considered in the analytic model described in the text.

The measurements of the fluctuating fields are usually restricted to root means square (rms) fields, b_{rrms} and $b_{\theta rms}$, at $r > a$, the limiter radius. We would like to know how this is related to the field components at the resonant surface, so that we can calculate associated island widths. Typically we want to determine b_{rmn} from a measured $b_{\theta rms}$ outside r_{mn}. There is no unique transformation from $b_{\theta rms}$ to b_{rmn}, so a model must be invoked.

We proceed by assuming the fluctuating self generated field $b_{\theta rms}$ measured with magnetic probes at $r > a$ is proportional to the required b_{rmn} at $r_{mn} \approx a$. Evidence for such a model comes from correlation measurements between Langmuir probes and magnetic probes; the measured $b_{\theta rms}$ at $r > a$ is apparently determined by plasma current fluctuations at $r \approx a$, i.e. at the plasma edge. Outside the fluctuating current filaments ($r > r_{mn}$) the magnetic fields can be approximated by

$$b_r = \sum_{m,n} (b_{rmn})_{r=r_{mn}} \left(\frac{r}{r_{mn}}\right)^{-(m+1)} \cos(m\theta + n\phi + \delta_{mn}) \qquad 17.29$$

with ϕ the toroidal angle, θ the poloidal angle, and δ_{mn} a random phase. This ignores toroidal effects, which introduce terms proportional to $(m\pm1)$, and is strictly valid only for small n. If a conducting wall is present at $r = b$ then the expression is modified by the factor $[1-(r/b)^{2m}]$. For stationary ergodic turbulence the time and spatial averages are the same, so that the root mean square is found as a spatial average. Outside the singular surface we measure

$$b_{rms} = b_{r,rms} = b_{\theta,rms} = \sqrt{0.5\sum_{m,n}|b_{rmn}|^2_{r=r_{mn}}\left(\frac{r}{r_{mn}}\right)^{-2(m+1)}}$$ 17.30

To go further and obtain a relationship between $b_{\theta rms}$ at $r > a$ in terms of b_{rmn} at $r = r_{mn}$ we must specify

   a given current density or safety factor profile $q(r)$,

   the dependence of b_{rmn} on m and n,

   locate all possible m and n pairs where $q = m/n$,

   specify upper and lower limits to either m or n.

In general this must be done computationally. However, some progress can be made analytically. We can approximately solve Equation 17.30 for $b_{\theta rms}$ at $r > a$ in terms of b_{rmn} at $r = r_{mn}$ if we take b_{rmn} independent of m and n over some range to be specified, and a q profile relevant to the plasma edge, for example $q = q_a\left(\frac{r}{a}\right)^2$. Then we can relate the resonance location r_{mn} to a given q,

$$\frac{r_{mn}}{a} = \left(\frac{q}{q_a}\right)^{\frac{1}{2}} = \left(\frac{m}{nq_a}\right)^{\frac{1}{2}}$$ 17.31

With $\rho = r/a$ defining the measurement position and $q = m/n$, Equation 17.30 is written as

$$\left(\frac{b_{rms}}{|b_{rmn}|}\right)^2_{\rho\geq1} = 0.5\sum_{m,n}\left(\frac{1}{\rho}\right)^{2(m+1)}\left(\frac{m}{nq_a}\right)^{(m+1)}$$ 17.32

$\rho \geq 1$ is a constant, namely the location of the magnetic pick-up coils used to measure b_{rms}.

We now replace the summation by integrals. The space we are considering is shown in *Figure 17.4*. The first integral, $\int dn$, is from m/q_a to m, allowing all n values in between. The second integral, $\int dm$, is from m_1 to m_2, with $m_2 \gg m_1$. In Figure 17.4 $m_1 = 6$ and $m_2 = 12$. Unfortunately our chosen profile allows $q \leq 1$ (when $r_{mn}/a \leq 1/\sqrt{q_a}$). To restrict $n \geq 1$ we should choose $m_1 \geq q_a \approx 3$. The result of the integration is

$$\frac{b_{rms}}{|b_{rmn}|} = \left[\begin{array}{c} \dfrac{1}{4q_a\ln(\rho)}\left(\dfrac{1}{\rho^{2(m_1+1)}} - \dfrac{1}{\rho^{2(m_2+1)}}\right) \\[2em] -\dfrac{1}{2(\ln(q_a)+2\ln(\rho))}\left(\dfrac{1}{q_a^{(m_1+1)}\rho^{2(m_1+1)}} - \dfrac{1}{q_a^{(m2+1)}\rho^{2(m2+1)}}\right) \end{array}\right]^{\frac{1}{2}}$$

17.33

This expression can be further simplified for $\rho > 1$ by noting $m_2 \gg 1$ (so all terms involving m_2 disappear) and $m_1 > 1$ (so the term involving $q_a^{(m_1+1)}$ disappears) to give

$$\frac{b_{rms}}{|b_{rmn}|} = \frac{1}{2\rho^{(m_1+1)}\sqrt{q_a \ln(\rho)}}$$

17.34

This is the required result, giving us b_{rmn} at the plasma edge in terms of the measured b_{rms} outside the plasma. Because the terms involving m_2 have been ignored in deriving Equation 17.34 it predicts $(b_{rms}/|b_{rmn}|)_{\rho \Rightarrow 1} \Rightarrow \infty$. The more complete expression, remains finite, and

$$\left(\frac{b_{rms}}{|b_{rmn}|}\right)_{r=a} \approx \sqrt{\frac{(m_2 - m_1)}{2q_a}}$$

17.35

We conclude that the measured rms field outside the plasma ($\rho > 1$) is determined only by the lowest m number (m_1); the higher m numbers fall off too rapidly to contribute. Indeed, if Equation 17.34 is taken to represent the results, then a fit of the form $b_{rms} \propto r^{-\gamma}$ gives the result

$$\gamma = m_1 + 1 + \frac{1}{2\ln(\rho)}$$

17.36

We can also measure the frequency of the fluctuations. We assume that the observed frequency is described by an expression of the form

$$f = \frac{\omega}{2\pi} = \frac{m}{2\pi r_{mn} B_\phi}\left(\kappa \frac{T_e}{|e|n_e}\frac{\partial n_e}{\partial r} - E_r\right)$$

17.37

This is consistent with experimental results, with κ a factor of order 1. We also know experimentally that the term involving E_r dominates the term involving κ, and that we can approximate the expression by

$$f \approx \frac{-cmE_r}{2\pi r_{mn} B_\phi}$$

17.38

with χ a factor ≈ 1.5. E_r is approximately constant for $\rho < 1$. We now relate r_{mn} to $q = m/n$ by assuming a specific q profile. For the simple q profile used in deriving the analytic results the transformation from r_{mn} to m and n is given by Equation 17.31. A more realistic q profile gives

$$\frac{r_{mn}}{a} = \left(\frac{q - q_0}{q_a - q_0}\right)^{\frac{1}{2}} = \left(\frac{\frac{m}{n} - q_0}{q_a - q_0}\right)^{\frac{1}{2}} \approx \left(\frac{\frac{m}{n} - 1}{q_a - 1}\right)^{\frac{1}{2}} \qquad \text{17.39}$$

Substituting either Equation 17.31 (edge model, $f = f_1$) or Equation 17.39 ($f = f_2$) for r_{mn} into Equation 17.38 gives an expression for the frequency of a mode of given m and n;

$$f_1 \approx \frac{-cE_r\sqrt{q_a}}{2\pi a B_\phi}\sqrt{mn} \qquad \text{17.40}$$

$$f_2 \approx \frac{-cE_r\sqrt{(q_a - 1)}}{2\pi a B_\phi}\sqrt{\frac{m^2}{\left(\frac{m}{n} - 1\right)}}, \qquad \text{17.41}$$

These can be normalized to the frequency $f_{m/n=2/1}$ of the m = 2, n = 1 mode, which is often measured, to give from Equation 17.40

$$f_1 \approx \sqrt{\frac{mn}{2}}f_{m/n=2/1} \qquad \text{17.42a}$$

and from Equation 17.41

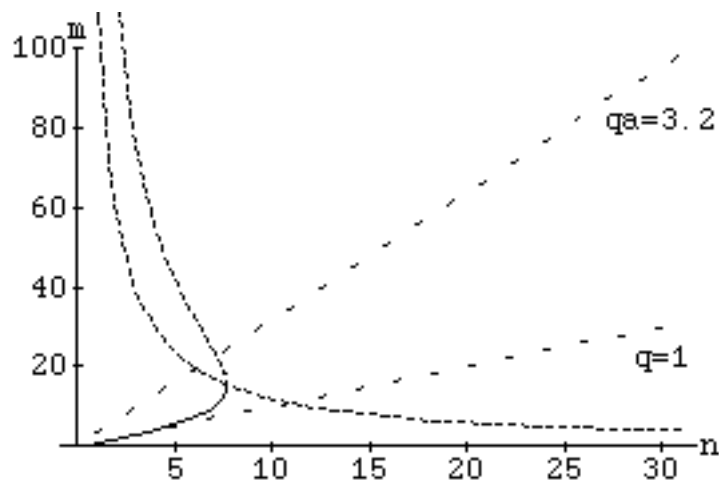$$f_2 \approx \sqrt{\frac{m^2}{4\left(\frac{m}{n} - 1\right)}}f_{m/n=2/1} \qquad \text{17.42b}$$

Figure 17.8 The values of m and n included and excluded by restricting f > 50 kHz, when $f_{m/n=2/1}$ = 6.5 kHz. The excluded area is to the left side of each filter line. The dashed straight lines represent the limits imposed by 1 < q < 3.2. The dotted curve

represents the limits imposed by the frequency filter from Equation 17.42a and Equation 17.42b.

If only modes with $f > f_{min}$ are considered, we can derive m_{lim}, a function of $f_{min}/f_{m/n=2/1}$ and n, which separates modes which are and are not included in any subsequent analysis. The results are shown in *Figure 17.8* for f_{min} = 50kHz, $f_{m/n=2/1}$ = 6.5 kHz. In general, frequency filtering should be considered more a restriction on n than on m.

18. INTERNAL PLASMA MEASUREMENTS

So far we have been concerned with measurements of fields taken outside the plasma.   In comparatively low temperature plasmas (say T_e < 50 to 100 ev), we can design pickup coils to make internal measurements. There is always the worry that the insertion of such a coil changes the very plasma characteristics we would like to determine. This fear is usually allayed by monitoring certain characteristic plasma features (sawtooth activity, Mirnov activity, loop voltage) to make sure they do not change significantly during probe insertion. *Figure 18.1* and *Figure 18.2* show a possible coil set up which might be used. The coil itself must be protected from the plasma, typically by a stainless steel case, possibly surrounded by a carbon shield. The geometry of the surrounding materials must be carefully chosen if we are looking at high frequencies so as not to cut off the very signals we want to measure.
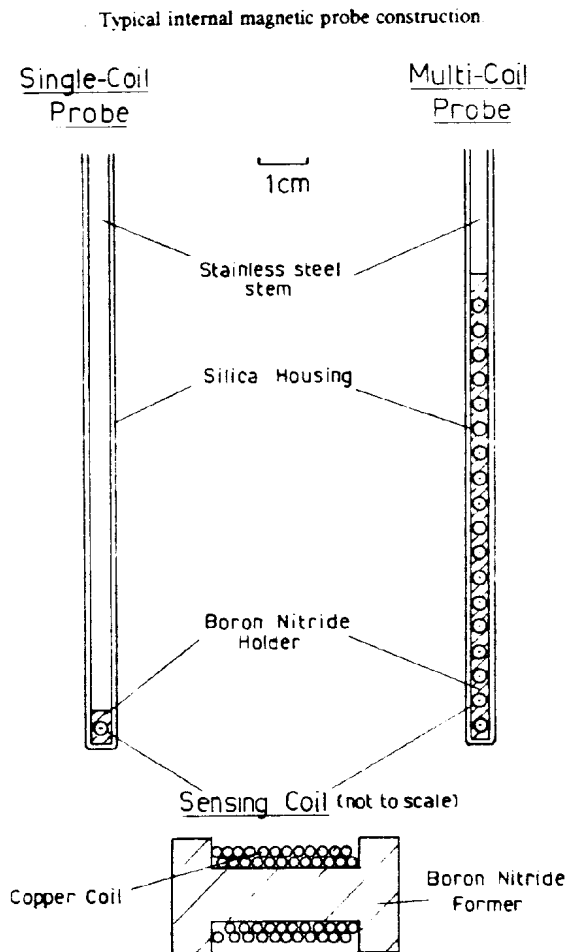

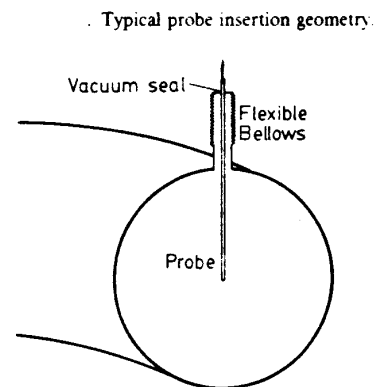
Figure 18.1. A possible internal coil construction.

*Figure 18.2.* A typical coil placement, showing the flexible belows.

Equilibrium

We first discuss the equilibrium. From the basic field measurements themselves we can, assuming circular straight geometry, reconstruct the current from the equations

$$j_\phi = \frac{1}{\mu_0 r}\frac{d}{dr}(rB_\theta)$$
18.1

$$j_\theta = -\frac{1}{\mu_0}\frac{d}{dr}(B_\phi)$$
18.2

i.e. to obtain $j_\phi(r)$ we only need the radial dependence of B_θ. Unfortunately we have to contend with non circularity and toroidicity. One technique which has been applied is illustrated by the results shown in *Figure 18.3*, where small pick-up coils were used to measure the poloidal magnetic field at current peak in a small tokamak (TNT inJapan).
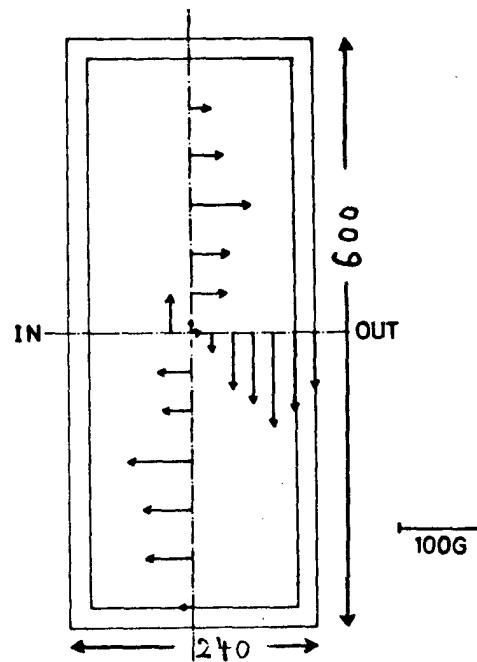
The measured poloidal magnetic field at
the current peak (700 μsec). The dimensions are
in millimeters.

Figure 18.3. Equilibrium poloidal fields measured in TNT

We move to the coordinate system of Figure 1.7. The radial component $B_R(R_0,z)$ is measured along a vertical line $R = R_0$, and the vertical component $B_z(R,0)$ is measured along a line $z = 0$. The results are fitted to expressions of the form

134

$$B_R(R_0, z) = \sum_{n=0}^{N} a_n z^n \qquad\qquad 18.3$$

$$B_z(R, 0) = \sum_{n=0}^{N} b_n R^n \qquad\qquad 18.4$$

The magnetic axis is found where from the zero crossing of the resulting polynomials. The flux function is found by integration:

$$\psi(R_0, z) = -R_0 \int \sum_{n=0}^{N} \left(a_n z^n \right) dz + const \qquad\qquad 18.5$$

$$\psi(R, 0) = \int \sum_{n=0}^{N} \left(b_n R^{n+1} \right) dR + const \qquad\qquad 18.6$$

The current density is then obtained as

$$\mu_0 j = \frac{\partial B_R}{\partial z} - \frac{\partial B_z}{\partial R} \qquad\qquad 18.7$$

The constants (giving $\partial B_R / \partial z$ at $z = 0$ and $\partial B_z / \partial R$ at $R = R_0$) must be determined by making some assumptions concerning the plasma shape, say that it is mostly elliptic. Some examples of the results of this analysis, where $N = 5$, are shown in *Figure 18.4* for the fluxes and *Figure 18.5* for the current density.
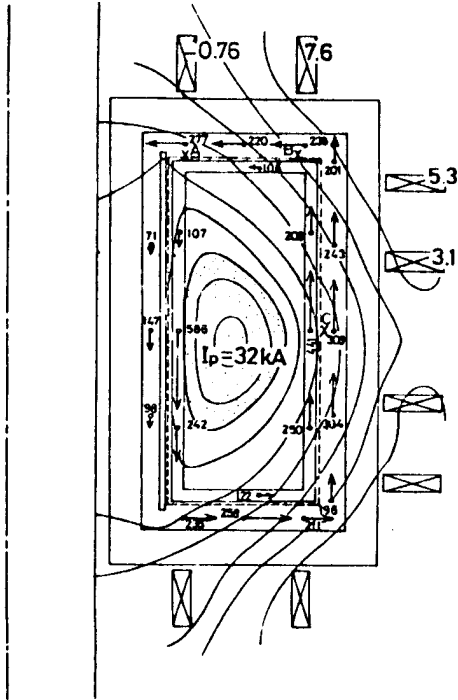
A rough sketch of magnetic
surface at the current maximum.
The equi-psi surfaces are drawn
for every $\pi \times 10^{-3}$ V·sec. Num-
bers at arrows show the field
component parallel to the arrows
in unit of gauss. The shaping
coil current is presented in
kAt, and minus sign means that
the coil current is parallel to
the plasma current. Coil current
has up-to-down symmetry.

Figure 18.4. Flux surfaces reconstructed for TNT.
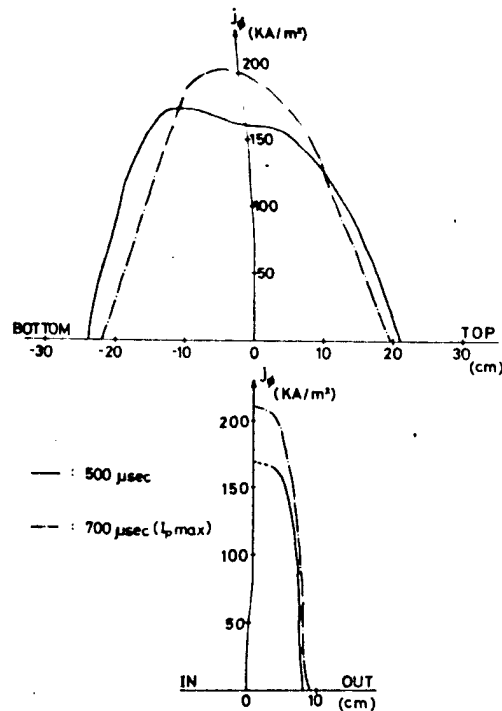
A typical example of the current density
profile at the current rising stage ($t = 500\ \mu$sec) and
at the current peak ($t = 700\ \mu$sec). Origins of the
graphs correspond to the center of the vacuum
vessel.

136

Figure 18.5. Current density profiles for TNT

Given the current density we can also attempt to deduce the safety factor q.

Internal magnetic measurements are also used to determine the internal electric field. From Faraday's law

$$\oint_l \mathbf{E} \bullet \mathbf{dl} = -\frac{d}{dt}\left(\int_S \mathbf{B} \bullet \mathbf{n} dS\right)$$
18.8

we have, applying this to the geometry of *Figure 18.6*,

$$E_\phi(r) = E_\phi(a) - \int_r^a \frac{d}{dt}B_\theta dr$$
18.9
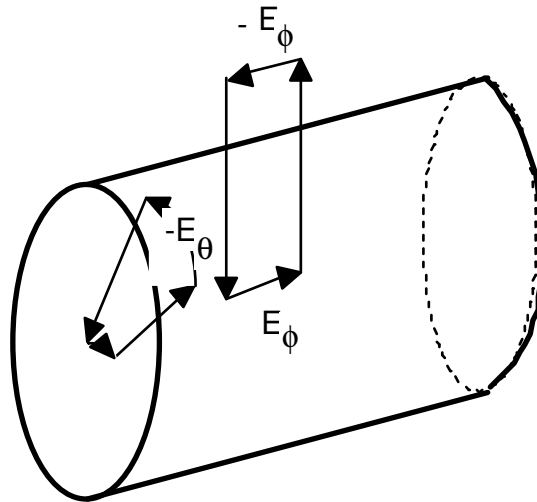
Figure 18.6. The geometry used to describe the measurements of internal electric field
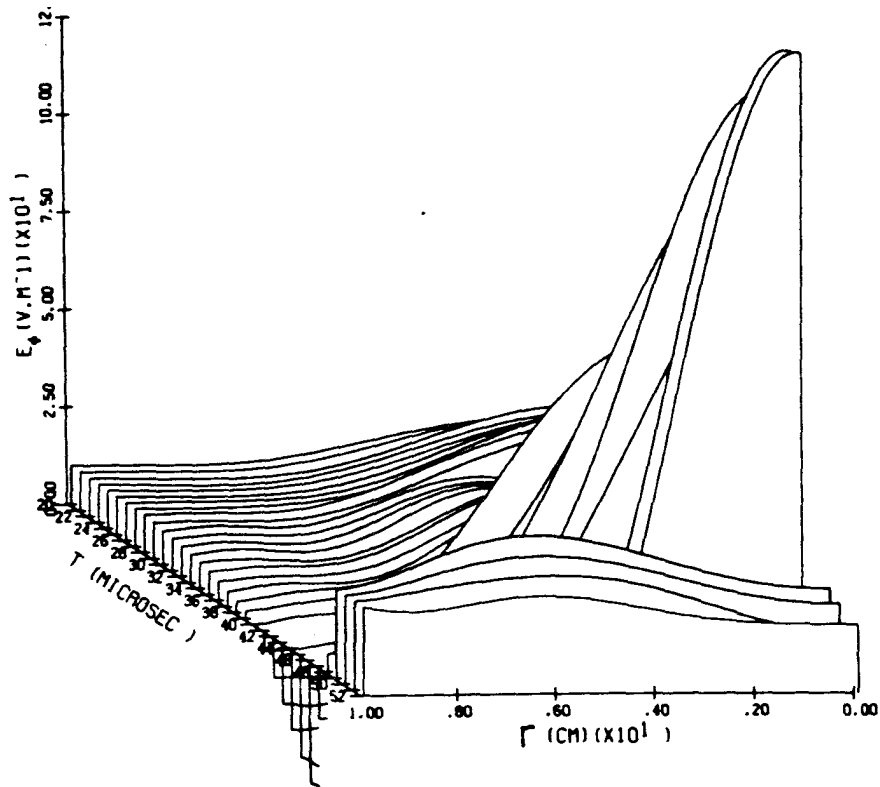
Toroidal electric field evolution

Figure 18.7. The internal electric field prior to a disruption (from Hutchinson)

Figure 18.7 shows some spatial profiles of E_ϕ from this analysis just before and at a disruption. Although the edge electric field goes negative (the negative voltage spike) the internal electric field strongly positive. In principle, having measured j and E we could derive the local conductivity.

Mirnov Oscillations

The same probes used to measure the internal equilibrium properties can be used to look at the Mirnov fluctuations (as long as the coils have a sufficiently high frequency response). Data from such experiments has isolated the radial dependence of the fluctuating b_r, b_θ fields, as shown in *Figure 18.8*. It agrees with our discussion in section 17, namely $b \propto (r_{mn}/r)^{m+1}$ for $r > r_{mn}$ without a vacuum vessel. In the presence of a conducting vessel at $r = r_w$ we must account for the image currents which flow, so for example we would expect
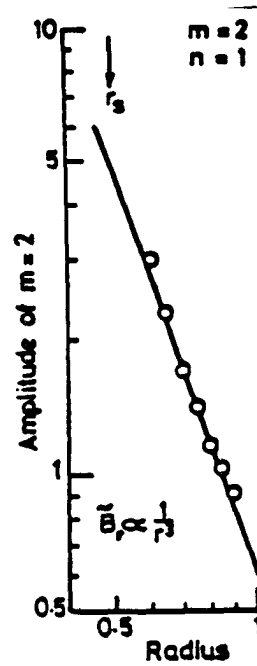
Figure 18.8. The measured radial dependence of the fluctuating poloidal fields
(Mirnov oscilations) from and m = 2 tearing mode (measurements in TOSCA).

19 . THE CONDUCTING VACUUM VESSEL

Skin depths

There is a vacuum vessel surrounding the plasma. Early experiments used insulating vessels (e.g. quartz or ceramic), which were later replaced by metal (stainless steel). In order to introduce the toroidal electric field necessary to initiate the discharge, this vessel must be highly resistive. This is ensured either by making a thin vessel, using convolutions, or adding at least one insulating break.

.　Circuit formation by the symmetrical (a) and non-symmetrical (b) components of the current in the casing in the presence of transverse gaps.
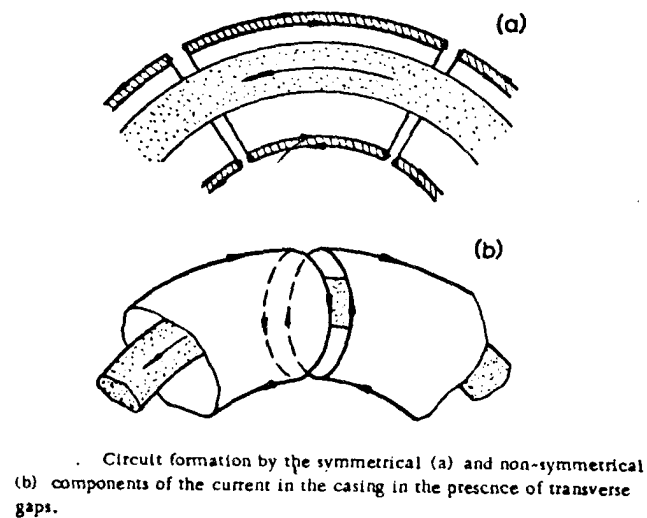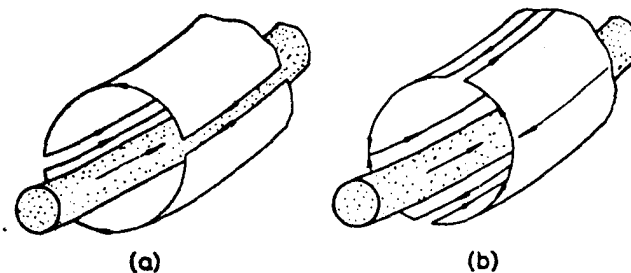
Figure 19.1. The currents flowing in a vessel or shell with a poloidal (or transverse) gap or insulating break.

Circuit formation by the non-symmetrical component of the current in the casing in the presence of longitudinal and transverse gaps:
(a) longitudinal gaps causing no distortions of the transverse field;
(b) longitudinal gaps distorting the transverse field.

Figure 19.2. The currents flowing in a vessel or shell with toroidal
(i.e. longitudinal) and poloidal (i.e. transverse) gaps.

There are two types of insulating breaks, as shown in *Figure 19.1* and *Figure 19.2, (taken from Mukhovatov and Shafranov)*. For transverse gaps (*Figure 19.1*) any symmetric component of current must flow on the vessel surfaces. However, non symmetric components, introduced for example by axisymmetric plasma motion, will produce volume currents. At the gap the non symmetric currents flow in opposite directions. They will produce a local vertical field, which must affect the plasma position, as well as the interpretation of magnetic coil signals. The two (surface and bulk) currents have different decay times, as discussed later.

If both a transverse and a longitudinal gap exists, *Figure 19.2* shows that for the non symmetric components the placing of the break in poloidal angle is important. A longitudinal gap at the outer equator does not distort the field, while a gap at the top or bottom does.
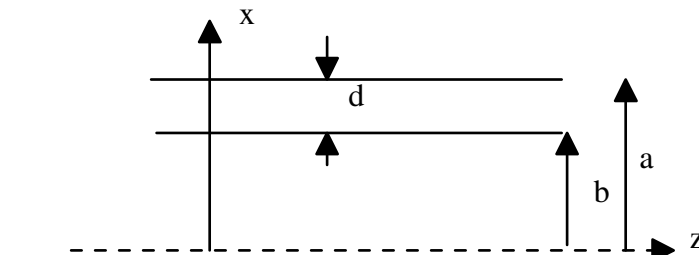
Figure 19.3. The geometry of a conducting shell or vessel.

We are concerned with the currents induced in a resistive vacuum vessel lying outside the plasma, and their effects on all the measurements we have discussed. As a characteristic example, consider a homogeneous field $B = B_0\sin(\omega t)$ parallel to the plane of a conducting plate; the inner and outer boundaries of the plate are at a distance b and a from the symmetry plane (see *Figure 19.3*). Maxwell's equations reduce to

$$\nabla \times (\nabla \times \mathbf{B}) = -\mu_0 \sigma \frac{\partial B}{\partial t} \qquad\qquad 19.1$$

When the ratio of the plate thickness to the layer thickness is much less than unity, i.e. $d/b \ll 1$, the penetration of the field is characterized by a time constant

$$\tau = \frac{\mu_0 \sigma b d}{2} \qquad\qquad 19.2$$

Now we can consider two cases, depending on the ratio of plate to skin depth, d/d_{skin}, where $d_{skin} = (2/(\mu\sigma\omega))^{1/2}$. If $d \gg d_{skin}$, (i.e. at high frequency) we have a thick plate, and we can consider

the plate to be perfectly conducting. If d << d_{skin} we have a thin plate, and then the characteristic penetration time is given by equation 19.2, namely $\tau = \mu\sigma bd/2$.

The result is the same for the penetration of a longitudinal field into a hollow cylinder, i.e. (approximately) a toroidal field into the toroidal vacuum vessel. τ is the L/Ω time for the decay of the poloidal current, with $L_\theta = \pi\mu_0 a^2$ the inductance per unit length, and $\Omega_\theta = 2\pi a/(\sigma d)$ the resistance per unit length. The same result applies for the penetration of a transverse field into a cylindrical shell, i.e. a vertical field into a toroidal vacuum vessel.

When we first initiate some perturbing field, the vessel will first appear as a thick plate, then change over to a thin plate after some time τ_σ. This time τ_σ is just the time it takes any dipole currents to become homogeneous, and is obtained from $\tau_\sigma \sim \pi/(2\omega)$, where ω is the value for which $d_{skin} = d/2$. We take (d/2) to allowing for penetration from both inside and outside the plate (from gaps in the plate), and obtain.

$$\tau_\sigma = \frac{\pi\mu_0\sigma d^2}{16}$$ 19.3

Application to a diamagnetic loop

Here we are considering poloidally flowing currents. Consider an N turn loop wrapped around a vessel with minor radius a_v, used to measure the plasma diamagnetic current $I_s = <p_\perp>/B_\phi$. After a time $t > \tau_\sigma$ we can consider the vessel as thin, and need correct only for the long time inductive time constant L/Ω. The voltage around the loop is

$$\frac{\varepsilon}{N} = M\frac{dI_s}{dt} + L\frac{dI_v}{dt}$$ 19.4

with I_s the diamagnetic current, I_v the vessel current, $M = \pi\mu_0 a_p^2$ and $L = \pi\mu_0 a_v^2$. The vessel current is given by

$$0 = \mathbf{\Omega} I_v + M\frac{dI_s}{dt} + L\frac{dI_v}{dt}$$ 19.5

where $\Omega = 2\pi a_v/(\sigma d)$. From 19.4 and 19.5, we have

$$I_s = \frac{1}{NM}\left[\int_0^t \varepsilon dt + \frac{L}{\mathbf{\Omega}}\varepsilon\right]$$ 19.6

Therefore we can correct the measured voltage ε to obtain the required diamagnetic current I_s.

Application to position measurement

Here we are considering toroidally flowing currents. If we are using the moment coil method to measure the plasma position, then the coils measure the current center of any currents within the contour on which the modified Rogowski and saddle coils are wound. Therefore, if these coils are outside the vacuum vessel, they will be sensitive to any currents induced in the vacuum vessel itself. If we consider times $t > \tau_s$, then we need only worry about the homogeneous vessel currents, driven by any non symmetric part of the flux function, Ψ_a. A vessel current with equivalent surface current density

$$i_v = \sigma_v E_\phi d_v = \frac{\sigma_v d_v}{2\pi R_v} \frac{\partial \Psi_a}{\partial t} i \qquad\qquad 19.7$$

will appear, where subscript v refers to the vessel. This asymmetric part of the flux function can be taken, for example, from the analytic expressions given in section 6.

Another method of calculating the induced vessel (toroidal) currents is to represent the vessel as a number of filaments, as discussed in section 1. Induced currents are then calculated through a mutual inductance matrix. The plasma might be specified analytically or as a single, or number of, filaments. Each vessel filament must be given a minor radius, which might be taken as $d_v/2$, half the vessel thickness, so that the self inductance is finite. Even the non homogeneous current components can be calculated in this way, if enough filaments suitably spaced and connected are included.

20 . THE IRON CORE

Many tokamaks have an iron core to ensure good coupling between the primary winding and the plasma.   This iron core has the additional advantage of keeping 'stray' fields away from diagnostic apparatus. However, it complicates the study of the plasma equilibrium, because the free space expressions for the fields produced by circular conductors are no longer applicable. Here all I want to do is to point out that iron is a pain to deal with.
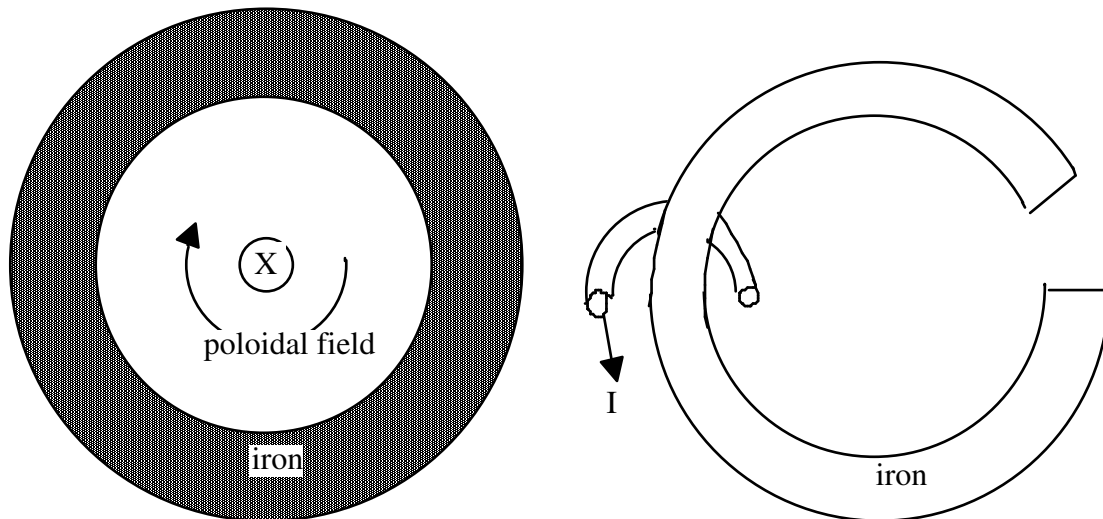
Figure 20.1. A straight iron cylinder *Figure 20.2*. An iron core with an air surrounding a plasma   gap, with a linked plasma (current I).

The iron core introduces a new boundary condition. It is often stated incorrectly that the lines of force enter a medium of infinite permeability (the iron) perpendicularly, but this is not always true. A simple example of a straight iron cylinder surrounding a straight wire with current shows this not to always be the case: in *Figure 20.1* the field lines are tangential to the iron boundary. A correct boundary condition, for the normal component of the induction, is

$$B_n(air) = \mu_0 H_n(air) = \mu H_n(iron) = B_n(iron) \qquad\qquad 20.1$$

For permeability u very large we can take H_n approaching 0 just inside the iron, so that

$$H_n(iron) = 0 \qquad\qquad 20.2$$

(from the continuity of B_n) and add the boundary condition

$$H_\tau \text{ is continuous} \qquad\qquad 20.3$$

In reality μ is not infinite, but the limit works well.

First consider an air gap inductor, as shown in *Figure 20.2*. We assume that inside the iron there are laminations which ensure no current, so that

$$\nabla \times \mathbf{H} = 0 \qquad\qquad 20.4$$

Then H is derived from a single valued potential given by Laplace's equation

$$\nabla^2 \psi = 0 \qquad\qquad 20.5$$

and the boundary condition on B_n (Equation 20.2) is equivalent to

$$\frac{\partial \psi}{\partial n} = 0 \text{ in the iron.} \qquad\qquad 20.6$$

The only possible solution of equation 20.5 and equation 20.6 is $\psi = $ constant . Therefore H (but not B) must be zero inside the iron. Continuity of the tangential component of H then shows that the lines of force in the air must be perpendicular to the iron. Therefore in air the magnetic fields are given by the usual equations, together with the boundary condition

$$\mathbf{e}_n \times \mathbf{H} = 0 \text{ on the iron surface.} \qquad\qquad 20.7$$

In the iron H = 0, but B is finite. Since $\nabla \times \mathbf{B} = 0$ in the iron, B(iron) = $\nabla\Phi$, and Φ satisfies

$$\nabla^2 \Phi = 0 \qquad\qquad 20.8$$

$$\frac{\partial \Phi}{\partial n} = B_n(air) \qquad\qquad 20.9$$
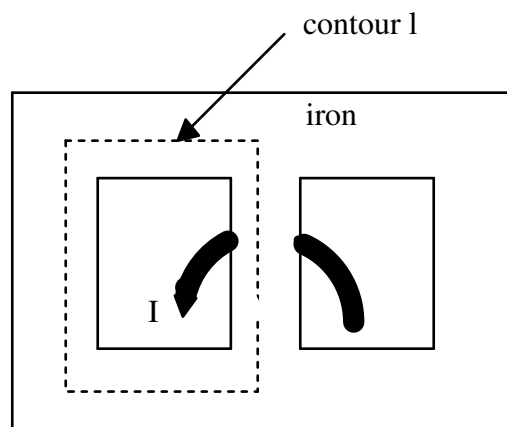
which is known.

Figure 20.3. The geometry of an iron core and
a linked plasma of current I. The contour l
considered in the text is shown.

Now consider the case shown in *Figure 20.3*, an iron core with a central limb as on TEXT. If the total number of turns linking the center core is 0, and there is no current in the iron (Equation 20.4) then $\int \mathbf{H} \cdot \mathbf{dl} = 0$ for any contour l inside the iron. Then H derives still from a single potential, and all our previous steps are valid. However, if a finite number of amp turns I links the iron, then $\int \mathbf{H} \cdot \mathbf{dl} = I$. This means that we can still write the field in the iron as $\nabla\Phi$, but now Φ is multi valued, increasing by ±I once around the contour l. That is, in this case, Equations 20.8 and 20.9 apply in the iron, but with the additional constraint

$$\oint_l \nabla\Phi \bullet \mathbf{dl} = I \qquad\qquad 20.10$$

In this case, had we assumed perpendicularity, we would have obtained $\int \mathbf{H} \cdot \mathbf{dl} = 0$, while in reality $\int \mathbf{H} \cdot \mathbf{dl} = I$. Thus the field lines only enter the iron core perpendicularly if no current flows in the iron, and the net ampere turns is zero.

The only place that the iron really affects magnetic diagnostics is in the equilibrium reconstruction. No longer can we use the free space expressions for a circular current filament, but they must be modified to satisfy the boundary condition. In toroidal plasma devices we almost always satisfy the conditions necessary for the boundary condition Equation 20.7. One way to model the effect of iron is by placing additional circular filaments inside the iron itself, with currents chosen to satisfy Equation 20.7 at a given number of locations. This is illustrated in *Figure 20.4*: the 'image" filaments must have a current flowing in the same direction as the filament in air, so that there is an attraction between the filament in air and the iron itself. As the filament in air gets closer to the iron, the "image" current must increase, and so the attraction must increase. This means that an iron core can lead to an axisymmetric, or n = 0, instability.
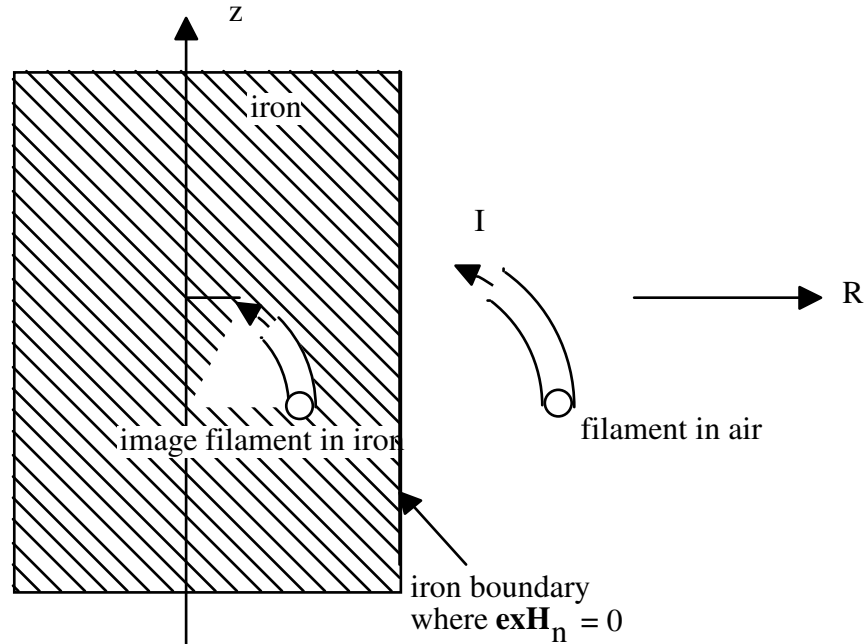
Figure 20.4. An iron core and plasma current (filament), together
with the image currents necessary to ensure the boundary condition
are satisfied.

In principle the method of images can model a true three dimensional iron core, although it would not help much because most of our equilibrium work involves two dimensions only. Therefore we often assume a two dimensional iron core which is produced by the toroidal revolution of the actual core. In this case there are analytic expressions for the additional field components produced by the iron.

Because the iron core is really three dimensional, it introduces a perturbation with a toroidal mode number n equal to the number of outside return limbs, N_l. As such any fields, such as the vertical maintaining field, will have an $n = N_l$ component. Calculations show that this perturbation can be as much as 10%, which might be thought to introduce a toroidally dependent plasma position. It does, but only by a very small amount. Suppose the toroidally symmetric vertical field B_z has an additional perturbing component $b_z \cos(N_l\phi)$. From the field line equation this variable field component will displace lines of force according to

$$\frac{dz}{b_z \cos(N_1\phi)} = \frac{Rd\phi}{B_\phi} \qquad\qquad 20.11$$

or

$$dz = \frac{R}{B_\phi} \int b_z \cos(N_1\phi) d\phi \qquad\qquad 20.12$$

Therefore the maximum displacement is

$$\Delta z_{\mathbf{max}} = \frac{R b_z}{N_1 B_\phi}$$ 20.13

which is typically a few mm.

21. TOKAMAK POSITION CONTROL

The axisymmetric instability

We first calculate the growth rate of an axisymmetric instability in a tokamak. We only consider vertical motion, because it is easier than the calculation for horizontal motion. The driving force is written in terms of the decay index n = -(R/B_Z)(dB_Z/dR). We consider a tokamak surrounded by a conducting vacuum vessel. There is assumed to be a transverse (poloidal) insulating gap in this vessel, so that only dipole currents can flow. The equation determining the vacuum vessel current I_s is

$$\frac{d}{dt}\left(L_s I_s\right) + \frac{d}{dt}\left(M_{sp} I_p\right) + \Omega_s I_{s=0}$$

21.1

Here I_p is the plasma current, L_s is the vessel inductance, Ω_s the vessel resistance, M_{sp} the mutual inductance between plasma and vessel. We introduce the vessel time constant $\tau_s = L_s/\Omega_s$. We can approximate the vessel as a circular shell, so that

$$L_s = \frac{\mu_0 \pi^2 R_s}{4}$$

21.2

$$\tau_s = \frac{\mu_0 \sigma \delta_s r_s}{2}$$

21.3

where R_s, r_s, δ_s are the vessel major radius, minor radius, thickness, and σ is the conductivity. Approximating the plasma as a filament initially centered within the vessel (R = R_0 = R_s, z = z_s = 0), the mutual inductance and its spatial derivative are given by

$$M_{sp} = \frac{\mu_0 \pi R_s z}{2 r_s}$$

21.4

$$\frac{\partial M_{sp}}{\partial z} = \frac{\mu_0 \pi R_s}{2 r_s}$$

21.5

From equations 22.1, 22.2 and 2.5 we can derive the relationship between the dipole current in the vessel and the plasma displacement z:

$$\frac{dI_s}{dt} + \frac{I_s}{\tau_s} = -2\frac{I_p}{\pi r_s}\frac{dz}{dt}$$

21.6

The equation determining the plasma displacement z is

$$m\frac{d^2z}{dt^2} \approx 0 = -2\pi R_p I_p \left[B_R + B_s + \Delta B \right]$$ 21.7

with B_R the equilibrium major radial field, B_s the major radial field from the vessel currents, and ΔB a perturbation to B_R. We can take the mass m of the plasma to be zero in the presence of the vessel; we will find the vessel slows the motion sufficiently for the $m(d^2z/dt^2)$ term to be vanishingly small. Using

$$B_R = \frac{nB_z z}{R}$$ 21.8

$$B_z = \frac{\Gamma \mu_0 I_p}{4\pi R_p}$$ 21.9

$$\Gamma = \ln\left(\frac{8R_p}{r_p}\right) + \frac{l_i}{2} + \beta_I - \frac{3}{2}$$ 21.10

$$K_s = \frac{B_s}{I_s} = \frac{-\mu_0}{4r_s}$$ 21.11

where r_p is the plasma minor radius, and we assume $R_s = R_p = R$. Taking $\Delta B = 0$, equation 22.7 can be written

$$0 = -\frac{n\Gamma \mu_0 I_p z}{4\pi R^2} + \frac{\mu_0 I_s}{4r_s}$$ 21.12

Equations 22.12 and 22.6 define the problem; they have solutions

$$z = z_0 e^{\gamma t}$$ 21.13

$$I_s = I_{s0} e^{\gamma t}$$ 21.14

The growth rate is

$$\gamma = -\frac{1}{\tau_s} \frac{n}{n + n_s}$$ 21.15

$$n_s = \frac{2R^2}{r_s^2 \Gamma}$$ 21.16

From equation 22.15 we see the plasma is unstable if n < 0.

Consideration of in-out motion is more complicated, because we must conserve poloidal magnetic flux. This is ensured by using the equation

$$\frac{d}{dt}\left[L_p I_p + \pi R_p^2 B_z + M_{ps} I_s\right] = 0 \qquad\qquad 21.17$$

where the plasma inductance is

$$L_p = \mu_0 R_p\left(\ln\left(\frac{8R_p}{r_p}\right) - 2 + \frac{l_i}{2}\right) \qquad\qquad 21.18$$

The unstable motion we nave derived for a plasma with decay index n < 0 must be controlled by feedback. *Figure 21.1* shows such a system. Sensing coils might be the multipole moment coils discussed in an earlier chapter, or single coils. Sensors can be placed inside or outside the vessel.
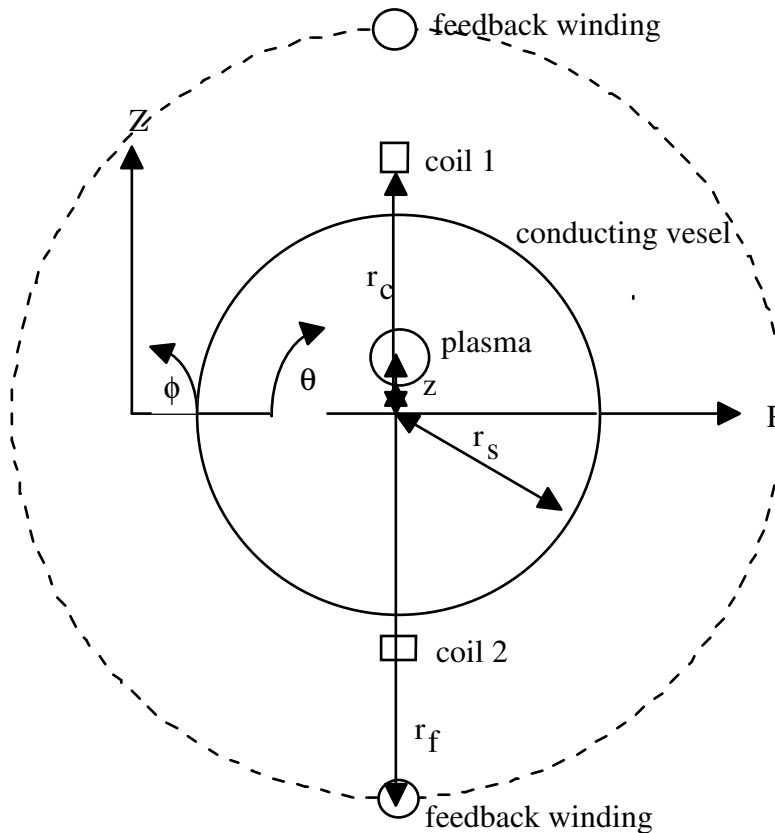

Figure 21.1. Geometry of a feedback system

Analysis of sensor coils allowing for vessel currents

If single coils were used, the analysis used to determine plasma displacement z is to take the difference signal, and divide by the sum signal. For a positive plasma current (into the plane) and a positive vertical plasma displacement z, the upper coil signal is $B_{\theta 1} = \mu_0 I_p/(2\pi(r_c-z))$ and the lower signal is $B_{\theta 2} = \mu_0 I_p/(2\pi(r_c+z))$, so that for $z << r_c$:

$$\frac{\mathbf{B}_{\theta 1} - \mathbf{B}_{\theta 2}}{\mathbf{B}_{\theta 1} + \mathbf{B}_{\theta 2}} = \left(\frac{\dfrac{1}{r_c - z} - \dfrac{1}{r_c + z}}{\dfrac{1}{r_c - z} + \dfrac{1}{r_c + z}} \right) \approx \frac{z}{r_c}$$

21.19

We now consider what happens when we allow for the presence of vacuum vessel currents I_s and feedback currents I_f, both of which produce fields seen by the sensing coils.

The dipole model

The feedback windings are represented by a shell of radius r_f and thickness δ_f with a dipole current distribution, with current (area) density $j_{\phi f} = j_{\phi f0}\sin(\theta)$. Then

$$I_f = \int_0^\pi j_{\phi f} r_f \delta_f d\theta = 2 r_f \delta_f j_{\phi f 0}$$

21.20

I_f is positive when the upper winding current is into the plane. This feedback circuit produces a major radial field for vertical position control, and ($r_c < r_f$):

$$B_f = K_f I_f, \qquad K_f = -\frac{\mu_0}{4 r_f}$$

21.21

That is, a positive I_f produces a signal $B_{\theta 1,f} = B_f$ (which will be negative for positive I_f) in the upper sensing coil and a signal $B_{\theta 2,f} = -B_f$ (which will be positive for positive I_f) in the lower sensing coil.

The vacuum vessel is also assumed to be a shell, of radius r_s and thickness δ_s, carrying a dipole current $j_{\phi s} = j_{\phi s0}\sin(\theta)$. Then

$$I_s = \int_0^\pi j_{\phi s} r_s \delta_s d\theta = 2 r_s \delta_s j_{\phi s0}$$

21.22

This produces a major radial field for sensors inside the vessel ($r_c < r_s$)

$$B_{s,i} = K_{s,i}I_s, \qquad K_{s,i} = -\frac{\mu_0}{4r_s} \qquad\qquad 21.23$$

Therefore the signals seen by the sensing coil are $B_{\theta1,s,i} = B_{s,i}$ in the upper coil and $B_{\theta2,s,i} = -B_{s,i}$ in the lower coil. If the sensing coils are outside the vacuum vessel ($r_c > r_s$), then the major radial field is

$$B_{s,e} = K_{s,e}I_s, \qquad K_{s,e} = \frac{\mu_0 r_s}{4r_c^2} \qquad\qquad 21.24$$

Therefore the upper coil sees a signal $B_{\theta1,s,e} = B_{s,i}$, and the lower sensing coil a signal $B_{\theta2,s,e} = -B_{s,e}$. These results are summarized in table 1.

**Table 1. Fields seen by the B_θ sensing coils,
dipole current model.**

	$B_{\theta1}$	$B_{\theta2}$
outside $(r_c \geq r_s)$		
plasma	$\dfrac{\mu_0 I_p}{2\pi(r_c - z)}$	$\dfrac{\mu_0 I_p}{2\pi(r_c + z)}$
feedback	$-\dfrac{\mu_0 I_f}{4r_f}$	$\dfrac{\mu_0 I_f}{4r_f}$
vessel	$\dfrac{\mu_0 I_s r_s}{4r_c^2}$	$-\dfrac{\mu_0 I_s r_s}{4r_c^2}$
inside $(r_s \geq r_c)$		
plasma	$\dfrac{\mu_0 I_p}{2\pi(r_c - z)}$	$\dfrac{\mu_0 I_p}{2\pi(r_c + z)}$
feedback	$-\dfrac{\mu_0 I_f}{4r_f}$	$\dfrac{\mu_0 I_f}{4r_f}$
vessel	$-\dfrac{\mu_0 I_s}{4r_s}$	$\dfrac{\mu_0 I_s}{4r_s}$

The apparent displacement z_{app} is derived using the equation

$$\frac{z_{app}}{r_c} = \frac{\sum B_{\theta1} - \sum B_{\theta2}}{\sum B_{\theta1} + \sum B_{\theta2}} = \frac{z}{r_c} + \alpha_s \frac{I_s}{I_p} + \alpha_f \frac{I_f}{I_p} \qquad\qquad 21.25$$

where the values of α_s and α_f, derived from the expressions in table 1, are given in table 2. Without the correction factors α_s and α_f, $z_{app} = z$. Moving the sensors from inside to outside changes the sign of α_s. When the plasma ($I_p > 0$, into plane) moves upwards ($z > 0$) it will induce a negative I_s. For sensors outside the vessel, the vessel currents then produce an apparent displacement smaller than the real displacement (i.e the vacuum vessel shields the sensing coils). For sensors inside the vessel, the apparent displacement is larger than the true displacement. The feedback windings complicate this simple process. If we wanted to, the effects of the feedback coupling to the sensors (i.e. finite α_f) can be removed by adding to each signal a term proportional to I_f itself. This cannot be done for the coupling from the vessel to the sensors, because we do not measure the vessel dipole currents.

Table 2. Correction coefficients α_s and α_f
for B_θ sensors.

	correction factor
outside $(r_c \geq r_s)$	
α_s	$\dfrac{\pi r_s}{2 r_c}, \geq 0$
α_f	$-\dfrac{\pi r_c}{2 r_f} \leq 0$
inside $(r_s \geq r_c)$	
α_s	$-\dfrac{\pi r_s}{2 r_c}, \leq 0$
α_f	$-\dfrac{\pi r_c}{2 r_f} \leq 0,$

For comparison, table 2 shows the coefficients α_s and α_f for the multipole moment coil system [1], with coils either inside or outside the vessel. Note that the multipole moment sensing coils are only sensitive to currents inside the contour on which they are wound, and thus $\alpha_f = 0$.

Table 3. Correction coefficients α_s and α_f
for multipole moment sensors.

	correction factor
outside $(r_c \geq r_s)$	
α_s	$\dfrac{\pi r_s}{2 r_c}, \geq 0$
α_f	0
inside $(r_s \geq r_c)$	
α_s	0
α_f	0

Numerical values applicable to TEXT are given in table 4, for r_c = 30 cm (inside) or 34 cm (outside), r_s = 32 cm, r_f = 50 cm. We see that, as far as pickup from the shell currents (α_s) is concerned, the B_θ coils outside the vessel are no worse than the moment coils.

Table 4. Numerical values of the correction factors α_s and α_f.

R = 100 cm, r_c = 30 (inside) or 34 (outside) cm, r_s = 32 cm, r_f = 50 cm

	α_s	α_f
dipole model, multipole coils outside	1.48	0
dipole model, multipole coils inside	0	0
dipole model, B_θ coils outside	1.48	-1.07
dipole model, B_θ coils inside	-1.67	-0.94

The feedback model

Here I want to illustrate how a feedback system is analyzed. We take the mass-less plasma model, in which the plasma is always in equilibrium due to currents in the vacuum vessel and the feedback windings, and the (unstable) driving term B_R. The vacuum vessel (i.e. conducting shell), feedback windings and plasma all having the same major radius R. The equations describing the plasma motion z, shell current I_s, feedback current I_f and feedback voltage V_f are :

$$m\frac{d^2z}{dt^2} = 0 = -2\pi R I_p \left(B_R + B_s + B_f \right)$$

$$\frac{d}{dt}\left(M_{ps}I_p \right) + L_s\frac{dI_s}{dt} + \Omega_s I_s + M_{sf}\frac{dI_f}{dt} = 0$$

$$\frac{d}{dt}\left(M_{pf}I_f \right) + M_{sf}\frac{dI_s}{dt} + L_f\frac{dI_f}{dt} + \Omega_f I_f = V_f \qquad\qquad 21.26$$

$$t_a\frac{dV_f}{dt} + V_f = -g\frac{\Omega_f B_z}{K_f R}\left(Z - t_d\frac{dZ}{dt} \right)$$

$$Z = z_0 - z_{app}$$

That is, in open loop the plasma displacement induces a dipole shell current as well as a dipole feedback current. The dipole currents in the shell and feedback circuits are themselves coupled. In closed loop a proportional (g) and derivative (gt_d) gain term are considered The mutual inductances M_{ij} and self inductances L_i between the various circuits (i,j = p for plasma, s for shell, i.e. vacuum vessel, and f for feedback) are:

$$M_{sf} = \frac{\mu_0 \pi^2 R r_s}{4 r_f}$$

$$M_{pf} = \frac{\mu_0 \pi R z}{2 r_f}$$

$$M_{ps} = \frac{\mu_0 \pi R z}{2 r_s}$$

$$L_f = \frac{\mu_0 \pi^2 R}{4}$$

$$L_s = \frac{\mu_0 \pi^2 R}{4}$$

21.27

$$L_p = \mu_0 R \left[\ln \frac{8R}{a_p} + \frac{l_i}{2} - 2 \right]$$

g is the linear gain in the feedback circuit, t_a is the time constant of the servo system, t_d is the time constant of the derivative gain, Ω_i is the resistance of the circuit i, z_0 is the required position. The equilibrium major radial field B_R is given in terms of the equilibrium vertical field $(-B_z)$ and the decay index n $= -(R/B_z)(\partial B_z/\partial R)$ as

$$B_R = \frac{n B_z z}{R}$$

$$B_z = \frac{\Gamma \mu_0 I_p}{4 \pi R_p}$$

21.28

$$\Gamma = \ln\left(\frac{8R}{a_p} \right) + \frac{l_i}{2} + \beta_I - \frac{3}{2}$$

For vertical (up/down) instability without feedback control n < 0; following a vertical displacement the plasma then experiences a major radial field B_R in a direction to cause further plasma displacement. We can model any unstable motion through the choice of n: without feedback but with vacuum vessel n should be chosen such that the measured growth rate is:

$$\gamma = \frac{1}{t_s} \frac{n}{n + n_s}$$

$$n_s = 2 \frac{R^2}{r_s^2 \Gamma}$$

21.29

Note that the vertical field required for major radial equilibrium is $-B_z$ as defined above. We normalize the equations, letting

$$\zeta = \frac{z}{R}, \qquad t_f = \frac{L_f}{\Omega_f}, \qquad t_s = \frac{L_s}{\Omega_s}, \qquad \tau = \frac{t}{t_s}, \quad i_s = \frac{I_s}{I_p}$$

$$i_f = \frac{I_f}{I_p}, \qquad v_f = \frac{V_f}{\Omega_f I_p}, \qquad m_{sf} = \frac{M_{sf}}{L_s} = \frac{r_s}{r_f}, \qquad m_{fs} = \frac{M_{fs}}{L_f} = m_{sf}$$

$$k_s = \frac{-K_s I_p}{B_z} = \frac{\pi R}{\Gamma r_s}, \; k_f = \frac{-K_f I_p}{B_z} = \frac{\pi R}{\Gamma r_f}, \qquad \mu_s = \frac{R}{L_s}\frac{\partial M_{ps}}{\partial z} = \frac{2R}{\pi r_s}$$

$$\mu_f = \frac{R}{L_f}\frac{\partial M_{pf}}{\partial z} = \frac{2R}{\pi r_f}$$

$$x_s = \frac{\alpha_s r_c}{R}, \; x_f = \frac{\alpha_f r_c}{R}$$

21.30

Values of x_s and x_f are derived from the values of α_s and α_f in table 4. Representative values for TEXT are given in table 5.

TABLE 5. values of x_s and x_f used in the modeling

	x_s	x_f
multipole outside	0.5	0
multipole inside	0	0
B_θ outside	0.5	-0.3
B_θ inside	-0.5	-0.3

The normalized equations are:

$$-n\zeta + k_s i_s + k_f i_f = 0$$

$$\mu_s \frac{d\zeta}{d\tau} + \frac{di_s}{d\tau} + i_s + m_{sf}\frac{di_f}{d\tau} = 0$$

$$\mu_f \frac{d\zeta}{d\tau} + m_{fs}\frac{di_s}{d\tau} + \frac{di_f}{d\tau} + \frac{i_f}{\tau_f} = \frac{v_f}{\tau_f}$$

21.31

$$v_f + \tau_a \frac{dv_f}{d\tau} = \frac{g}{k_f}\left[\left(\zeta_0 - \zeta - x_s i_s - x_f i_f\right) - \tau_d \frac{d}{d\tau}\left(\zeta_0 - \zeta - x_s i_s - x_f i_f\right) \right]$$

These can be solved either numerically or by Laplace transforming. These equations are then Laplace transformed (a superscript "~" denotes a Laplace transform, s is the Laplace variable) to give

$$-n\tilde{\zeta}(s) + k_s\tilde{i}_s(s) + k_f\tilde{i}_f(s) = 0$$

$$\mu_s s\tilde{\zeta}(s) + (s+1)\tilde{i}_s(s) + m_{sf}s\tilde{i}_f(s) = 0$$

$$\mu_f s\tilde{\zeta}(s) + sm_{fs}\tilde{i}_s(s) + \left(s + \frac{1}{\tau_f}\right)\tilde{i}_f(s) - \frac{\tilde{v}_f(s)}{\tau_f} = 0$$

21.32

$$\tilde{v}_f(s) = \frac{g}{k_f}\left[\tilde{\zeta}_0(s) - (1 - \tau_\Sigma s)\left(\tilde{\zeta}(s) + x_s\tilde{i}_s(s) + x_f\tilde{i}_f(s)\right)\right]$$

where $\tau_\Sigma = \tau_a + \tau_d$. Solutions for the displacement ζ, vessel current i_s, feedback current i_f and

feedback voltage v_f can be obtained; for the displacement ζ is given by:

$$\frac{\tilde{\zeta}(s)}{\tilde{\zeta}_0(s)} = \frac{A + Bs}{D + Es + Fs^2}$$

21.33

where

$$A = gk_f$$

$$B = -g\left(k_s m_{sf} - k_f\right) = 0$$

$$D = k_f(n+g) + \mathbf{ngx_f}$$

$$E = -gx_s m_{sf}(n + k_s\mu_s) + k_f\left[n + k_s\mu_s + (n + k_f\mu_f)\tau_f\right] - gk_f\tau_\Sigma + \mathbf{gx_f(n + k_s m_s - nt_s)}$$

$$F = m_{sf}\left[gx_s\tau_\Sigma + \tau_f k_s(1 - m_{sf}m_{fs})\right]n + k_s\mu_s\right] - \mathbf{t_s x_f g(n + k_s m_s)}$$

21.34

The term appearing due to the coupling between sensors and feedback windings are in bold. The remaining terms are identical to those previously derived, except that the values of x_s to be considered are different (negative values are now permitted).

For stability, the Routh criteria can be applied, which requires 1) $D > 0$, 2) $E > 0$, and 3) $F > 0$. These three criteria define the available operating space in (g, τ_Σ) space for a given instability (i.e. for a given decay index n).

Application of stability criteria.

Values relevant to TEXT Upgrade are $t_s = 7$ms, $t_f = 137$ms, $\tau_f = 20$, $m_{sf} = m_{fs} = 0.67$, $k_s = 2.26$, $k_f = 1.5$, $\mu_s = 1.59$, $\mu_f = 1.06$, and the pairs of values for x_s and x_f given in table 5. Experimental observations of open loop vertical motion show $\tau_{instability} = 1/\gamma \sim 100$ ms, so that   a suitable

value for the decay index in the modeling is n = -0.2. We now compute the stable regions in $(g, \tau_\Sigma$ space), the results of which are shown in *Figures 21.2 through 21.5*. For the values considered the best system is that of multipole sensing coils inside the vessel (Figure 21.2), closely followed by the single B_θ coils inside the vessel (*Figure 21.4*). For sensing coils outside the vessel the operational space is restricted, more so in the case of single B_θ sensors than for multipole sensors. This is seen by comparing *Figures 21.3 and 21.5*.
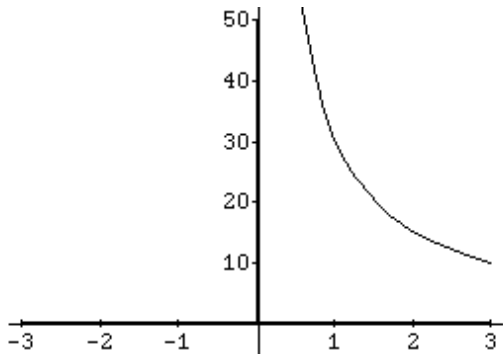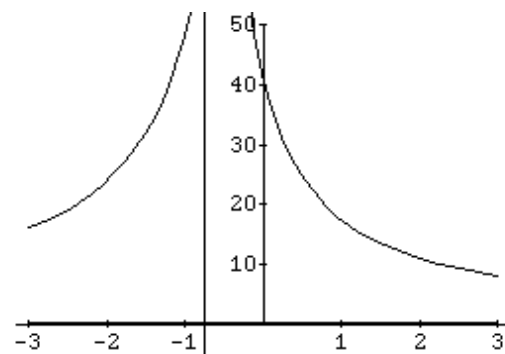
Figure 22.2. Moment coils, inside vessel.   *Figure 22.3.* Moment coils outside vessel.
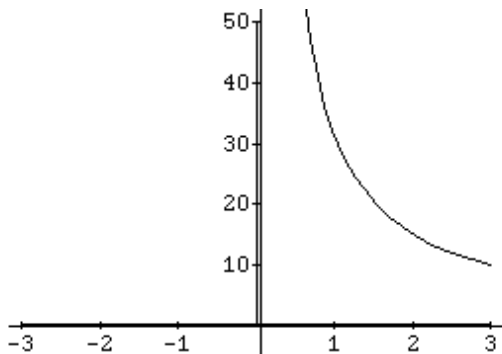
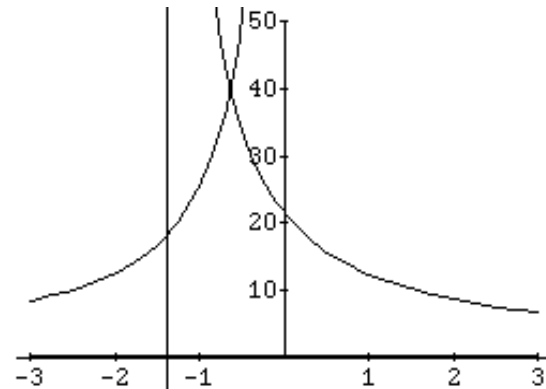*Figure 22.4.* Single B_θ coils inside vessel.   *Figure 22.5. Single B_θ coils outside vessel.*

22. MAGNETIC ISLANDS

We consider the effect of a helical perturbation on a tokamak equilibrium. We will not consider anything other than vacuum fields, i.e. we will not allow the plasma to respond to the applied fields in any way. I have adapted the work of S. Matsuda and M. Yoshikawa, in Japanese Journal of Applied Phys. **14** (1975) 87.

The field line equation is

$$\frac{dl}{B} = const.$$ 22.1

i.e. working in a quasi cylindrical system based on the plasma center

$$\frac{d\theta}{d\phi} = \frac{R}{r}\frac{B_\theta}{B_\phi} = \frac{1}{q(r)} = \iota(r)$$ 22.2

q is the safety factor, ι the rotational transform. Expanding $\iota(r)$ near $r = r_0$, the radius of the resonant surface, we obtain

$$\frac{d\theta}{d\phi} \approx \iota(r_0) + \frac{d\iota(r)}{dr}\left(r - r_0\right) = \iota_0 + \iota' x$$ 22.3

where $x = r - r_0$, $\iota_0 = \iota(r_0)$, and $\iota' = \left.\frac{d\iota(r)}{dr}\right|_{r=r_0}$. To lowest order in the perturbing field we also have

$$\frac{dr}{rd\theta} = \frac{dx}{rd\theta} = \frac{b_r(r,\theta,\phi)}{B_\theta(r)}$$ 22.4

where $b_r(r,\theta,\phi)$ is the radial component of the error field. We ignore the θ component because it is small compared to the equilibrium field B_θ. Assuming small islands, we also ignore any radial dependencies of b_r and B_θ. b_r is expanded as a Fourier series

$$b_r(r_0,\theta,\phi) = \sum_{m,n}\left[\begin{array}{l} a_{m,n}\sin(m\theta - n\phi) + a'_{m,n}\sin(m\theta + n\phi) \\ +c_{m,n}\cos(m\theta - n\phi) + c'_{m,n}\cos(m\theta + n\phi)\end{array}\right]$$ 22.5

Because we shall see that only resonant components matter near $r = r_0$, we keep only the first and third terms which satisfy

$$\frac{m}{n} \approx \frac{1}{\iota_0} = q_0 \qquad\qquad 22.6$$

Then

$$b_r(r_0, \theta, \phi) = b_{m,n} \sin(m\theta - n\phi + \beta) \qquad\qquad 22.7$$

with $b_{m,n} = \sqrt{a_{m,n}^2 + c_{m,n}^2}$ and $\tan(\beta) = \dfrac{b_{m,n}}{a_{m,n}}$

Next we define a new variable

$$\eta = m\theta - n\phi + \beta \qquad\qquad 22.8$$

so that equation 22.4 becomes

$$\frac{dx}{r_0 d\theta} = \frac{b_{m,n} \sin(\eta)}{B_\theta(r_0)} \qquad\qquad 22.9$$

We also obtain from equations 22.3 and 22.8

$$\frac{d\eta}{d\theta} = -\frac{n}{\iota_0 + \iota' x} + m \qquad\qquad 22.10$$

Substituting equation 22.9 into equation 2.10 gives us a non linear equation

$$\frac{d^2\eta}{d\theta^2} = -n\frac{d}{d\theta}\left[\frac{1}{\iota_0}\left(1 - \frac{\iota'}{\iota_0}x\right)\right] = n\frac{r_0 \iota'}{\iota_0^2}\frac{b_{m,n}\sin(\eta)}{B_\theta(r_0)} = -A\sin(\eta) \qquad\qquad 22.11$$

where

$$A = -n\frac{r_0 \iota'}{\iota_0^2}\frac{b_{m,n}}{B_\theta(r_0)} \qquad\qquad 22.12$$

We can take $A > 0$ for convenience. We see the behavior of the field lines is analogous to the motion of a particle in a periodic potential $U = A(1-\cos(\eta))$, when we regard η and θ as position and time. Multiplying equation 22.11 by $d\eta/d\theta$ and integrating over θ gives

$$\frac{1}{2}\left(\frac{d\eta}{d\theta}\right)^2 = E - A(1 - \cos(\eta)) \qquad\qquad 22.13$$

with $E = \dfrac{1}{2}\left(\dfrac{d\eta}{d\theta}\right)^2_{\eta=0}$ a constant of integration analogous to a kinetic energy. Let $k^2 = \dfrac{E}{2A}$, so that

$$\left(\frac{d\eta}{d\theta}\right)^2 = 4A\left(k^2 - \sin^2\left(\frac{\eta}{2}\right)\right)$$ 22.14

Two types of solution are possible, as shown in *Figure 22.1*. If E < 2A the field lines move periodically within a limit of η. Field lines with E > 2A are "passing".

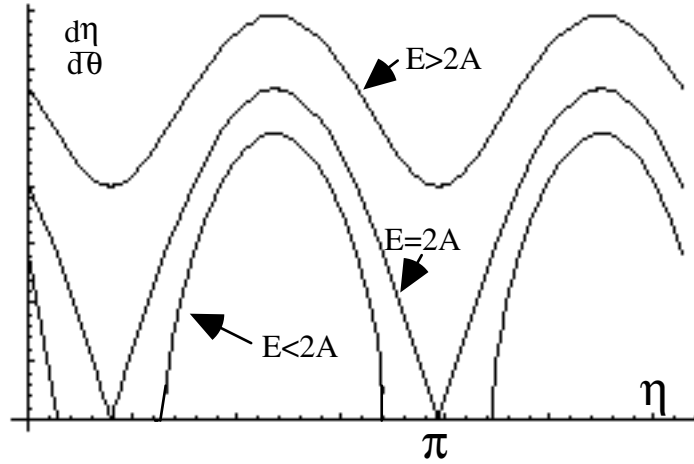*Figure 22.1*. Behavior of field lines in phase space.

The maximum excursion is found when E = 2A, or k = 1. Then from equation 22.9 we have

$$w = \int dx = \int \frac{r_0 b_{m,n} \sin(\eta) dx}{B_\theta(r_0)\frac{d\eta}{d\theta}}$$ 22.15

Using equation 22.14 the integral in equation 22.15 is found to be $\dfrac{4}{\sqrt{A}}$, so that we finally obtain

$$w = 4r_0\sqrt{\left|\frac{b_{m,n}}{mB_\theta(r_0)}\right|\left|\frac{\iota}{-r_0\iota'}\right|} = 4\sqrt{\frac{b_{m,n}r_0 q^2}{mB_\phi\frac{dq}{dr}}}$$ 22.16

23. SOME EXPERIMENTAL TECHNIQUES

Coils winding

The rogowski coil is simply made by obtaining a delay cable, and returning the wire down the center of the delay line (to ensure no net single turn is left). More complicated coils must be made by using variable winding densities (i.e. changing the pitch) or varying the cross sectional area of the former on which the coil is wound.

Interference suppression

Electrical equipment designed to produced RF energy such as generators, and switching phenomena in electrical circuits, create RF spectra which must be contended with.

interference

propagation

lines
dc coupled

radiation
capacitive coupling
(inductive coupling)

- -

suppression

line
attenuation

decoupling
attenuation

components
capacitiors
inductors
filters

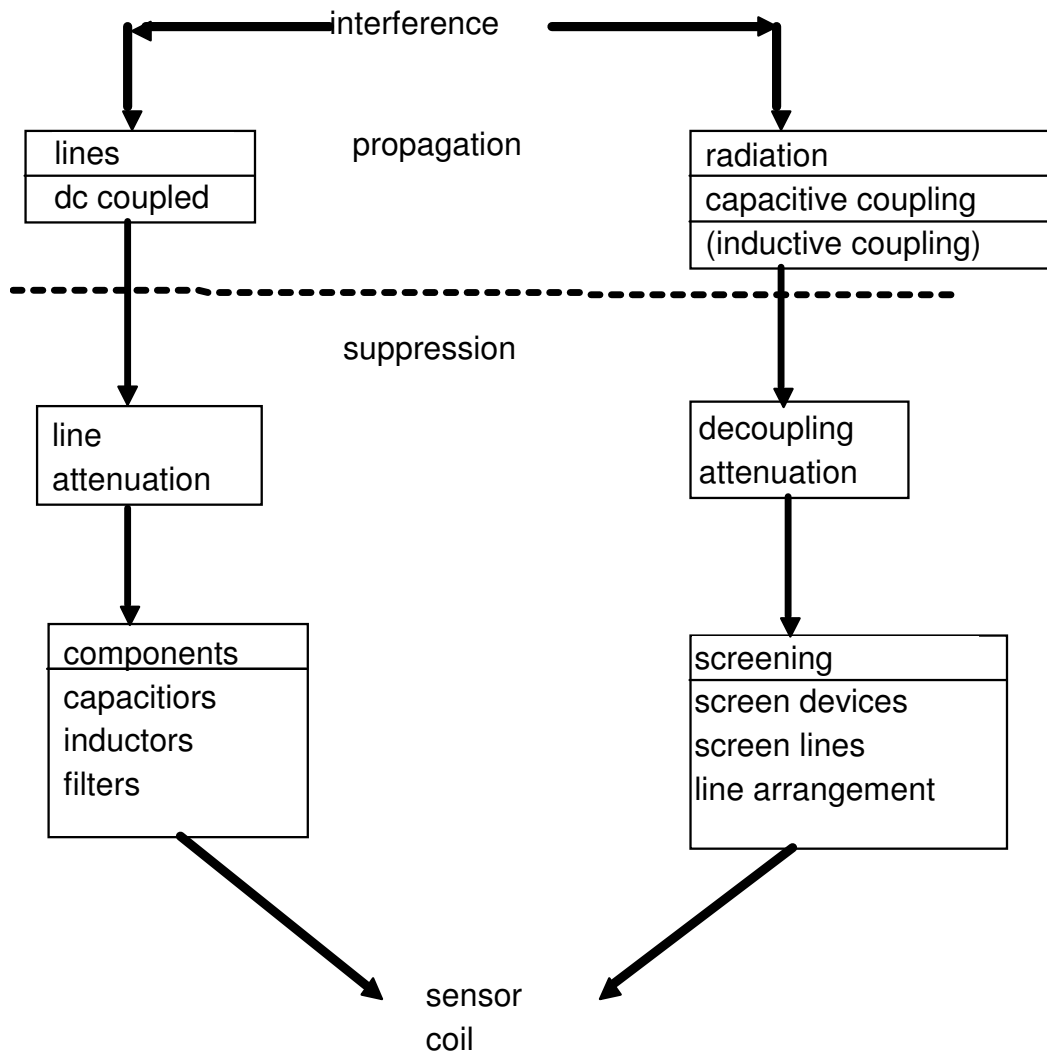| screening |
|---|
| screen devices |
| screen lines |
| line arrangement |

sensor

coil

Figure 23.1. An illustration of interference paths and suppression techniques.

The sources of interference are illustrated in *Figure 23.1.* The interference propagates either down lines (cables) or by direct radiation. If the wavelength is large compared to the dimensions of the interference source only minor radiation will result, which is mostly found along the lines. This is the case for frequencies up to 30 MHz. When the dimension of the interference source is about that of the wavelength the interference energy will travel by radiation. The dominant frequencies are those where the interference source are l/4 or multiples of it. Favorable radiation conditions imply reduced line propagation (because of increased line attenuation) . Therefore the two propagation paths, comprising direct and capacitive or inductive coupling, suggest two means of suppression, either line attenuation or de-coupling attenuation. Line attenuation is effected by filters. De-coupling attenuation is effected by the construction of the sensor coil and the associated connecting lines.

A common problem with probes is capacitive pick-up. To test for this pick up on simple sensor coils, two identical and adjacent coils can be connected in series. Depending on the orientation, the signal obtained should be twice that measured with a single coil, or zero. If the coils connected in opposition do not give a zero signal, then capacitive coupling effects should be considered as a possible source of error. Capacitive coupling can be over using a grounded screen or can around the sensor.

Screened rooms

The requirement is to screen a room in which a sensitive measurement is being performed from external interference, or to accommodate apparatus which radiate interference in a screened room to keep the surroundings free from interference. The basic method is to use cages of wire mesh, or metal sheet. Both electric and magnetic field components must be considered. Units used for effectiveness are the decibel :

$$s = 20\log\left(\frac{E, B_{noscreen}}{E, B_{withscreen}}\right)$$

and the Napier

$$s = \ln\left(\frac{E, B_{noscreen}}{E, B_{withscreen}}\right)$$

The wire mesh works to screen electric fields because the external flux lines mainly end on the mesh. The effectiveness depends primarily on the size and type of the mesh. Magnetic screening is effected by induced currents; DC magnetic fields are not screened, and low frequency AC magnetic fields are only poorly screened by non magnetic materials. With increasing frequency the magnetic shielding improves and approaches a finite value. Double screens, insulated from each other except at one point, improve the screening. These rooms work well to 20 MHz. Above this the screen room size can equal the cage dimension, causing resonances.

Sheet metal rooms have better screening properties than double walled wire mesh, but breathing is a problem. The screening against electric fields is ideal since no flux can penetrate. The screening of the magnetic component improves with increasing frequency due to the skin effect.

Honeycomb inserts are also used. The grids are wave guides (with the frequencies considered below cut-off), the screening effectiveness of which depends on the ratio of depth to width of the honeycomb up to cm wavelengths. They are used for 100 kHz < f < 1000 MHz.

Misaligned sensor coils

Typical tokamak requirements include the measurement of poloidal fields in the presence of a much larger toroidal field. A small misalignment of the coil will then introduce unwanted field components. There are a number of solution to overcoming this problem

a) subtract data obtained with only the (unwanted) field component by energizing only the offending windings

b) make use of the differential nature of a pick-up coil signal. For example, consider the toroidal field to be the offending field, so that the pick-up coil measures $\frac{dB}{dt} = \frac{dB_{poloidal}}{dt} + \frac{dB_{toroidal}}{dt}$. If the toroidal field is almost steady state (d/dt ≈ 0) during the times of interest, then the differential signal during this time is approximately that required (i.e. from the poloidal field component only). Therefore the temporal integration should be started as late as possible.